Advanced control of large-scale wind turbines: Structural load reduction and lifetime control

Von der Fakultät für Ingenieurwissenschaften,
Abteilung Maschinenbau und Verfahrenstechnik
der
Universität Duisburg-Essen
zur Erlangung des akademischen Grades
eines
Doktors der Ingenieurwissenschaften
Dr.-Ing.
genehmigte Dissertation

von

Mạnh Hùng Đỗ
aus
Hanoi, Vietnam

Gutachter: Univ.-Prof. Dr.-Ing. Dirk Söffker
Univ.-Prof. Dr.-Ing. Andreas Reuter

Tag der mündlichen Prüfung: 30. November 2020

Acknowledgements

First and foremost, I would like to sincerely thank Univ.-Prof. Dr.-Ing. Dirk Söffker for his mindful supervision at the Chair of Dynamics and Control. His guidance and advice not only for the academic works but also for the management and real-life problems help me a lot to complete this thesis.

I also want to thank Univ.-Prof. Dr.-Ing. Andreas Reuter for his review and comments on my thesis as the second supervisor.

Special thanks to my colleagues at the Chair of Dynamics and Control (SRS) and the former member Dr.-Ing. Jackson G. Njiri for their kind support and cooperation.

I am grateful for my family who always believes and encourages me.

Finally, I would like to thank the Vietnam International Education Development Department (VIED) and Hanoi University of Science and Technology (HUST) for the funding during my research period.

Duisburg, December 2020 Đỗ Mạnh Hùng

Abstract

Global warming is a major consequence of high carbon dioxide emissions due to the burning of fossil fuels. In addition, the use of fossil fuels also emits mercury, sulfur dioxide, nitrogen oxides, and particulate matter into the air and water leading to many health problems. These factors in combination with the depletion of fossil fuel motivate the requirement for low-carbon and renewable energy sources.

Wind energy takes an important role in the transformation of the global energy system towards clean and sustainable sources. The main development of wind energy technology in recent decades is the growth of Wind Turbine (WT) size motivated by economic factors. The larger turbine size helps to increase power output and energy efficiency, however, it leads to challenges in wind turbine operation and maintenance. Larger and more flexible turbines experience higher mechanical stress on the turbine components such as gearboxes, blades, and towers. These structural loads may lead to early failure limiting the turbine size and performances.

To further reduce the cost of wind energy, advanced control approaches are developed focusing on power maximization, structural load mitigation, lifetime extension, and reliability improvement ultimately reduce the cost of wind energy. This multi-objective problem is difficult to solve due to design conflicts. The optimal trade-off between goals is varying and depends on actual operating situations such as on-site wind characteristics, system aging, and grid requirements.

Advanced control approaches are applied for utility-scale WTs to maximize power production and reduce structural loads. When the structural loads are considered, wind turbines become Multi-Input Multi-Output (MIMO) systems. Because of the coupling between control inputs and outputs, traditional Single-Input Single-Output (SISO) controllers are difficult to design and not suitable for such systems. Multi-input multi-output control approaches consider system internal connections so they can realize multiple objectives simultaneously. Multi-objective advanced MIMO control algorithms reduce the loads while maximizing the power generation. Related control approaches need to be robust and able to reduce the effects of unknown variable wind speed disturbances and modeling errors.

Load mitigation helps to expand the turbine lifetime, reduce the maintenance cost, and allows to build larger WTs. However, load reduction often comes with the consequence of decreasing power production and increasing blade pitch activities. To define an optimal compromise with these contrary goals, complete knowledge about various elements affecting control performance is required. Besides, the contribution of each aspect to the addressed conflicting objectives as load mitigation, and energy maximization, need to be evaluated by suitable measures.

Modern utility-scale wind turbines are equipped with numerous sensors providing useful information about turbine components operation status. With the huge de-

velopment of computation capability and big data analytics techniques, the turbine performance and state-of-health information could be obtained and evaluated through historical logged data using Prognostics and Health Management (PHM) systems. The information aids the optimal operation and maintenance of wind energy systems. In recent years, the integration of state-of-health information into the closed-loop control system begins to attract the attention of the wind energy researcher community. Controllers are adapted based on current and future aging behaviors optimizing the trade-off between service life expansion and power production maximization.

This thesis develops multi-objectives MIMO control strategies to maximize power production, reduces fatigue loading, and improves the reliability of large-scale WTs. Firstly, the thesis proposes novel measures based on time-series historical data obtained from wind turbines, such as blades/tower bending moments and rotor/generator speed, and the covariance of the data to assess the overall control performance of a wind turbine. New parameters defining the relation between control goals are introduced, which add new measures for controller assessment and design. The measures are able to express multi control objectives graphically and related mathematical values. Secondly, robust control algorithms regulating the generator power, and reducing fatigue loads are developed considering wind disturbances and model errors due to the use of linearized models and unmodeled dynamics. The approaches utilize an unknown input observer scheme to estimate wind disturbances. The WT nonlinearities and unmodeled dynamics are assumed as additive inputs so they also can be estimated by the observer. The effects of unknown inputs including wind disturbance, nonlinearities, and unmodeled dynamics are accommodated using suitable feed-forward controllers. The overall control system including observers and controllers are optimized by minimizing the H_∞ norm of the generalized system with uncertainties. The optimization problem defines optimal control parameters guaranteeing both performance and robustness. Finally, a PHM module providing current and future health information is integrated into the control loop to define the optimal balance of the trade-off between power production and loads mitigation. The PHM module predicts the Remaining Useful Life (RUL) of the system in real-time, so the lifetime of the WTs can be controlled to ensure the turbine survivability to the next maintenance schedule. A novel adaptive lifetime control scheme using RUL prediction is proposed to avoid unwanted failures. The proposed control strategy provides an optimal balance between maximize power production and reduce fatigue loading objectives. The reliability and lifetime of the WTs are controlled guaranteeing the systems reach designed lifetime, reducing unscheduled maintenance cost.

Kurzfassung

Die globale Erwärmung ist eine Hauptfolge der hohen Kohlendioxidemissionen aufgrund der Verbrennung fossiler Brennstoffe. Darüber hinaus werden bei der Verwendung fossiler Brennstoffe Quecksilber, Schwefeldioxid, Stickoxide und Partikel in die Luft und in das Wasser abgegeben, was zu vielen gesundheitlichen Problemen führt. Diese Faktoren in Kombination mit dem Abbau fossiler Brennstoffe begründen den Bedarf an kohlenstoffarmen und erneuerbaren Energiequellen.

Windenergie spielt eine wichtige Rolle bei der Umstellung des globalen Energiesystems auf saubere und nachhaltige Quellen. Die Entwicklung der Windenergietechnologie in den letzten Jahrzehnten beruht auf dem Größenwachstum von Windkraftanlagen (WT), motiviert durch wirtschaftliche Faktoren. Die Steigerung der Turbinengröße führt zur Erhöhung von Leistung und Energieeffizienz, stellt jedoch beim Betrieb und der Wartung von Windkraftanlagen eine Herausforderung dar. Größere und flexiblere Turbinen sind einer höheren mechanischen Belastung der Turbinenkomponenten wie Getriebe, Schaufeln und Türme ausgesetzt. Diese strukturellen Belastungen können zu einem frühen Ausfall führen, der die Turbinengröße und -leistung einschränkt.

Um die Kosten für Windenergie weiter zu senken, werden fortschrittliche Steuerungsansätze entwickelt, die sich auf Leistungsmaximierung, strukturelle Lastminderung, Verlängerung der Lebensdauer und Verbesserung der Zuverlässigkeit konzentrieren und letztendlich die Kosten für Windenergie senken. Dieses Problem mit mehreren Zielen ist aufgrund von Designkonflikten schwer zu lösen. Der optimale Kompromiss zwischen den Zielen variiert und hängt von den tatsächlichen Betriebssituationen ab, wie z. B. den Windeigenschaften vor Ort, der Systemalterung und den Netzanforderungen.

Für Windkraftanlagen im Versorgungsmaßstab werden erweiterte Regelungsansätze angewendet, um die Stromerzeugung zu maximieren und die strukturelle Belastung zu verringern. Die Berücksichtigung strukturellen Belastungen führt zu MIMO-Systemen (Multi-Input Multi-Output). Aufgrund der Kopplung zwischen Ein- und Ausgängen sind herkömmliche SISO-Regler (Single-Input Single-Output Regler) schwierig zu konstruieren und für solche Systeme nicht geeignet. Regelungsansätze mit mehreren Ein- und Ausgängen berücksichtigen systeminterne Verbindungen, sodass mehrere Ziele gleichzeitig realisiert werden können beispielsweise die Reduktion der Lasten und die Maximierung der Stromerzeugung. Die verwendeten Regelungsansätze müssen robust sein, um die Auswirkungen unbekannter variabler Windgeschwindigkeitsstörungen und Modellierungsfehler reduzieren zu können.

Die Lastminderung hilft, die Lebensdauer der Turbine zu verlängern, die Wartungskosten zu senken und größere Windkraftanlagenzu bauen. Eine Lastreduzierung führt jedoch häufig zu einer Verringerung der Stromerzeugung und einer Erhöhung der

Blattneigungsaktivitäten. Um einen optimalen Kompromiss zwischen diesen entgegengesetzten Zielen zu definieren, sind vollständige Kenntnisse über Elemente erforderlich, die die Performance des Reglers beeinflussen. Außerdem muss der Beitrag jedes Aspekts zu den angesprochenen widersprüchlichen Zielen wie Lastminderung und Energiemaximierung durch geeignete Maßnahmen bewertet werden.

Moderne Windkraftanlagen im Versorgungsmaßstab sind mit zahlreichen Sensoren ausgestattet, die nützliche Informationen über den Betriebsstatus der Turbinenkomponenten liefern. Mit der enormen Entwicklung von Rechenfunktionen und Big-Data-Analysetechniken konnte die Turbinenleistung und der Zustand der WT mithilfe historischer protokollierter Daten unter Verwendung von Prognostics and Health Management (PHM) -Systemen abgerufen und ausgewertet werden. Die Informationen unterstützen den optimalen Betrieb und die Wartung von Windenergieanlagen. In den letzten Jahren hat die Verwendung von Informationen über den Zustand der WT im Regelungssystem an Bedeutung gewonnen. Die Regler werden basierend auf dem aktuellen und zukünftigen Alterungsverhalten angepasst, um einen optimalen Kompromiss zwischen Verlängerung der Lebensdauer und Maximierung der Stromerzeugung zu erreichen.

In dieser Arbeit werden MIMO-Regelungsstrategien entworfen, die darauf abzielen die Stromerzeugung zu maximieren, die Ermüdungsbelastung zu verringern und die Zuverlässigkeit von WTs in großem Maßstab zu verbessern. Erstens werden in der Arbeit neuartige Kenngrößen zur Performance-Bewertung der Regelung von Windkraftanlagen entwickelt. Diese Kenngrößen basieren auf historischen Zeitreihen von Windkraftanlagen wie z. B. Schaufel- / Turmbiegemomente und Rotor- / Generatordrehzahl, die im Hinblick auf Kovarianz ausgewertet werden. Es werden neue Parameter eingeführt, die für den Entwurf und die Bewertung der Regler verwendet werden können. Die Maßnahmen erlauben es das Erreichen der Regelungsziele grafisch zu bewerten und mittels mathematischer Kenngrößen zu quantifizieren. Zweitens werden robuste Regelungsalgorithmen entwickelt, die die Generatorleistung regulieren und Ermüdungslasten reduzieren, wobei Windstörungen und Modellfehler berücksichtigt werden. Die Modellfehler entstehen aufgrund der verwendeten linearisierten Modelle und der nicht berücksichtigten Dynamiken Die Ansätze verwenden ein unbekanntes Eingangsbeobachterschema, um Windstörungen abzuschätzen. Die WT-Nichtlinearitäten und die nicht modellierte Dynamik werden als additive Eingaben angenommen, damit sie vom Beobachter geschätzt werden können. Die Auswirkungen unbekannter Eingänge, einschließlich Windstörungen, Nichtlinearitäten und nicht modellierte Dynamiken, werden mithilfe geeigneter Vorwärtsregelungen berücksichtigt. Das gesamte Steuerungssystem einschließlich Beobachtern und Regler wird optimiert, indem die H_∞ Norm des verallgemeinerten Systems minimiert wird. Das Optimierungsproblem definiert optimale Reglerparameter, die sowohl Leistung als auch Robustheit garantieren. Schließlich wird ein PHM-Modul, das aktuelle und zukünftige Informationen zum Zustand der WT bereitstellt, in den Regelkreis integriert, sodass ein optimales Gleichgewicht zwischen Stromerzeugung und Lastmin-

derung erreicht werden kann. Das PHM-Modul sagt die verbleibende Nutzungsdauer (RUL) des Systems in Echtzeit voraus, sodass die Lebensdauer der WT gesteuert werden kann und die Funktionsfähigkeit der Turbine bis zum nächsten Wartungszeitpunkt sichergestellt ist. Ein neuartiges adaptives Lebensdauersteuerungsschema unter Verwendung der RUL-Vorhersage wird vorgeschlagen, um unerwünschte Fehler zu vermeiden. Die vorgeschlagene Regelstrategie bietet ein optimales Gleichgewicht zwischen der Maximierung der Stromerzeugung und der Reduzierung der Ermüdungsbelastung. Die Zuverlässigkeit und Lebensdauer der WT wird kontrolliert, um sicherzustellen, dass die Systeme die vorgesehene Lebensdauer erreichen, wodurch die außerplanmäßigen Wartungskosten gesenkt werden.

Contents

List of Figures

List of Tables

Nomenclature

Symbols

ρ	Air density
β	Blade pitch angle
R	Control input weighing matrix
T_g	Electrical generator torque
$GS()$	Gain scheduling coefficient function
N_g	Gearbox ratio
$\|\|.\|\|_\infty$	$\mathcal{H}_\infty$ norm
K_i	Integral gain
β_{opt}	Optimal pitch angle in region 2
λ_{opt}	Optimal tip speed ratio in region 2
C_p	Power coefficient
K_p	Proportional gain
$J_{_{LQR}}$	Quadratic performance index
R	Rotor radius
ω_r	Rotor rotational speed
Q	States weighing matrix
λ	Tip speed ratio
K_g	Torque controller gain
ζ	Tower fore-aft deflection
v	Wind speed

Abbreviations

ACM+P	Prognostics-enhanced Automated Contingency Management
CBM	Condition-Based Maintenance
COE	Cost Of Energy
CPC	Collective Pitch Controller
DAC	Disturbance Accommodating Controller
DEL	Damage Equivalent Load
EU ETS	European Union Emissions Trading System
FAST	Fatigue, Aerodynamics, Structures, and Turbulence
FTC	Fault-Tolerant Control
HAWT	Horizontal Axis Wind Turbine
IPC	Individual Pitch Controller
IPHMC	Integrated PHM Control
KF	Kalman Filter
LCOE	Levelized Cost Of Energy
LIDAR	Light Detection And Ranging

LMI	Linear Matrix Inequality
LQG	Linear Quadratic Gaussian
LQR	Linear Quadratic Regulator
LTI	Linear Time Invariant
MBC	Multi-Blade Coordinate transformation
MIMO	Multi-Input Multi-Output
MPC	Model Predictive Control
MPPT	Maximum Power Point Tracking
NREL	National Renewable Energy Laboratory
O&M	Operation and Maintenance
PHM	Prognostic and Health Management
PIO	Proportional-Integral-Observer
PSF	Power Signal Feedback
RUL	Remaining Useful Life
SHM	Structural Health Monitoring
SISO	Single-Input Single-Output
SoH	State-of-Health
SRCE	Safety and Reliability Control Engineering
TSR	Tip Speed Ratio
VAWT	Vertical Axis Wind Turbine
WECS	Wind Energy Conversion System
WT	Wind Turbine

1 Introduction

1.1 Motivation and problem statement

Global warming is a major consequence of high carbon dioxide emissions due to the burning of fossil fuels. To combat climate change, the Paris agreement was built to limit the temperature increase to 1.5 degrees Celsius in comparison with pre-industrial levels by reducing the total global greenhouse gas emissions [RDEH+16]. In 2018, coal-fired power plants account for 37 % of the European Union Emissions Trading System (EU ETS) emissions [Ago19]. In addition, the use of fossil fuels also emits mercury, sulfur dioxide, nitrogen oxides, and particulate matter into the air and water leading to many health problems [BLB+16]. These factors in combination with the rising cost and depletion of fossil fuel motivate the requirement for low-carbon and renewable energy sources.

Wind energy plays a significant role in scaling up renewable electricity sources for the decarbonization of the global energy generation system. It is forecasted that more than 30 % of electrical demand by 2050 is provided by wind power [IRE19]. To fulfill the growing requirements, wind turbines are scaled up in size to access more power from the wind driven by technology innovation and the use of advanced materials. The largest wind turbine was installed in 2018 with a power rating of 8.8 MW and a rotor diameter of 164 m [KFB19]. Larger rotors aid in increasing capacity factor and efficiency ultimately reducing the cost of wind energy. The wind Levelized Cost Of Energy (LCOE) has been reducing in the last decade [Koo16, SBHS18]. In the US, the average rotor diameter in 2018 increased by 35 % over 2010, while the average LCOE reduced by over 50 % in the same period [WB19]. The production cost of wind energy is continuing to decrease, and it begins to outcompete even the cheapest fossil fuel-fired source of new electricity (fig. 1.1) [IRE20]. The global weighted-average LCOE of onshore wind is USD 0.053/kWh in 2019 [IRE20].

The larger turbine size improves power output and energy efficiency, however, it leads to challenges in wind turbine operation and maintenance. Larger and more flexible turbines experience higher mechanical stress on the turbine components. These structural loads may lead to early failure limiting the turbine size and performances [Bos03b]. To further increase the turbine size, structural loads need to be reduced or considered/monitored.

Advanced control approaches are applied for utility-scale WTs to maximize power production and reduce structural loads [NS16]. The variation of turbine components such as blades, tower, drive-train, or gear-box are controlled along with the power production by modifying the blade pitch angles. When the structural loads are considered, it is helpful to understand the wind turbine as a Multi-Input Multi-Output (MIMO) system. Because of the coupling between control inputs and outputs, traditional Single-Input Single-Output (SISO) controllers are difficult to design and

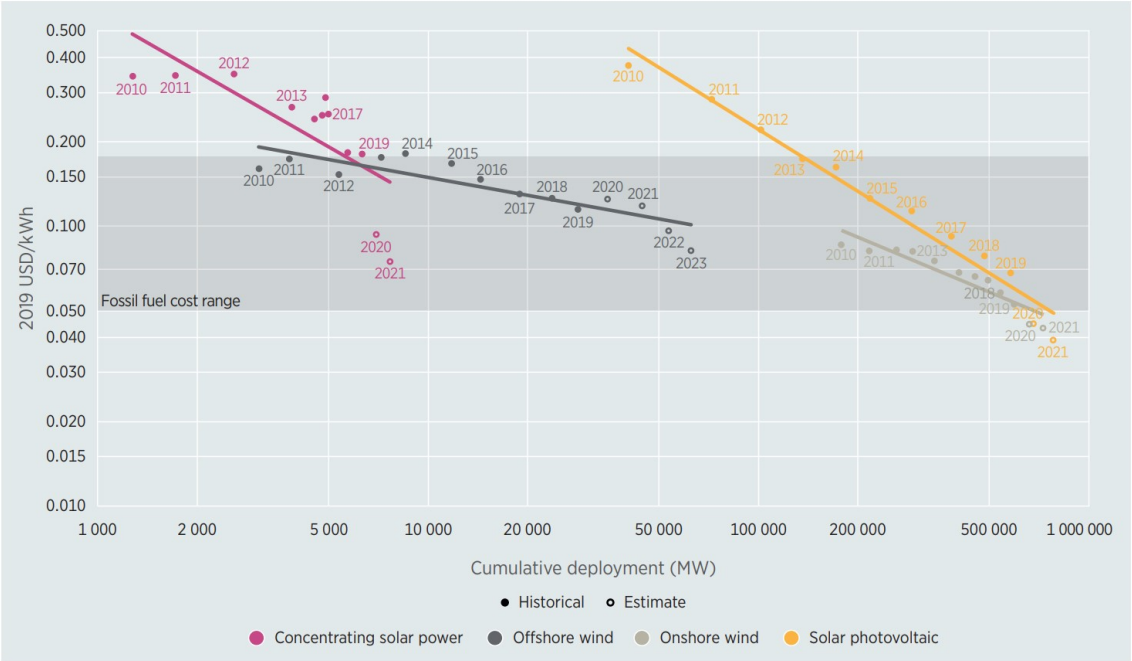

Figure 1.1: The global weighted-average price of renewable energy [IRE20]

not suitable for such systems [WB03]. Multi-input multi-output control approaches consider system internal connections so they can realize multiple objectives simultaneously. Multi-objective advanced MIMO control algorithms reduce the loads while maximizing the power generation. Related control approaches need to be robust and able to reduce the effects of unknown variable wind speed disturbances and modeling errors [DNS18]. Load mitigation helps to expand the turbine lifetime, reduce the maintenance cost, and allows to build larger WTs. However, load reduction often comes with the consequence of decreasing power production and increasing blade pitch activities [Bos03b]. Balancing and optimizing this trade-off is challenging and still is an open problem.

To make wind energy more competitive, the related Cost Of Energy (COE) needs to be reduced either by evolution in turbine design, applied materials or optimal Operation and Maintenance (O&M). The O&M cost can account for 30 % of wind power COE [DMR+13, CMM16], so it is important to reduce the cost by expanding the turbine service lifetime or reducing unplanned maintenance cost which takes over 50 % of total O&M cost [Woo19].

With the recent development in sensor techniques, computation capacity, as well as PHM algorithms, the current and predicted health status information is integrated into WT O&M processes to minimize the cost [TJWD11]. The information can be used to defined optimal maintenance schedules as in Condition-Based Maintenance (CBM) or optimal control configurations as in Fault-Tolerant Control (FTC) based

on actual situations. The PHM information also can be integrated with control system targeting system performances, safety and reliability [SR97, TKG+08, EPN12]. The decision-making concerns control objectives, maintenance, and repairs strategies can be integrated into a closed-loop automation concept considering system SoH, safety, reliability, and performance.

Despite the potential of the PHM and control combination, this strategy has not widely applied in the field of wind energy yet. So it is necessary to develop a throughout framework for this combination focusing on performance and reliability of WTs ultimately further reducing the cost of wind energy.

1.2 Thesis objectives and scope

This thesis aims to develop multi-objective MIMO control strategies with integrated PHM information to maximize power production, reduce fatigue loading, and improve the reliability of large-scale WTs. The related approaches need to deal with typical challenges of wind turbine control such as unknown varying wind speed, inaccurate system model as well as the conflict between power maximization and structural load mitigation. A general framework is established to integrate PHM into the control loop with a novel application of lifetime control for WTs. The thesis also discuss the requirement for multi-objective performance metrics to compare and evaluate control approaches.

A high fidelity simulation software and nonlinear megawatt-scale off-shore wind turbine model are used to evaluate the developed approach with different wind conditions reflecting real operations. Within the thesis, fatigue damage, which strongly relates to vibration of WT components such as blades, towers, and gearboxes, is considered as the structural load. The reduction of this structural load increases the fatigue life of WT components thus expands the WT service lifetime.

The thesis is based on the results and development steps published/submitted in the following journal papers [NBDS19, DNS20, DS20a, DS20d] and conference proceedings [DNS18, DS19, DS20b, DS20c].

1.3 Thesis outline

The thesis contains six chapters. In the first chapter, the motivation and problems of developing advanced control systems for large-scale wind turbines focusing on load mitigation, power generation performances, and reliability to reduce the cost of wind energy are introduced.

In the second chapter, an overview of standard wind turbine control systems is given along with the simulation tool and wind turbine model used in the thesis. Literature

reviews on structural load reduction control and novel integrated Prognostic and Health Management Control (IPHMC) are provided. Challenges and open research questions are discussed in the chapter.

In the third chapter, the need for multi-objective control performance evaluation metrics and requirements of PHM approaches for integrated control are considered. A novel performance measure based on power and load distribution covariant is developed to compare and evaluate the control performance for both power production and load mitigation objectives.

In the fourth chapter, novel load mitigation control approaches considering wind disturbances and model inaccuracy are developed for wind turbines in both region 2 and region 3. The control performances are evaluated and compared with baseline controllers by several metrics using simulation results with different wind conditions.

In the fifth chapter, the general concept of IPHMC and a novel lifetime control approach are presented. The approach combines PHM information with the load mitigation controller introduced in chapter fourth to regulate the lifetime of wind turbine components avoiding early failures and optimizing the trade-off between power production and load mitigation.

Finally, summary, conclusions, and outlook for future works are given in chapter sixth.

2 Background and literature review

The figures, tables, and content in this chapter are partly based on the submitted journal paper [DS20a].

2.1 Wind turbine control system overview

Wind turbines are devices converting the kinetic energy of the wind into electricity. Wind turbines are typically classified into two main types based on the axis of rotation: Horizontal Axis Wind Turbines (HAWT) and Vertical Axis Wind Turbines (VAWT) (fig. 2.1). Most of the large-scale wind turbines are HAWTs due to the higher efficiency in comparison with VAWTs [Hau13]. However, VAWTs have advantages in urban areas that have high turbulence low-speed wind conditions and noise restrictions [KRF18].

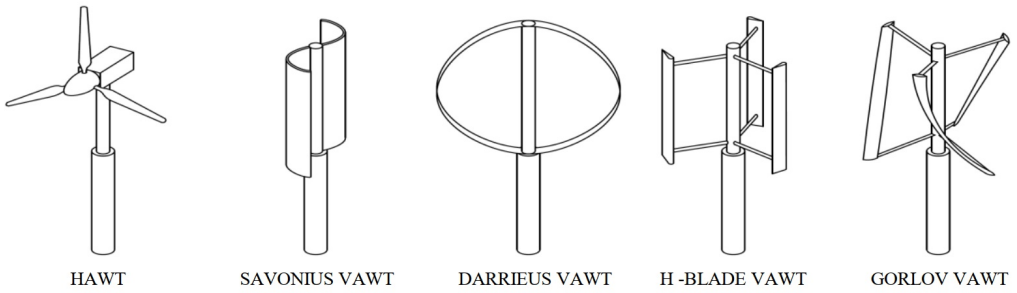

Figure 2.1: Types of wind turbines [Cas16]

The main components of a HAWT are shown in fig. 2.2. Horizontal axis wind turbines operate based on lift aerodynamic forces that are perpendicular to the flow of the wind. The forces caused by the difference in pressure on two sides of the blades when interacting with the wind flow. These forces convert wind kinetic energy to the rotational energy of the rotor. Most of the large-scale wind turbines are equipped with pitch drives to change the blade attack angle (fig. 2.3). The change allows to control of the aerodynamic forces affected the blades thus control the rotor rotational speed. Blade pitch angles can be controlled collectively (Collective Pitch Control - CPC) or individually with a different angle for each blade (Individual Pitch Control - IPC) [Bos03a]. Because the wind direction changes overtime, WTs have yaw mechanisms to track the wind direction maximizing power production. The relatively slow rotation speed of the rotor is transferred to high-speed rotation of the generator by a gearbox to produce electricity. The generator electrical torque also can be modified to control the rotor speed. The overall control system for wind turbines is shown in fig. 2.4.

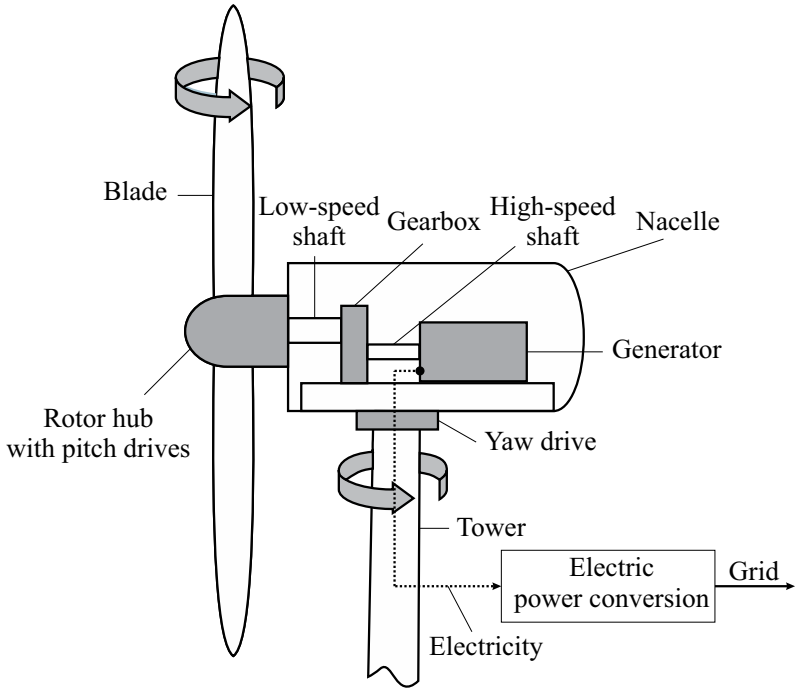

Figure 2.2: Main components of wind turbines

Because of the improvements of semiconductor power converter technologies, the rotational speed of WTs can be decoupled from the output electrical frequency. This allows WTs to operate at variable speeds. Variable speed WTs operate closer to the optimal rotational speed thus have higher efficiency than fixed speed WTs [PJ11].

The operation of wind turbines can be divided into 3 main regions (fig. 2.5). Region 1 is below cut-in wind speed, where wind energy is not enough to operate the turbine, so turbine is stopped. Region 2 is between cut-in and rated wind speed. In this region, the main goal is to maximize power production, typically by fixing the pitch angles at a predefined optimal value and varying the generator torque to tracking the maximal coefficiency. In region 3 which is above rated speed, wind energy is higher than the turbine capacity, so the goal here is to regulate rotor speed or generator power at a rated value to guarantee the system safety.

In low wind speed region or part-load region, the main goal is to maximize energy extracted from the wind. Large wind turbines often have variable-speed configuration due to the ability to optimally operate over a wide range of wind speed. The amount of extractable wind power is strongly related to the turbine operating point defined by wind speed, rotor rotational speed, and blade pitch angle. The wind speed varies stochastically in nature, so to make wind turbines operate at the optimal point, the rotor speed and blade pitch angles need to be controlled accordingly by Maximum Power Point Tracking (MPPT) control methods [AYTS12, TB16].

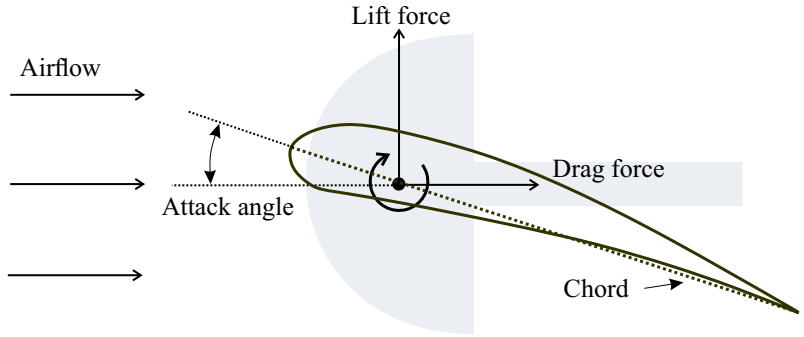

Figure 2.3: Wind turbine aerodynamic forces

The MPPT methods determine optimal operating point using the information of wind speed, output power, or the characteristic curve of the wind turbine [AYTS12]. Typical MPPT control algorithms applied to wind turbines are Tip-Speed-Ratio (TSR) control, Power Signal Feedback (PSF), Hill-Climb Searching (HCS), Optimal Torque Control (OTC), and soft computing techniques. Both the TSR and PSF control methods require prior knowledge of wind turbine parameters and feedback measurements. The HCS control method is based on an iterative search of optimum power point using power and rotational speed measurements or converter duty cycles. The tip-speed-control method requires knowledge of optimum tip speed ratio λ_{opt} and the measurement of effective wind speed to give accurate results. The error between the actual torque and the reference torque defined by maximum power point at particular wind speed is used to modify the generator torque in OTC methods. Soft computing methods including Fuzzy Logic Controller (FLC) and Artificial Neural Network (ANN) on the other hand do not require prior knowledge of wind turbine parameters [TB16].

One of the most common MPPT control algorithms applied to WTs is tip-speed-ratio control. The method maintains the optimal TSR λ_{opt} to maximize the power coefficient C_p, which is a nonlinear function of TSR λ and blade pitch angle β. In region 2, β is held at a constant optimal value β_{opt} that yields the maximum aerodynamic lift, so C_p depends on λ only.

The power available in the wind P_{wind} is proportional to the cube of wind velocity as

$$P_{wind} = \frac{1}{2}\rho\pi R^2 v^3, \tag{2.1}$$

where ρ denotes the air density, R the rotor radius, and v the wind velocity.

Wind turbines are able to convert a part of the wind power into mechanical energy. The maximum extractable energy is limited to a theoretical value 59.3% of available wind power (Betz limit).

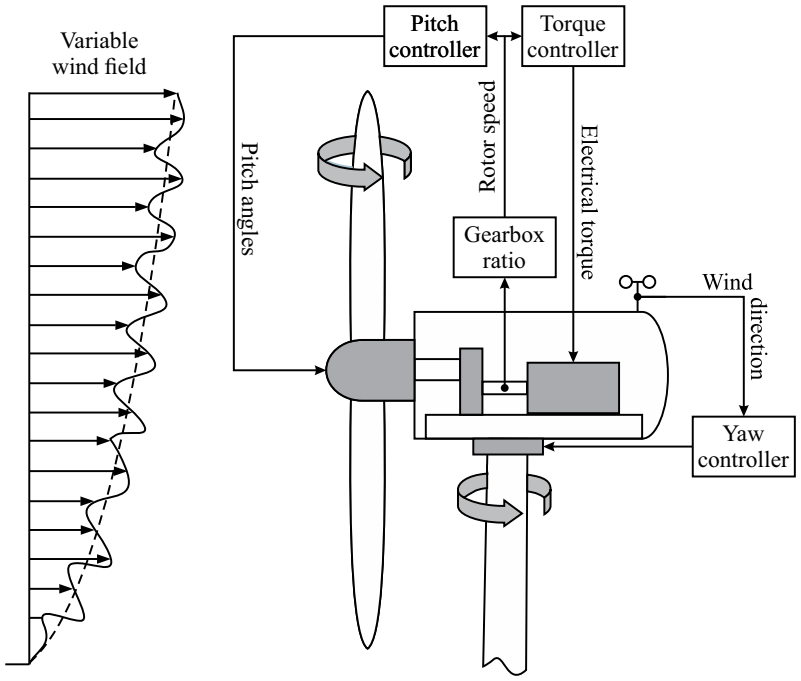

Figure 2.4: Wind turbine control system

The performance of wind turbines is defined by the power coefficient C_p as

$$C_p(\lambda, \beta) = \frac{P}{P_{wind}}, \tag{2.2}$$

where P denotes the wind turbine power.

Wind turbine power coefficient C_p is a nonlinear function of tip-speed-ratio λ and blade pitch angle β. Tip-speed-ratio λ is defined as the ratio between rotor speed ω_r and active wind speed as

$$\lambda = R\frac{\omega_r}{v}. \tag{2.3}$$

In most of MPPT control methods, blade pitch angle β is held at a constant optimal value β_{opt} that yields the maximum aerodynamic lift such that the power coefficient depends on tip-speed-ratio λ only. The aim of MPPT algorithms is to keep wind turbines operate at optimal tip-speed-ratio λ_{opt} maximizing C_p. The maximum power coefficient $C_p(\lambda_{opt}, \beta_{opt})_{max}$ and the optimal operation values λ_{opt} and β_{opt} can be determined either through experiment or theoretical methods such as Blade Element Momentum (BEM) theory.

To maintain the optimal tip-speed-ratio, the rotor speed ω_r needs to follow the stochastically vary wind speed v. The standard method for optimal tip-speed-ratio

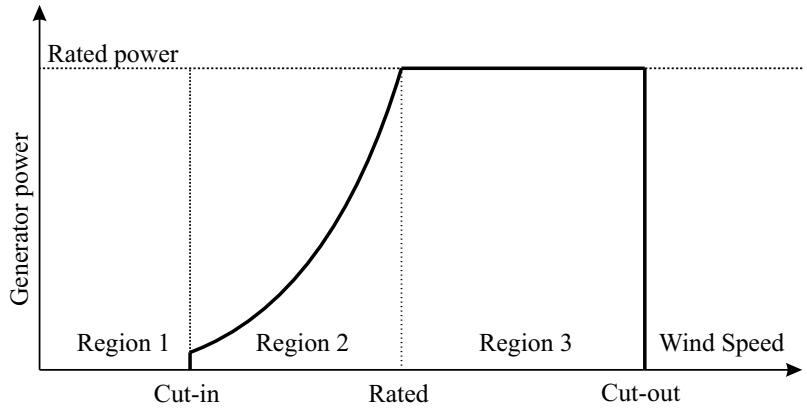

Figure 2.5: Operation regions

tracking is to control generator torque T_g using rotor speed feedback as

$$T_g = \frac{1}{2N_g}\rho\pi R^5 \frac{C_p(\lambda_{opt}, \beta_{opt})_{max}}{(\lambda_{opt})^3}\omega_r^2 = K_g\omega_r^2, \tag{2.4}$$

where N_g denotes the gearbox ratio between generator and rotor speed, K_g the gain of the torque controller. The standard torque controller for WTs in region 2 is shown in fig. 2.6.

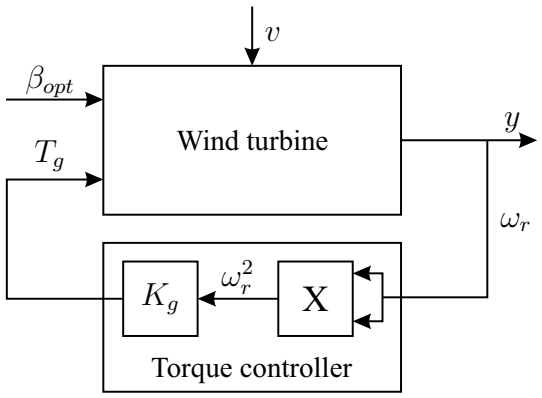

Figure 2.6: Standard torque controller for region 2

A detail explanation of the region 2 standard controller can be found in [JFBP04].

In high wind speed regime (region 3) which is above rated wind speed, the wind energy is beyond the extraction capacity of the turbines. The main goal in this region is to keep the turbines operate under the electrical and mechanical safety limits. Two typical strategies for region 3 wind turbines control are constant power and constant torque. In the constant power strategy, the generator power is kept constant by varying the generator torque inversely proportional to the generator

speed [JBJ09]. In the second strategy, the generator torque is held constant while the rotor/generator speed is regulated to the desired rated value by modifying the blade pitch angles [MH06]. In this thesis, the constant generator torque approach is used. The generator torque is kept at the rated value T_{rated}, the generator speed is regulated to rated speed.

Proportional and Integral (PI) control approach is the most widely used method of commercial wind turbines control in region 3. A PI controller formula can be written as

$$u(t) = K_p e(t) + K_i \int e(\tau) d\tau, \tag{2.5}$$

here K_p and K_i denote the coefficients for the proportional and integral terms respectively, $u(t)$ the control variable which is the collective demanded pitch angle, $e(t)$ the difference between desired rated speed ω_{rated} and measured rotor speed ω_r. The design parameters K_p and K_i depend on the linearized model of the system which varies according to the operation points. To compensate the effects of changing operation points, a variable gain controller should be used. In this thesis, a gain scheduling PI controller as described in [DR18] is used as baseline controller (fig. 2.7).

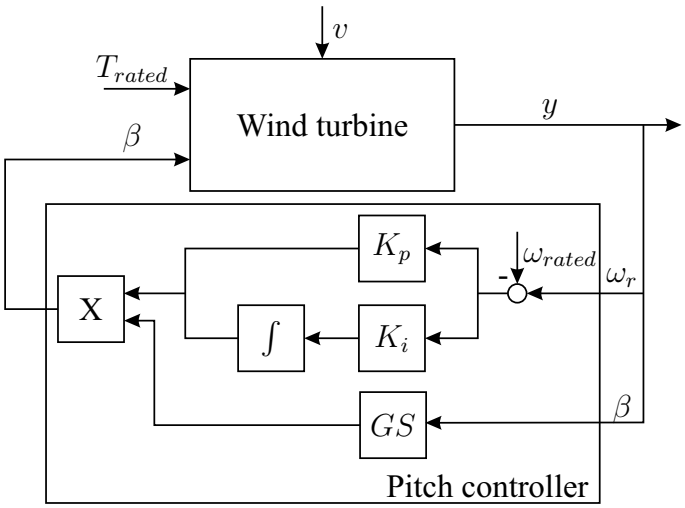

Figure 2.7: Gain scheduling pitch controller for region 3

The gain scheduling PI controller is realized by multiplying the PI control output with a coefficient depending on operational point. The operational point is defined by the actual blade pitch angle β. In this thesis, the WindPACT baseline wind turbine models developed by the US National Renewable Energy Laboratory

(NREL) are used [DR18]. The scheduling coefficient function for WindPACT WTs are defined as follow [DR18]

$$GS(\beta) = \begin{cases} 1 & \beta < 0.0454 \\ 0.213\beta^{-0.5} & 0.0454 \leq \beta \leq 0.5236 \\ 0.2944 & \beta > 0.5236 \end{cases} \tag{2.6}$$

here the blade pitch angle β is in radians.

2.2 Wind turbine model and simulation tool

This section gives a brief introduction about control model and simulation tools used in the thesis for designing and evaluation of control approaches.

Fatigue, Aerodynamics, Structures, and Turbulence (FAST) code [JBJ05] developed by NREL is used to obtain dynamic responses of different control schemes and operation scenarios. The code can simulate important turbines' motions such as the translational (surge, sway, and heave) and rotational (roll, pitch, and yaw) motions of the support platform relative to the inertia frame, the tower motion, the yawing and nacelle motion, the generator motion, variable rotor speed and drive-shaft flexibility, the drive-train motion, the blade flap-wise tip motion for the first and second mode, the blade edge-wise tip displacement for the first mode, and lastly the rotor and tail-furl. These motions can be disabled during the simulation or linearization to obtain less complex models for designing controllers.

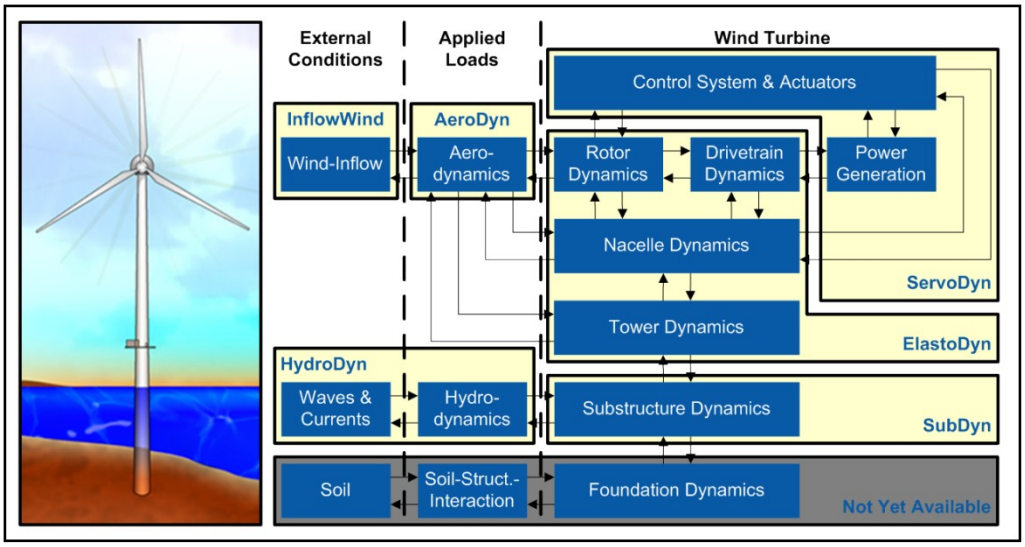

Figure 2.8: FAST simulation tool structure [JBJ05]

A three-bladed upwind reference WindPACT 1.5 MW onshore wind turbine model developed by NREL [DR18] is considered as a reference system based on the FAST code. The model is built based on an actual commercial wind turbine and was used most extensively in the WindPACT program for studies of wind turbine technology innovations. The turbine's characteristics are outlined in table 2.1. In this thesis, all of the DOFs of the onshore wind turbine are enabled for simulation. However only the generator speed, drive-train torsional, first mode blade flap-wise, and tower fore-aft DOFs are enabled to obtain a reduced order linearized model for controller design.

Table 2.1: WindPACT 1.5 MW reference wind turbine specifications

Rated rotor speed	20.463 rpm
Hub height	84 m
Configuration	3-blades, upwind
Cut_in, Rated, Cut_out wind speed	4 m/s, 12 m/s, 25 m/s
Gearbox ratio	87.965
Rotor diameter	70 m
Rated power	1.5 MW
Blade pitch range	0-90^o

Wind turbine dynamics can be described using a nonlinear model as

$$\begin{aligned} \dot{x} &= f(x, u, d) \\ y &= h(x, u, d), \end{aligned} \tag{2.7}$$

where x denotes the state vector of the turbine, u the control inputs, d the disturbances, and y the measured outputs with proper dimensions.

The nonlinear wind turbine model of the WindPACT 1.5 MW reference WT is linearized about a given steady state operating point to receive a linear model for controller design numerically using FAST. First, a constant speed wind is used as input for FAST linearization analysis, the blade pitch angles are kept constant. The software automatically computes the periodic steady-state operation points and the corresponding linearized models. The periodic state-space matrices then are azimuth-averaged to obtain the final model [JBJ05]. In this contribution, the nonlinear model (2.7) is linearized about the operating point. In the above-rated wind speed region, with hub-height wind speed of v_{op} = 18 m/s, collective pitch angles of β_{op}= 20 degrees, and nominal rotor speed of y_{op} = 20.463 rpm are selected as steady state operating points. In region 2, the operation point is chosen as $v_{op} = 8$ m/s, β_{op} 2.9 degrees, and y_{op} = 14.8 rpm. The controller of each region is computed based on the corresponding linearized model.

During the linearization process using FAST, certain DOFs are enable to obtained the reduced order model. The reduced order linearized model has to contain the most important aspects of the wind turbine dynamics representing the control objectives. In this study, structural load is considered, so the related model has to consist of corresponding load variables representing blade, tower, drive-train loads, and the rotor speed. Generally, the variables of the linearized model are small variations about the selected steady state operating point. The mechanical state vector $x \in \mathbb{R}^{11x1}$ of the corresponding model is

$$x = \begin{bmatrix} \text{tower fore-aft displacement} \\ \text{drivetrain torsional displacement} \\ \text{blade 1 flap-wise displacement} \\ \text{blade 2 flap-wise displacement} \\ \text{blade 3 flap-wise displacement} \\ \text{generator speed} \\ \text{tower fore-aft velocity} \\ \text{drivetrain torsional velocity} \\ \text{blade 1 flap-wise velocity} \\ \text{blade 2 flap-wise velocity} \\ \text{blade 3 flap-wise velocity} \end{bmatrix}. \tag{2.8}$$

The measured output $y \in \mathbb{R}^{2x1}$ include rotor speed ω calculated from the generator speed through gearbox ratio and tower fore-aft displacement ζ which can be easily obtained from typical sensors of modern turbines. The control input $u \in \mathbb{R}^{1x1}$ denotes the perturbed collective blade pitch angle $\Delta\beta$, and the disturbance $d \in \mathbb{R}^{1x1}$ denotes the perturbed hub-height wind speed Δv. All variables are initialized with zero.

The linearized reduced order model is represented in state-space form in suitable coordinates as

$$\begin{aligned} \dot{x} &= Ax + Bu + B_d d \\ y &= Cx, \end{aligned} \tag{2.9}$$

where $A \in \mathbb{R}^{11x11}$ denotes the system matrix, $B \in \mathbb{R}^{11x1}$ the control input matrix, $B_d \in \mathbb{R}^{11x1}$ the disturbance input matrix, and $C \in \mathbb{R}^{2x11}$ the output matrix.

The FAST code does not integrate pitch actuator dynamics, hence, to represent the effects of the blade actuator dynamics, an additional actuator model is required. Due to the larger bandwidth of the pitch actuator dynamics relative to the wind turbine dynamics, here for simplicity, the actuator dynamics is considered as a first-order lag (PT1) linear model

$$\frac{\beta}{\beta_{com}} = \frac{1}{s\tau_\beta + 1}, \tag{2.10}$$

where β_{com} represents the desired pitch angle, β the actual pitch angle, and τ_β the actuator lag time. The actuator model can be expressed in state space form

$$\dot{\beta} = -1/\tau_\beta \beta + 1/\tau_\beta \beta_{com}. \tag{2.11}$$

From (2.9) and (2.11) the extended wind turbine model including the pitch actuator dynamics

$$\begin{aligned} \begin{bmatrix} \dot{x} \\ \dot{\beta} \end{bmatrix} &= \underbrace{\begin{bmatrix} A & B \\ 0 & -1/\tau_\beta \end{bmatrix}}_{A_a} \underbrace{\begin{bmatrix} x \\ \beta \end{bmatrix}}_{x_a} + \underbrace{\begin{bmatrix} 0 \\ 1/\tau_\beta \end{bmatrix}}_{B_a} u + \underbrace{\begin{bmatrix} B_d \\ 0 \end{bmatrix}}_{B_{da}} d \\ y &= \underbrace{\begin{bmatrix} C & 0 \end{bmatrix}}_{C_a} \begin{bmatrix} x \\ \beta \end{bmatrix}, \end{aligned} \tag{2.12}$$

is obtained, here u denotes β_{com} instead of β. In following sections the extended model included actuator dynamics is used instead of the original one.

The simulation tool (FAST code) can be used in combination with MATLAB Simulink for more powerful and flexible controller designing and validating (fig. 2.9). The FAST code provides complete nonlinear aeroelastic wind turbine equations of motion considered as a real plant. The pitch, torque, and yaw controllers can be designed in MATLAB Simulink environment and interacted with the nonlinear WT model through an S-Function block [JBJ05]. This combination allows for fast development and evaluation of advanced control approaches without the use of costly real turbines.

2.3 Structural load reduction control

Structural loads affecting tower, blades, and drive-train mainly result from gravity and wind forces affecting the wind turbine rotor area [NS16]. The wind aerodynamic forces shown in fig. 2.3 not only rotate the rotor to produce energy but also make the turbine structures to deflect. The main deflection modes of the tower and blades can be seen in fig. 2.10. Unbalanced and varying aerodynamic loads caused by the difference in phase of each blade when rotating also induce stresses on turbine structures. The wind speed changes stochastically in both direction and magnitude. The speed is usually larger at the upper part and lower at the bottom part of the turbine due to the vertical wind shear (fig. 2.10). This leads to each blade experiences different and continuously changing wind speed increasing asymmetrical aerodynamic forces. Another source of structural loads is gyroscopic forces yielding cyclic stresses to the drive-train and the blades resulting in fatigue loads [HMN12]. Wake effect which is the reduction of wind speed and increase of turbulence intensity in downstream also contributes to increasing fatigue loads in wind farms [TS99].

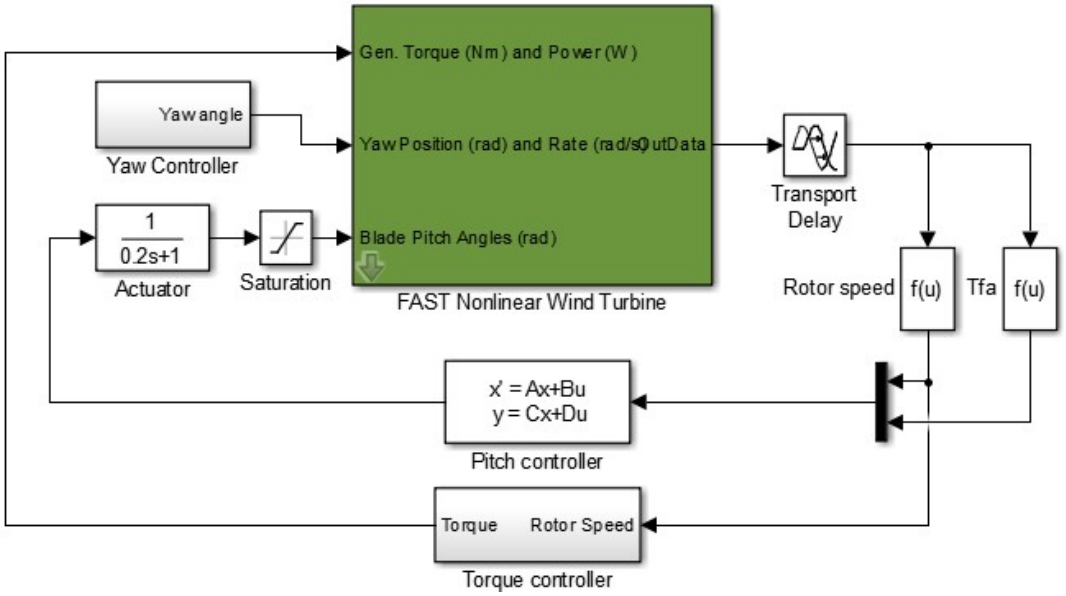

Figure 2.9: FAST Simulink interface

These effects are stronger when the turbine sizes become larger leading to the increase in structural loads. The reduction of such periodic and stochastic loads could reduce the operating cost and increase the wind turbines' expected lifetime, which would lower the cost of wind energy.

Most large-scale wind turbines nowadays are characterized by variable-pitch and variable-speed control to maximize the energy extracted. The turbine rotor speed is controlled to track the optimal speed in region 2 (under-rated wind speed) and to regulate the rotor speed at a rated value in region 3 (above-rated wind speed) by adjusting the generator torque and the pitch angle of blades (Section 2.1). Classical proportional-integral (PI) collective pitch control (CPC) controllers only regulate the rotor without considering structural loads. In modern large-scale wind turbines, structural loads such as tower, blades, and drive train torsional vibration are reduced by using additional control loops for active damping at resonant frequencies [Bos03a, DS14]. Because of the strong coupling between control modes, special attention is required when designing control loops individually for different goals to avoid performance deterioration or unstabilizing the closed-loop system. To deal with the decoupling problem of SISO approaches, advanced MIMO controllers have been developed by wind energy researchers in order to realize multiple objectives such as regulating the rotor speed and mitigating structural loads at the same time.

The MIMO control system for wind turbines is shown in fig. 2.11. The wind turbine is assumed to operate only at region 2 or region 3. The transition region (region $2_{1/2}$) is not considered in this thesis. The region 2 control system includes a baseline torque controller described in section 2.1. The MIMO controller adjusts the

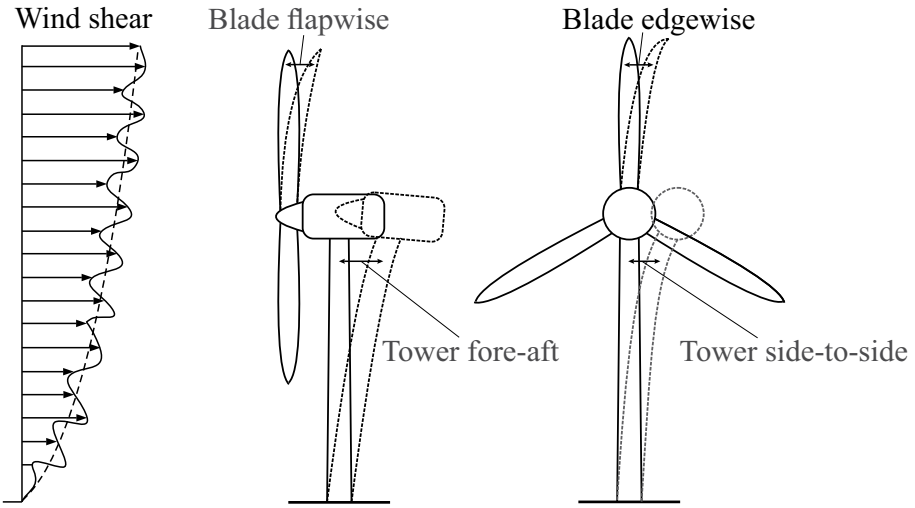

Figure 2.10: WTs structural loads

blade pitch angles around the optimal value to provide additional damping to the structural load variation modes. In region 3, the torque is kept constant at rated value, the objectives of the MIMO controller in this region are to regulate the rotor/generator speed and reduce structural variations. Note that the two MIMO controllers have different parameters calculated from different linearized models depending operational points.

The PI controller described in the previous section only regulates the rotor speed without considering the structural load. To reduce structural load as well, a MIMO multi-objective controller is needed. The dynamic behavior of the system described by (2.9) depends on its eigenvalues λ defined by

$$det(\lambda I - A) = 0. \tag{2.13}$$

Assuming (2.9) as fully controllable, new dynamical properties of the system can be designed by a full-state feedback controller

$$u = -Kx, \tag{2.14}$$

where matrix K denotes controller gain. The controlled system eigenvalues are calculated by

$$det(\lambda I - (A - BK)) = 0, \tag{2.15}$$

and can be arbitrarily located by common approaches like pole placement or LQR to add damping to blade and tower bending modes.

A linear quadratic regulator LQR is designed such that the objective function J_{LQR}

$$J_{LQR} = \int \left(x^T(t)Qx(t) + u^T(t)Ru(t)\right) dt, \tag{2.16}$$

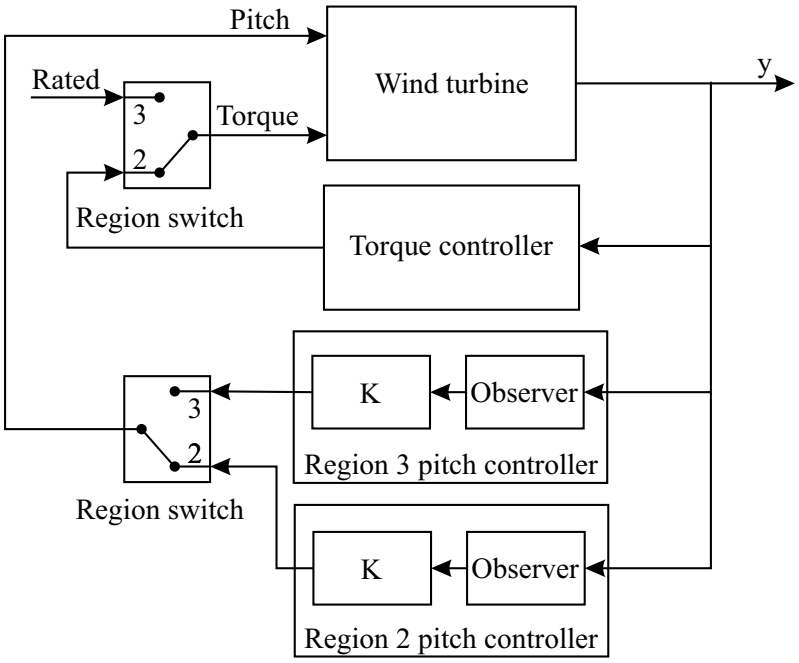

Figure 2.11: MIMO control approach for wind turbines [DNS20]

is minimized, where Q and R are state and control input weighting matrices respectively. The weighting matrices, provide a trade-off between state regulation and control efforts. A typical way to choose suitable weighting matrices is to keep R constant (let say $R = I$) and vary Q. To realize the objective of reducing structural load on blades and tower vibration, the elements of the Q weighting matrix related to blades and tower motions can be tuned. For each attempts, performance measures are applied and compared until the desired values are obtained.

The controller gain is calculated as

$$K = -R^{-1}B^{T}P. \tag{2.17}$$

The matrix P is obtained by solving the Algebraic Riccati Equation (ARE) as

$$AP + PA^{T} + Q - PR^{-1}B^{T}P = 0. \tag{2.18}$$

The controller requires the feedback state values, however some of the states are not always available or expensive to measure. Assuming (2.9) as fully observable, the values of x can be estimated using measured outputs applying an observer as

$$\begin{aligned} \dot{\hat{x}} &= A\hat{x} + Bu + L(y - \hat{y}) \\ \hat{y} &= C\hat{x}, \end{aligned} \tag{2.19}$$

where matrix L denotes the observer gain and can be designed by the same procedure used for controller gain with faster dynamics. Estimated states $\hat{x}$ then used for the controller as feedback information.

From (2.14) and (2.19), changing the feedback states x by the estimated ones $\hat{x}$, the formulation of the observer-based controller can be written as

$$\begin{aligned} \dot{\hat{x}} &= (A - BK - LC)\hat{x} + Ly \\ u &= -K\hat{x}. \end{aligned} \tag{2.20}$$

The dynamics of the overall system including the observer and controller only depend on the matrix K and L. The gain K and L can be designed separately due to the separation principle. However, the observer design may affect the performance of the overall system. Another problem is that the controller is designed based on the linearized model which is only precise near the chosen operation point. However, the operation point defined by the wind speed always varies leading to modeling errors. These errors need to be considered to ensure the system's robustness.

In [PCPB11] and [IHS14] Linear Quadratic Gaussian (LQG) approach is used to calculate an optimal controller for speed regulation and loads alleviation. Model Predictive Control (MPC) is commonly used for load reduction due to the ability to deal with constraints [ECK14]. In [MSPN13] a Light Detection And Ranging (LIDAR) sensor is used to provide wind speed disturbance information in combination with MPC. The effects of wind variation on wind turbines can be mitigated by Disturbance Accommodating Control (DAC). The method uses a predefined disturbance model to estimate the wind speed as unknown disturbances. The blade flapwise bending moment is mitigated while regulating constant rotor speed thanks to the DAC independent pitch controller [WWB17]. To reduce the drive train and tower loads and control the generator speed, in [DCPAE+12] two robust H_∞ controllers are used for torque and pitch control. The simulation results show that the H_∞ controllers provide better performance than classical control approaches. In [YT17] Direct Model Reference Adaptive Control (DMRAC) is proposed to consider the varying wind speed and model uncertainties. The trade-off between generator speed regulation and load mitigation effect can be adjusted by modifying the weighting matrices of the adaptive laws. Both energy capture and fatigue loads are considered in [MSC15], an algorithm to avoid tower resonance operating frequency is developed to mitigate the tower loads. The trade-off between power production and structural loads is considered by designing the parameter of an internal PI controller. In [XLR16] structural loads are taken into account by maximizing power using modified objective function of the Extremum Seeking Control (ESC) method. In general, the wind speed varies with height leading to unbalance forces that each turbine blades have to withstand.

To reduce these asymmetrical loads, Individual Pitch Control (IPC) is widely used [Bos03a, Bos05]. Instead of using collective pitch for all blades, IPC controls each

blade pitch individually. The core idea of IPC is to transform the blades rotating coordinate to a fixed frame by Multi-blade Coordinate Transformation (MBC) methods [Bir08]. Controllers can be designed in the fixed frame by above-mentioned methods, the control outputs then are converted back to rotating coordinate by the inverse transformation to produce individual pitch commands. Among modern control approaches, IPC full-state feedback controls combined with observers are proved to have potential in load reduction by field tests on a real turbine [BFW12].

The main objectives of wind turbine control systems are to maximize the energy extracted from the wind, to minimize structural loads, and to guarantee system safety. The structural loads including blade bending moment and tower bending moment can be reduced by control the blade pitch angles collectively or individually with a proper algorithm. The challenge is while trying to mitigate structural loads by modifying blade angles, the rotor speed will be affected, leading to performance degradation resulting in conflicts between structural loads mitigation and power control. The conflicts differ in different operating regions of wind turbines. When the wind speed is under the rated value which is defined as region 2, the main control goal here is to maximize the generated power. The trade-off needs to be optimized in this region is between energy efficiency and structural loads. To keep the wind turbine operating under safety limits in region 3, the rotor/generator speed is kept constant at the rated value. Now a compromise between speed regulation performance and loads reduction arises. To define an optimal compromise, complete knowledge about various elements affecting control performance is required. In addition, the contribution of each aspect to the addressed conflicting objectives as load mitigation, speed regulation, and energy maximization need to be evaluated by suitable measures.

2.4 Integrated PHM control for wind turbines

System Health Diagnostic and Prognostic (PHM) techniques provide the system State-of-Health (SoH) information and look for variation in system performance. Based on the provided information, suitable actions such as adjusting controllers or maintaining damaged components are realized to help the system working at maximum performance. State-of-health of a system is defined by health indicator variables. For WT applications, accumulated fatigue damage is widely used as a health indicator [AWRF11].

The wind turbine is a complex system, a failure in one of the WT components may lead to un-schedule downtime increasing the Operation and Maintenance (O&M) costs. To avoid an early failure of the system, the design lifetime of the components needs to be ensured. System health diagnostic and prognostic techniques are widely applied to wind turbine operation and control to improve system reliability reducing

O&M cost. Most of the research focuses on condition-based maintenance and fault-tolerant control applications [GDC15, GS18].

To diminish the unplanned costs due to failures, PHM approaches are recently developed for wind turbines to provide the information of turbine SoH and prediction of the Remaining Useful Life (RUL) [EOGA+17]. Using the measured data, maintenance schedules of each component of the turbine and each turbine of the wind farm can be optimized to minimize the overall maintenance cost while guaranteeing the failure probability thresholds [TJWD11]. The maintenance strategy using health condition monitoring is classified as Condition-Based Maintenance (CBM). Diagnostic and prognostic information about the system's health allows making suitable decisions on emergency actions and repairs. Condition-Based Maintenance techniques are adopted to reduce the wind turbine probability of failure thus to reduce the O&M cost [TJWD11]. The main challenge of wind turbine CBM is the uncertain wind makes it is difficult to predict future health degradation behavior [YWPH18]. The complexity in the signal analysis technique for WT PHM also hinders the real-time application of the approach [FC14].

Unscheduled maintenance due to failures can be reduced using Fault-Tolerant Control (FTC) systems to improve the system reliability and survivability [SES10]. The FTC systems are designed to continue the turbine operation at reasonable performance in case of restrictive faults [OSK13]. The effects of faults are accommodated by modifying or switching the related controllers with sacrifices in power production [HHS18]. Real-time monitoring of systems is needed for detection and isolation of faults. Applying FTC allows avoiding the entire turbine failure resulting in total losses of power generation. However, due to the fact that the turbine operates with faulty components, the power output is restricted. Repairs are required to make the system operate with full capacity.

The FTC approach works only when a fault is detected, or the system is already in a faulty condition. To avoid the fault, control strategies need to be adapted with system health indicators before the fault appears. The idea of integrating knowledge about system SoH and predicted RUL into the control loop to adapt the controller targeting system safety and reliability was first introduced in [SR97]. The concept named Safety and Reliability Control Engineering (SRCE) considers the reliability function and lifetime extension of the system by continuously optimizing control strategy based on the information provided by PHM systems (fig. 2.12). With this concept, system reconfiguration decisions are made not only at the faulty conditions but also when changes in the system reliability are detected. The approach allows optimizing the system dynamic behavior and reliability characteristics in the fault-free state.

In [TKG+08], online information from an PHM system is used to adapt the control law to current and future fault and contingency situations with the so-called Prognostics-enhanced Automated Contingency Management (ACM+P) approach.

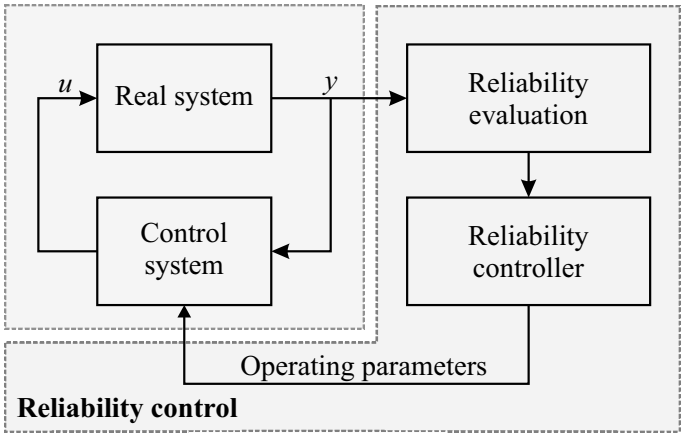

Figure 2.12: Safety and Reliability Control Engineering (SRCE) concept [DS20a]

The system life can be managed by considering future assumptions in control law if performance requirements can be relaxed. The ACM+P system can accommodate faults or mitigate failures using short-term prognosis (with a RUL estimate in terms of minutes or hours in the future) by reconfiguring controllers or/and control objectives accordingly. Similar ideas to consider and control the current and future system SoH are proposed in [EPN12, Kad12] with the related paradigm name Health-Aware Control (HAC). The HAC concept allows adapting controllers before faulty events happen improving the system reliability and providing wider space to optimize the maintenance schedules. The decision-making concerns control objectives, maintenance, and repairs strategies can be integrated into a closed-loop automation concept considering system SoH, safety, reliability, and performance. The system components aging is also monitored allowing situation-based optimal operation of the system depending on the actual degradation level.

There are several reviews on PHM approaches and advanced control for wind turbines [NS16, YTC$^+$14, BS16, HHS18]. The review [NS16] focuses on load mitigation multi-objective control schemes for large-scale wind turbines. The trade-off between power maximization and structural load reduction is pointed out in the paper as an open problem. The authors of [HHS18] provided references about model-based fault detection and fault-tolerant control approaches for WTs to improve reliability. Signal-based methods for WT fault detection are reviewed in [BS16]. The paper gives a detailed description of sensor types and measurement techniques for WT structural health monitoring. An evaluation of the online applicability of the methods is also provided in the review. Commercial aspects of PHM methods are considered in [YTC$^+$14]. The authors review data-mining techniques for WT structural health monitoring used commercially. The cost, advantages, and disadvantages of each approach are also discussed.

The aforementioned reviews only focus on PHM or control, the integration of PHM into the control loop is only briefly discussed. Applying integrated PHM control

(IPHMC) approaches allows the improvement of system reliability and performance ultimately reducing the O&M cost. The approaches require reliable and online SoH monitoring methods. The knowledge about the health degradation characteristics and the relation between system dynamics behavior and health degradation are important to establish optimal control strategies. Most of the research focuses on condition-based maintenance and fault-tolerant control applications [GDC15, GS18]. Recently, the combination of PHM and control applied for non-faulty wind turbines to avoid unwanted failure begins to attract attention. There are several names for this strategy such as contingency control [FGO13] or health aware control [SEPO18], however, the overall idea is the integration of PHM information into control systems to improve performance and reliability of fault-free systems. With the development of digitalization and data-driven techniques, the integration approaches have the potentials to further improve the wind energy system performances. Till now, there was no throughout review on this new research direction for wind energy systems. So it is necessary to generalize and provide the most recent developments in the field for establishing research gaps and challenges.

The existing integrated PHM control (IPHMC) approaches for wind turbines can be briefly classified into two categories: direct damage control [JBBWS15, SEPO18, CCC$^+$19, LFGS20] and reliability adaptive/supervisory control [FGO13, OZZ$^+$13, NBDS19, BNS18].

2.4.1 Direct damage control

Structural load reduction is one of the main objectives of large wind turbine control. Most of the current load mitigation control methods reduce the load indirectly through the reduction of certain norms of measured signals such as stress variations [JBBWS15, LFGS20]. The control performance is evaluated later through measured outputs using some off-line metrics like Root Mean Square (RMS), Power Spectral Density (PSD), or Damage Equivalent Load (DEL) [DNS20]. Direct damage control strategies use on-line PHM modules as virtual sensors providing damage information thus allow to control the damage directly [CCC$^+$19].

Model Predictive Control (MPC) is used in combination with an on-line estimation of the turbine shaft fatigue damage in [JBBWS15]. Fatigue damage is considered as the weakening of materials subjecting to cyclic stress so it can represent the system's health status. In the wind energy control field, fatigue is often reduced indirectly by variation suppression of wind turbine components. Within the IPHMC context, fatigue damage is integrated directly into the control loop as a feedback measurement. The on-line fatigue estimation is based on using a Preisach hysteresis operator. The operator provides similar results as the Fain-Flow Counting (RFC) method, however, the proposed method does not require a large history measurement data so it is more suitable for on-line applications. The estimated damage information is used

to modify the weighting matrix Q adding extra weights to the cost function of the original MPC algorithm. The accumulated damage is reduced without deterioration in output power using the extra health information.

In [SEPO18], a health-aware MPC algorithm for wind turbines is proposed. A linear approximation version of the RFC model for on-line application is used to provide the blade fatigue. The damage linear equation is included in the MPC algorithm state-space model as a new output, an additional objective corresponding to damage is added to the MPC cost function. Depending on the feedback health value and the corresponding weight of the damage reduction objective, the health-aware MPC derates the wind turbine producing less power and accumulated damage. A trade-off between maximizing the extracted power and minimizing the accumulated damage is observed and needs to be optimized.

Nonlinear Model Predictive Control (NMPC) is used in [LFGS20] considering tower fatigue load reduction and energy maximization. The fatigue damage is estimated via an Artificial Neural Network (ANN). The cycle-based fatigue damage obtained from the RFC algorithm is transformed into a time series by calculating the damage for each segment of time. Parameters of the ANN is trained using the obtained damage time series. Eventually, the estimated fatigue damage using ANN is included directly in the cost function of the NMPC controller. The proposed strategy considers the fatigue in closed-loop control thus can directly minimize the fatigue damage.

A virtual fatigue sensor for on-line damage estimation is presented in [CCC+19]. Fatigue sensing is based on the application of the RFC algorithm to a floating window defined in the time domain instead of the whole stress time series. The use of time windows reduces the computational burden of the classic RFC and provides the damage as a function of time. For control integration, the damage function is approximated in the least-squares sense using a recursive ARX model. A sliding mode collective pitch controller with fatigue damage feedback is used in combination with a standard generator torque controller to mitigate the turbine tower damage. The approach is able to reduce the tower damage equivalent load with the exchange of power output reduction.

2.4.2 Reliability supervisory control

Reliability adaptive/supervisory control schemes focus on improvement/control of WT reliability using current and future health status provided by PHM modules. Generally, the approaches have a cascade structure with a primary control loop realizing structural load and power regulation objectives. An adaptive/supervisory control loop reconfigures or modifies the set-point of the primary control loop according to the feed-back health status information for reliability control. Fault-tolerant control is one case of reliability supervisory control for faulty systems. The primary

controller is reconfigured depending on faults detected by health diagnostic algorithms (fig. 2.13). The goal of FTC is to ensure the system's reliability avoiding serious failures that may stop the system. Reliability supervisory control approaches also can apply for non-faulty systems. In this case, the control system reconfiguration is realized before the faults appear. The approaches depend on the observation of health indicators representing system health status and RUL prognostic information.

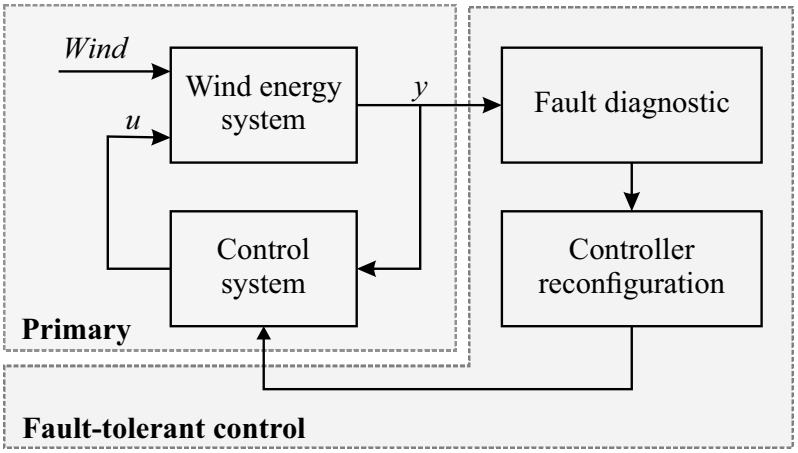

Figure 2.13: Fault-tolerant supervisory control [DS20a]

In [FGO13], a structural health management system is integrated with contingency control to deal with the trade-off between power production and the potential blade damage. The goal is to operate the turbine at a reasonable reduced capacity avoiding extreme damage caused by the blade SoH deterioration and highly turbulent operating conditions. The heath indicator used is the blade stiffness obtained from recorded blade tip deflections through proper models. Base on the provided health information, the contingency controller may de-rate the turbine with a proper value to prevent exceeding some damage threshold resulting in unscheduled downtime. The information about operating conditions defined by measured wind characteristics is also considered in the paper. In the case of highly turbulent wind, the turbine power set-point is smoothly reduced by the contingency controller to ensure system safety and reliability.

A method to control the remaining lifetime of the WT component is proposed in [OZZ+13]. Here the term 'remaining lifetime' denotes the average time until the component fails in the current operating conditions. The remaining lifetime is adjusted so that the WT components can survive to the next maintenance schedule avoiding unwanted repairs. A PHM module is required to determine the health status and estimate the remaining lifetime. The health status indicates the likelihood of failure of the component and is classified by levels using several thresholds. Depending on the health status level and remaining lifetime, the suitable control scheme

regarding different power degradation level is selected to maximize the profit. In the contribution, the health status is obtained from simple measured temperature, vibrations, and stress data, no signal analysis method is given. The remaining lifetime is determined through a function of time that WT spends on each power level, the parameters of RUL function are obtained from the experiment data via regression methods. The authors suggested that the control scheme can be selected automatically or manually based on additional operational requirements. However, there is no guideline for establishing control schemes.

In [NBDS19, BNS18], the optimal trade-off between generation power and lifetime extension is considered. The structural load reduction or lifetime extension level is determined by the observed fatigue damage accumulation. An on-line RFC algorithm is adopted to provide the fatigue damage as the system health indicator. The on-line RFC algorithm considers the extreme values of the measured time series as they occur instead of processes the whole spectrum reducing the computational time and providing instantaneous damage value. Depending on the health status of the turbine components defined by the accumulated fatigue damage, the optimal distribution between power production and structural load mitigation is made. Different MIMO controllers are precomputed with respect to different load mitigation levels defined by different weights. Higher structural load mitigation capacity leads accordingly to lower power production. The controllers are designed by the LQG technique, different levels of load mitigation are realized by tuning the corresponding elements of the LQG weighting matrices. The decision of sacrificing harvested power to improve lifetime is made with support from the structural health monitoring systems. The ultimate goals are to improve system reliability and minimize the overall cost.

The switching between different controllers is triggered by damage accumulation thresholds in [NBDS19]. The aging of the turbine is considered by the damage diagnostic and prognostic model. At first, the power production is maximized without considering load reduction. When the accumulated damage reaches a certain predefined threshold due to system aging and/or failures, the load mitigation controller is activated. The load mitigation level is continuously adjusted depending on the damage level to guarantee the pre-defined turbine service lifetime.

In [BNS18], an additional case of controller selection based on the damage increments or the rate of change in accumulated damage at particular moment information is provided. In this case, when the damage accumulation rate is high due to either strong variation wind or system failures, the load mitigation needs to be high to accommodate the related effects. Otherwise, the controller can ignore load mitigation to maximize power production in the normal working condition. The Remaining Useful Life (RUL) is controlled by switching between different load mitigation levels indirectly regulating the damage accumulation rate. Lifetime control is realized as a secondary control loop affecting the primary load reduction level.

In figure 2.14 the IPHMC concept is summarized. The direct damage/health control approaches consider the accumulated damage or health status of the system as controllable states. The approaches require the real-time and precise calculation of health indicator features which typically can not be measured directly. The dynamics of health degradation or damage accumulation process also need to be suitably modeled for designing controllers. Most of the existing literature in the wind energy field uses fatigue damage as a health indicator. Fatigue damage and fatigue damage dynamics are typically estimated by approximated models of RFC schemes. However, wind energy systems are complex and contain multiple failure modes driven by different mechanisms thus the obtained models might not cover all of the heath degradation characteristics. Data-driven PHM approaches can represent multiple failure modes and degradation stages. However, the actual lack of wind turbine run-to-failure data makes it is difficult to train and validate the models. The complexity and computation time of data-driven approaches are also important aspects that need to be considered for real-time control applications.

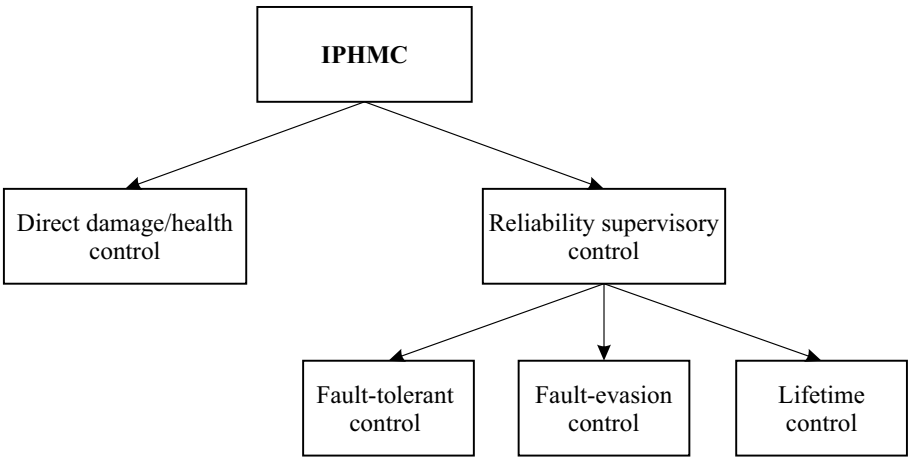

Figure 2.14: IPHMC classification [DS20a]

The real-time requirements of PHM approaches are relaxed in the reliability supervisory control scheme. Due to the much slower dynamics of reliability characteristics compared to that of wind turbines, the time interval of the supervisory control loop is typically chosen higher than that of the primary control loop. Considerations on the relation between control system configurations and reliability characteristics are required in this situation. Faults can be avoided by reconfiguring the primary controller based on the current and future health status information provided by PHM modules.

Lifetime control is possible using the reliability supervisory control scheme as mentioned in [OZZ+13]. The remaining useful life of each component can be regulated to reach the next maintain schedules avoiding unscheduled repairs. However, no method is provided yet in [OZZ+13]. In [NBDS19, BNS18] the RUL is controlled

indirectly using damage accumulation thresholds. The required lifetime might not be guaranteed due to the lack of RUL feedback.

2.5 Open research problems

From the previous review, some open problems of advanced wind turbine control can be detected:

(i) Wind turbines are complex systems having many relevant variables hard or expensive to be measured. To obtain the value of unmeasured outputs for control purposes, observers are commonly used. Although the observer design does not affect system stability, it can introduce variations in control performance. For fast convergence and precise estimation, high observer gain is required, however, it makes the observer more sensitive to noise and model errors.

(ii) The varying and unknown wind significantly affects wind turbine performances. To mitigate the effects of wind disturbance, wind speed can be estimated using disturbance observer techniques or measured using LIDAR. However, it is a challenge to define a suitable disturbance rejection controller to guarantee system stability and totally cancel the wind disturbance effects.

(iii) It can be observed that most of the existing solutions face the problem of modeling errors due to the use of linearized and reduced-order models. The aerodynamics of wind turbines are nonlinear in nature, the control input gains vary with blade pitch angle, rotor speed, and wind speed. When the turbines operate at continuous changing wind speed, the gains may defer from that of the linear model used for control design leading to poor performance or even unstable closed-loop behavior.

(iv) Load mitigation approaches for WTs not only reduce the structural load but also affect the rotor speed regulation performance leading to power production performance degradation. This conflict between structural loads mitigation and power control need to optimize depends on operation situation to minimize the cost.

(v) Prognostics and health management techniques can be used in combination with load mitigation control approaches to improve performance and reliability. The main challenge of the combination approaches is the requirement of reliable and simple enough on-line PHM methods. The methods need to handle various loading operating conditions and multiple failure modes driven by different mechanisms. The relations between control system configurations and health degradation dynamics are needed for establishing the supervisory control loop. Due to various loading conditions and multiple degradation

states, situation-based multiple models may be needed to fully represent the relations.

In the next sections, a robust disturbance accommodation control approach is developed to reduce structural load while maximizing power production. Several performance measures are presented to evaluate the proposed approach. A lifetime control scheme based on the IPHM concept and the proposed load mitigation controller is developed to improve system reliability and optimize the trade-off between power and load reduction.

3 The need of performance evaluation and requirements for control-oriented PHM

The figures, tables, and content in this chapter are partly based on the journal paper [DNS20].

The main objectives of wind turbine control systems are to maximize the energy extracted from the wind, to minimize structural loads, and to guarantee system safety. The structural loads including blade bending moment and tower bending moment can be reduced by control the blade pitch angles collectively or individually with a proper algorithm. The challenge is while trying to mitigate structural loads by modifying blade angles, the rotor speed will be affected, leading to performance degradation resulting in conflicts between structural loads mitigation and power control. The conflicts differ in different operating regions of wind turbines. When the wind speed is under the rated value which is defined as region 2, the main control goal here is to maximize the generated power. The trade-off needs to be optimized in this region is between energy efficiency and structural loads. To keep the wind turbine operating under safety limits in region 3, the rotor/generator speed is kept constant at the rated value. In this region, a conflict between speed regulation performance and loads reduction arises. To define an optimal compromise, complete knowledge about various elements affecting control performance is required. In addition, the contribution of each aspect to the addressed conflicting objectives as load mitigation, speed regulation, and energy maximization need to be evaluated by suitable measures.

In the mentioned literature, to evaluate and compare the load mitigation performances of control algorithms for wind turbines, Power Spectral Density (PSD) [NK03] based on Fourier Transform and Damage Equivalent Load (DEL) [Hay12] based on fatigue damage are commonly used. The methods use time-series historical data of blades and tower bending moment to calculate the strength of structural loads that the wind turbine has to withstand. The metric PSD analysis can calculate the strength of blades or tower variation at certain frequencies which can generally describe the structural loads. On the other hand, DEL relates the cumulative fatigue damage representing the structural loads over a period of time. The metrics PSD and DEL only consider loads without referring to other goals, and the relationship between them makes it difficult to evaluate the overall performance including power production or rotor speed regulation criteria. The mentioned metrics need to be used in combination with other performance metrics to assess and design multi-objective controllers for wind turbines.

This section proposes novel measures based on time-series historical data obtained from wind turbines, such as blades/tower bending moments and rotor/generator speed, and the covariance of the data to assess the overall control performance of a wind turbine. The proposed measures can represent multi control performances in

a graph avoiding using separate metrics in designing controllers. A new parameter defines the relation between control goals is introduced, which introduces a new measure for controller assessment and design. The measures are able to express multi control objectives graphically and also in combination with related mathematical values. These illustrations give control engineers and control designers quantitative and qualitative insights into control performance criteria, enabling designers to modify control parameters to reach desired results. The usages of the new measures are illustrated by comparing and tuning two commonly applied control approaches for wind turbines, PI and MIMO observer-based state feedback controllers. The proposed measure is used to assess the control performance of the different approaches. As an example, standard approaches introduced in chapter 2 are used for illustration. Results for wind speed region 2, region 3, wind turbulence effects, and control parameters effects is realized for the application demonstration.

System reliability and health status are important metrics for WT advanced control approaches. The PHM methods are developed to calculate the health status and estimate the remaining useful life of wind turbine components as well as reliability. The obtained information is used for optimal operation, maintenance, and control of wind energy systems. PHM modules can be integrated into the control loop to improve system reliability and performance ultimately reducing the O&M cost. The knowledge about the health degradation characteristics and the relation between system dynamics behavior and health degradation is important to establish optimal control strategies. The integration approaches require reliable and online SoH monitoring methods, thus requirements of PHM and control approaches for the combination are also reviewed and discussed in this section.

3.1 Power spectral density

Power spectral density analysis is a type of frequency-domain analysis methods describing the distribution of power or the strength of variation into frequency components [NK03]. In other words, PSDs show the strength of variation at certain frequencies.

For load analysis of wind turbines, PSDs are often used to determine blade and tower variation power at rotor frequency (1P - one-per-revolution) and multiples of rotor frequency (2P, 3P, and so on) which correspond to structural loads.

To obtain PSDs, time series data of tower and blades variation are transformed to frequency domain by truncated Fourier Transform over a finite interval T as

$$x(\omega) = \frac{1}{\sqrt{T}} \int_0^T x(t) e^{-i\omega t} dt. \tag{3.1}$$

The power spectral density or power spectrum is calculated as

$$P(\omega) = \lim_{T\to\infty} E[|x(\omega)|^2], \tag{3.2}$$

where E denotes the expected value [GS01].

3.2 Fatigue damage

Wind turbine components are subjected to variable mechanical stresses due to variability of wind speed leading to gradual degradation of individual components. In the field of wind energy, fatigue damage is widely used to assess health status wind turbines and is recommended by the IEC 61400-1 standard [IEC05]. Fatigue is the weakening of a material due to cyclically applied loads which are beyond certain thresholds [Sch96]. Accumulated fatigue damage can express the aging of the system thus providing helpful information for optimizing the health degradation behavior. Because the fatigue damage generally can not be measured directly, methods to calculate the accumulated fatigue damage are needed. Fatigue calculation methods suitable for wind turbine control are introduced in the next section.

3.2.1 Rain flow counting

For certain materials, the relation between the number of cycles to failure with the stress level or cycle amplitude was established. This relation can be represented by the stress-cycle (S-N) curve. The S-N curves are typically derived from experiments on samples of the material. For a given stress history, assuming there are k different load amplitude levels, namely $S_i, (1 \leq i \leq k)$, each level S_i appear in n_i cycles, and the number of cycles to failure at the stress level S_i is N_i defined by the S-N curve. The damage accumulation D_{ac} can be calculated using Miner's rule as

$$D_{ac} = \sum_{i=1}^{k} D_i = \sum_{i=1}^{k} \frac{n_i(S_i)}{N_i(S_i)}, \tag{3.3}$$

with D_i denotes contributed damage of stress level S_i and D_{ac} denotes accumulated damage over the whole time history. In general, when the damage accumulation D_{ac} reaches a defined limit ≥ 1, the system is considered as failed.

To define stress levels and the number of cycles of each level, the rain flow counting (RFC) algorithm is used. The algorithm transforms a spectrum of varying stress levels to a set of simple stress range allowing the application of Miner's rule (fig. 3.1).

The RFC algorithm is widely used to calculate the fatigue damage with the highest accuracy regarding complex loading [BBW16]. However, the standard form of RFC

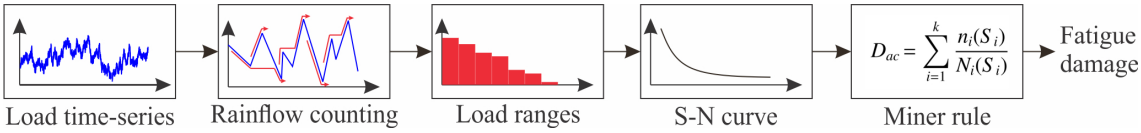

Figure 3.1: Fatigue calculation using RFC and Miner rule [DS20a]

is computationally expensive due to the requirement of the whole load history. The RFC method is a procedure rather than a mathematical function [BBW16, LFGS20]. The relation between fatigue damage and the measured stress obtained from the RFC algorithm is typically nonlinear and difficult to compute the gradient.

To reduce the computational and memory load, the RFC method can be realized on a floating time window rather than the whole time history [CCC+19, LFGS20]. An online RFC algorithm is proposed in [MJ12]. Instead of tracking the complete time history data, the algorithm store and processes extremal value (minimum and maximum) simultaneously as they occur to provide the equivalent full and half cycles.

To justify the damage in a period of time, damage equivalent load (DEL), which is a constant-amplitude fatigue-load defining the equivalent damage as the variable spectrum of loads [Hay12], can be calculated as

$$DEL = (\frac{\sum_i n_i S_i^m}{N})\frac{1}{m}, \tag{3.4}$$

where N denotes total equivalent fatigue counts, m the Wöhler exponent, both are defined by experiments.

3.2.2 RFC approximation

As mentioned in [BBW16], RFC algorithm is widely used and has an active standard [AST17]. However, the approach is nonlinear and hard to calculate its gradients make it is difficult to apply the approach directly for control. Typically for control integration, the RFC algorithm is approximated using mathematical models.

In [SEPO18], the RFC algorithm is approximated using a linear model establishing the relation between the generator torque T_g, system states ω_r, disturbance v_w with the damage z of the blade

$$\begin{aligned} z(k) &= \frac{m}{L}(a_0 + a_1\frac{\partial P_g}{\partial \omega_r}\omega_r(k) + a_1\frac{\partial P_g}{\partial T_g}T_g(k) + a_2 v_w(k)) \\ Z_{acc}(k+1) &= Z_{acc}(k) + z(k), \end{aligned} \tag{3.5}$$

here Z_{acc} denotes the accumulated damage, P_g the generator power output, L the number of samples per cycle, and m the slope of the accumulated damage curve. The

model parameters a_0, a_1, and a_2 are obtained using least square algorithm using the results from RFC. Figure (3.2) shows the comparison between the fatigue damage calculated from RFC and the approximated model.

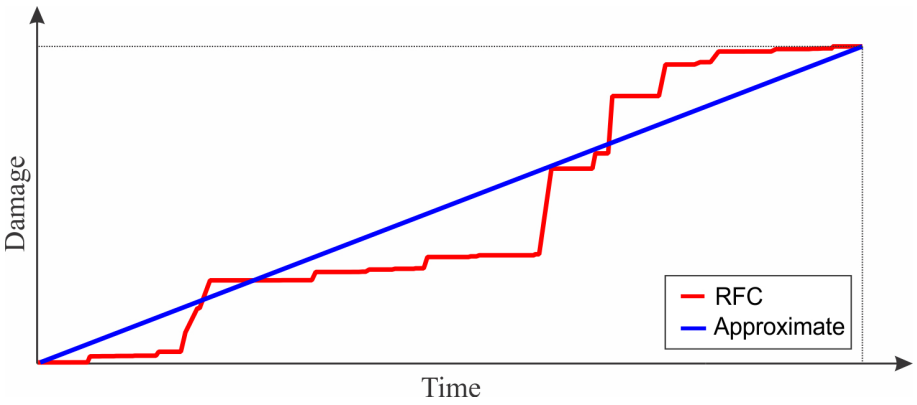

Figure 3.2: Linear approximation of RFC algorithm [DS20a]

A recursive ARX model is used in [CCC+19] to approximate the relationship between the tower damage equivalent load (DEL) and the tower top velocity. Damage equivalent load, which is a constant-amplitude fatigue-load defining the equivalent damage as the variable spectrum of loads [Hay12], can be calculated using the results of the RFC algorithm. The approximated model is used as a damage sensor for a sliding mode controller to reduce the fatigue damage of the turbine tower.

In [LFGS20], a nonlinear autoregressive networks with exogenous inputs (NARX) artificial neural network (ANN) is for the function approximation. The tower fatigue damage is calculated from the stress time series using RFC for different wind speeds. The obtained stress and damage data is used for training and testing of the ANN. Several ANNs with a different number of neurons are considered. The results show that ANNs can approximate the RFC algorithm with high accuracy. The number of neurons required is low thus integration of the model does not increase much the computational time.

3.3 Prognostic of remaining useful life

Remaining Useful Life (RUL) is a mandatory information for optimal operation and maintenance of wind energy systems. Based on the RUL information, suitable maintenance and control strategies can be chosen to reduce the O&M cost and improve system reliability. Remaining useful life estimation methods are broad and can be classified considering different aspects. Roughly, wind turbine RUL estimation methods are grouped as model-based, data-based, and hybrid approaches [WW14, DBS18].

Model-based methods aim to establish physical or mathematical degradation models to represent the correlation between input signals and RUL. The models are built based on the knowledge about the mechanisms leading to failure such as wear, fatigue damage, crack growth [AL14]. Wind turbines contain multiple failure modes driven by different mechanisms thus it is difficult to establish a model covering all of the modes. Typically, only dominated phenomena are considered. For wind turbine applications, the most common model-based method is the fatigue life prediction based on the S-N curve and Palmgren-Miner rule [WW14]. The accumulated fatigue damage D_k of a component at the time T_k can be calculated from historical measured data using (3.3). When the accumulated damage reaches a predefined limit D_f, the component is considered as failed. Assuming that the wind turbine operates in the same conditions in the future, the time to failure L_f is estimated as

$$L_f = \frac{T_k}{D_k} D_f. \tag{3.6}$$

The estimated RUL is calculated as

$$RUL = L_f - T_k = T_k(\frac{D_f}{D_k} - 1). \tag{3.7}$$

Data-based or data-driven approaches depend on measured data, detailed knowledge about system physics is not required. The methods establish the correlation between RUL and physical signals by learning from stored data. Multiple failure modes can be presented without knowledge about the failure mechanisms behind, however, great efforts need to be put into obtained and process failure data. The quantity and quality of data greatly affect the prediction accuracy [AL14]. Typically, raw data from measurement systems need to be processed using noise reduction and feature extraction techniques before using for training the data-driven models.

Artificial Neural Networks (ANN) are used to model the normal behavior of wind turbine gearboxes in [GSBDP06]. Possible anomalies or faults can be detected according to the difference between the real measured output and estimated output from the models. The time remaining still the failure or remaining useful life is predicted using another ANN model. The prediction ANN model represents the dynamics of the difference between real and estimated data (residual) of a historical failure case. The residual dynamics of the system can be predicted using the ANN residual model and current gearbox life status. The remaining useful life can be predicted if the failure can be detected by the ANN normal behavior model.

In [ESLM19], a regression model and ANN are combined to model the relationship between wind turbine bearing variations and health status. The regression model provides the bearing degradation information through the root mean square of vibration signals. The results from the regression model are used to improve the ANN

RUL prediction. The combined model shows better accuracy than the single ANN model.

Stochastic data-driven models based on probability and statistical theory such as Bayesian networks, Markov process, or Levy processes are also used for fault detection and RUL estimation of wind turbines [WW14]. The methods consider deterioration behavior as random processes and provide RUL prediction results as probabilities [LSFB+13]. Stochastic methods can deal with uncertainties in measurements and parameters, however, they require the observation of health or degradation indicators. Based on the data, the most fit stochastic model needs to be chosen for good predictions [WW14]. The authors of [CQZ+18] use an interval whitenization Gaussian process (IWGP) to estimate RUL of wind turbine bearings. The effects of the non-stationary operation of wind turbines on health indicators are reduced using the interval whitenization methods. The RUL prediction model is established using the processed health indicators and Gaussian process.

A model-based and data-based hybrid approach for WT RUL prediction is proposed in [DBS18]. The method applies a physical-based approach to model the normal and faulty operation behavior of the system. The obtained models are used for generating related normal and faulty data. A data-based clustering algorithm is used to separated the simulated data into clusters representing normal operation and different failure scenarios states. An on-line monitoring system continuously measures data from the real system to identify and calculate the Euclidean distance between the current operation cluster and identified clusters from the previous off-line step (fig. 3.3). When the degradation process begins, the current cluster of the real system will move toward a faulty cluster. The distance and the degradation speed to the faulty cluster are used to calculate the related RUL.

Wind turbines are complex systems operating in non-stationary conditions due to varying wind speeds. Wind turbine components also are affected by various fault mechanisms. These make it is difficult to estimate accurately the RUL of WT components. Generally, several approaches are combined to deal with WT prognostics and diagnostics challenges such as non-stationary operating conditions, the lack of labeled data, or multi states degradation. These combinations often require complex computation thus limit on-line applications [FC14, YWPH18]. For integrated PHM control, the problem becomes more severe due to the requirement of quick reactions against the change in health status and health degradation behaviors. So the development of accurate and simple enough diagnostic and prognostic methods is crucial for the applicability of the IPHM strategy.

3.4 New covariance distribution diagram measure

Existing measures for structural loads mentioned above only consider loads without referring to the relationship between loads and other control performance aspects

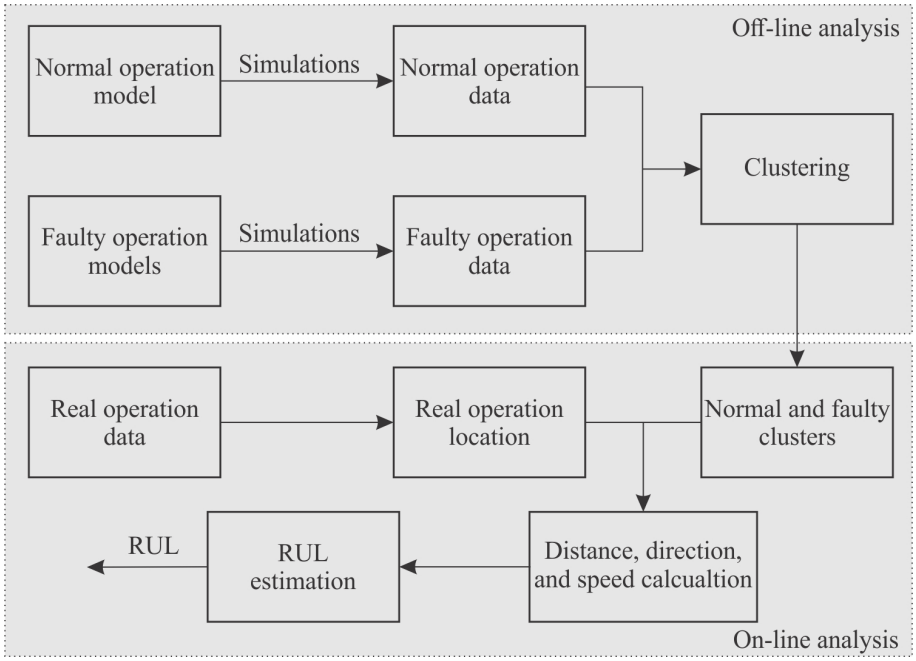

Figure 3.3: Hybrid RUL prognosis [DS20a]

such as the power regulation or the power extracted. To illustrate exactly this relationship, this contribution proposed to place structural loads and generator power together in a covariance distribution diagram (fig. 3.4) as a base to form new measures.

For the uniform between region 2 and region 3, the power regulation is use to represent the speed regulation, since the power is proportional to the speed when the torque is constant. In fig. 3.4, for a given load profile each point represents the instantaneous values at a sample time of the bending moment of the tower (structure load) and the generated power related to a certain wind speed applying a specific control structure and parameter set combination. Thus for given wind profile and a control system, an unique distribution can be obtained. The behaviors can be clearly distinguished and characterized by the area, density, and 2D-width of related distributions (here: MIMO controller: blue; PI-controller: red).

To describe the related characteristics of the controllers more clearly, the covariance matrix of the relevant structural loads damage data D and generator power data P has to be calculated. Based on the covariance matrix, ellipse iso-contours are determined for controllers. Each ellipse is characterized by the center point m, the angles between the ellipse axes and the coordinate axes α, and the widths in both directions σ_x, σ_y. These variables can be used as performance measures namely CS_x (CS is the acronym for controller sensitivity) for wind turbine control system. The ellipse then is scaled by a factor determined by the Chi-square probabilities table (3.11). The higher scale factor, the bigger ellipse containing more data points. In

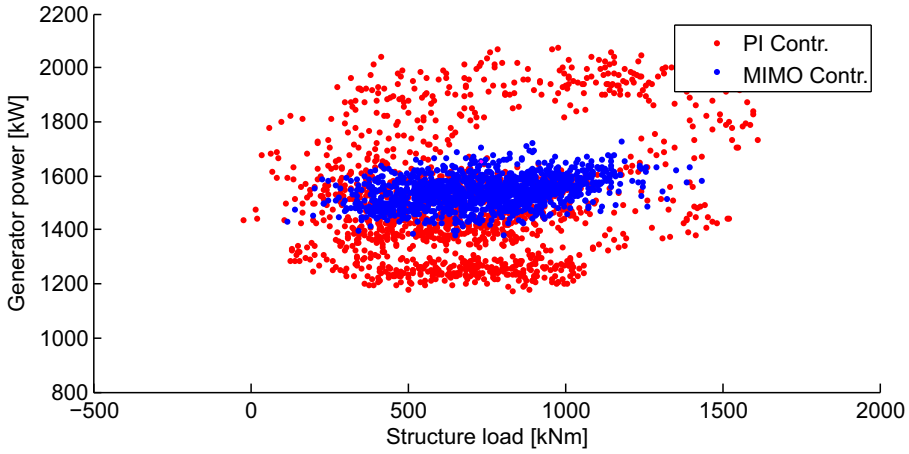

Figure 3.4: Comparison of load and power contributions (red: PI, blue: MIMO controller) [DNS20]

this paper, the scale factor is chosen to defining the ellipse containing 95 % of all data (fig. 3.5).

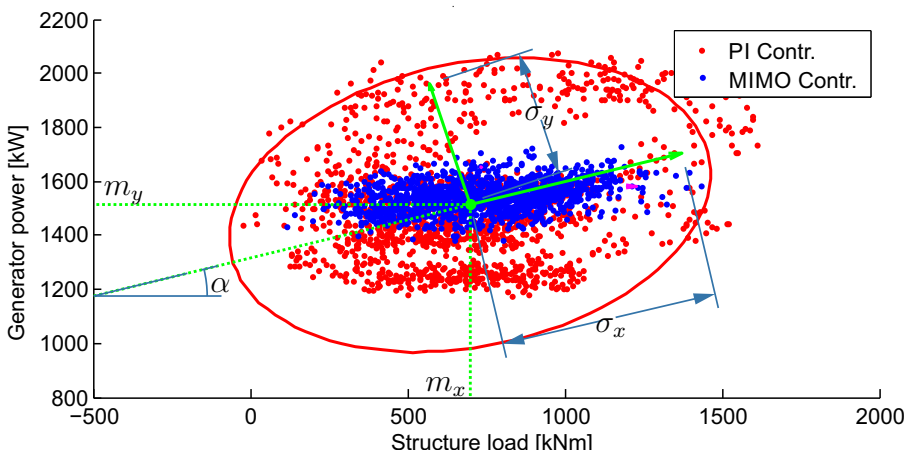

Figure 3.5: Illustration of the introduced measures CS_{1-5} applied to the result of PI controller [DNS20]

The center points are determined by the average value of the load variations m_x (CS_3) and the generated power m_y (CS_4). The average load m_x is expected to be low. The higher m_y is better in wind speed region 2 since it indicates that more power is produced. However, in wind speed region 3, the control goal is to keep generated power constant at rated value, so m_y is expected to be close to the set-point.

The angle α ($0 \leq \alpha \leq 90$) denotes the relationship between the loads and power, if the ellipse axes and the coordinate axes are aligned or the angle α equals to zero

or 90^o, the structural loads and generated power are uncorrelated. To illustrate the correlation level of the data, the newly measure CS_5 can be defined as

$$CS_5 = min(\alpha, 90 - \alpha). \tag{3.8}$$

Higher value of CS_5 defines that higher power production will be connected with higher structural loads, so CS_5 are considered as a measure for the sensitivity of controllers (controller sensitivity - CS). The lower the value of CS_5 is the better due to the related controller introduces lower additional structural loads; it can produce more power without increasing the loads.

The magnitudes σ of the ellipse axes define the variance of the data. The value of σ_x (CS_1) represents the strength of structural load variation, so the control goal for both wind speed regions is to keep σ_x as small as possible. In wind speed region 2, power production related to σ_y (CS_2) and m_y (CS_4), higher σ_y and m_y means more power is produced. Typical control strategy for region 2 is using an additional loads reduction control loop with the baseline controller. The loads reduction controller only modifies the pitch angles around the optimal value to mitigate loads, so the mean generated power m_y is nearly the same as the baseline case (see chapter 2). On the other hand, in wind speed region 3, generated power is regulated to rated value, so σ_y need to be small in this region.

In table 3.1, the proposed measures are summarized. The list of proposed measures is given in the first column with the corresponding variables given in the second column. The next two columns represent the application of proposed measures in region 2 and region 3. In each region, the '+' sign denotes the higher of the corresponding measure, the better the performance. The '-' sign denotes the lower value of the measure is better.

Table 3.1: New measures summary [DNS20]

CS measures	Variables	Region 2	Region 3
CS_1	σ_x	-	-
CS_2	σ_y	+	-
CS_3	m_x	-	-
CS_4	m_y	+	NA
CS_5	α	-	-

Note:		
	+	Higher is better
	-	Lower is better
	NA	Not defined

Based on the ellipses representing the results of each controller, control performance information include structural load levels, generator power, and the relationship

between loads and power is extracted and compared. This allows to justify the effectiveness of different control approaches, as well as to give criteria for tuning the control parameters.

The covariance of the two variable vectors X and Y are defined as

$$cv(X,Y) = \frac{1}{N-1}\sum_{i=1}^{N}(X_i - m_x) * (Y_i - m_y), \tag{3.9}$$

here m_x and m_y denote the mean of X and Y, $*$ denotes the complex conjugate. The covariance matrix of X and Y is calculated as

$$C = \begin{bmatrix} cv(X,X) & cv(X,Y) \\ cv(Y,X) & cv(Y,Y) \end{bmatrix}. \tag{3.10}$$

Using the covariance matrix, the ellipse equation is formulated as

$$\left(\frac{x}{\sigma_x}\right)^2 + \left(\frac{y}{\sigma_y}\right)^2 = s, \tag{3.11}$$

here s denotes the scale factor of the ellipse determined by the Chi-square probabilities table (95 % confidence level corresponds to $s = 5.99$), σ_x and σ_y are standard deviations of structural load and generator power data, which are related to the eigenvalues λ of the covariance matrix C as

$$CS_{1/2} = \sigma_i = \sqrt{\lambda_i}, \tag{3.12}$$

$$det(C - \lambda I) = 0. \tag{3.13}$$

The ellipse is centered at the mean values of data (m_x, m_y), and rotated around the X-axis an angle α equal to the angle of the largest eigenvector v_{max} of C towards the X-axis

$$\alpha = arctan\frac{v_{max}(y)}{v_{max}(x)}. \tag{3.14}$$

As example in fig. 3.6 and table 3.2 the results comparison of the PI and MIMO controllers for wind speed region 3 are given. In wind speed region 3, the rotor speed is regulated to the design rated value to avoid too high mechanical stresses by governing the blade angles, while the generator torque is held constant. It can be obtained that MIMO controller has much better speed regulation performance than classical PI controller (79 % smaller CS_2 or generator speed variation). In addition, by applying full state feedback controller, the structural loads (tower bending

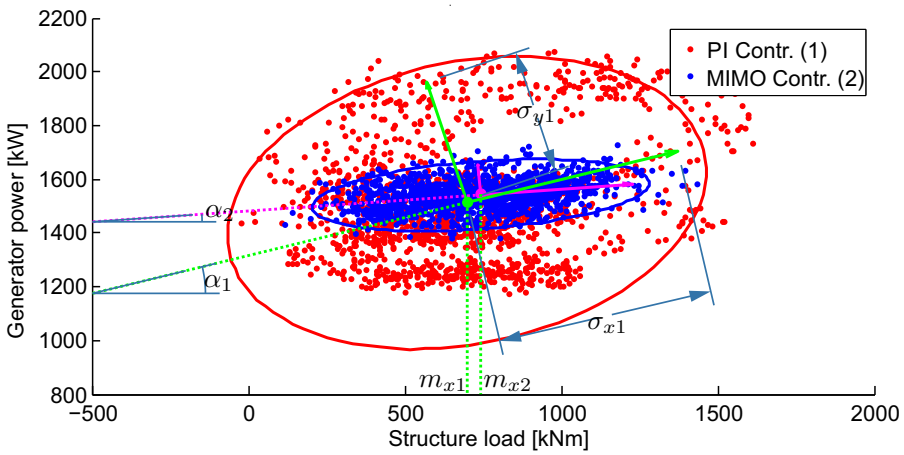

Figure 3.6: Illustration of the introduced measures CS_{1-5} applied to the results of two controllers (red: PI, blue: MIMO) [DNS20]

Table 3.2: PI and MIMO controller comparison [DNS20]

CS measures	CS_1	CS_2	CS_3	CS_4	CS_5
Variables	σ_x	σ_y	m_x	m_y	α
PI (1)	328	218	697	1512	17
MIMO (2)	238	46	744	1540	5

Note: Better results

moment) that the turbine has to withstand also reduce by 27 % indicated by reduction in CS_1, the correlation between structural loads and generated power also be reduced (smaller orientation angle CS_5).

For comparison with the new measures, the tower DELs of both controllers are calculated (fig. 3.7) using Mlife [Hay12]. The results show that by using the MIMO controller, the tower DEL reduce by 29 % which is a good agreement with the results of the new measures. However, in the DEL metric, only structural load is considered, no information regarding the speed regulation performance and the correlation is provided.

It can be easily observed from the new measures graphically represented in fig. 3.6 that the MIMO controller has advantages over the PI controller with respect to both objectives, rotor speed regulation and structural loads mitigation. In the new measures, CS_{1-4} define a generalized representation of commonly used load amplitude measure for load analysis, CS_5 is completely new and introduces an additional measure for controller assessment and design. All new measures are visualized graphically in one figure, it is convenient for designers to assess and compare the performances of each controllers.

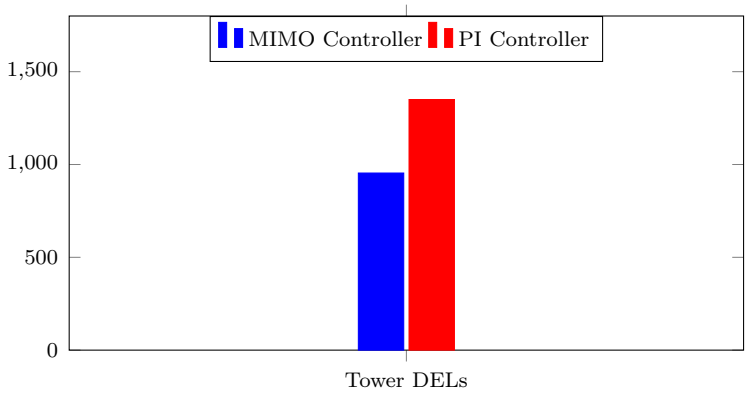

Figure 3.7: Damage equivalent loads [DNS20]

3.4.1 Illustrative examples

The proposed measures are applied to compare PI and MIMO controller in both wind speed regions 2 and 3 to illustrate the ability of performance evaluation using the measures introduced. The normal power production design load case DLC 1.2 for fatigue according to the IEC 61400-1 standard is used [IEC05]. The results are obtained using FAST code with the wind turbine model and standard control methods described in chapter 2.

Turbulence wind profiles used for simulation are generated using IEC von Karman wind turbulence model by TurbSim [JBJ09]. The wind has a mean value of 8 m/s for region 2 and 18 m/s for region 3 simulation, the linear vertical wind shear power law exponent is 0.2. The turbulence intensity of the wind is chosen as 12 % corresponding to standard IEC category C. Three different random seeds are used for each wind profiles to analyze the fatigue loads which are the tower bending moments of the turbine.

Wind turbulence level effects

To study the effects of wind turbulence level on the control performances using the new measures, two wind profiles with different turbulence intensity of 12 % (IEC type C) and 17 % (IEC type A) are used in comparison with the same controller (fig. 3.8).

The results are obtained for both wind profiles with MIMO controller. From fig. 3.9 it can be observed that the representative ellipses have identical center points and angles shown by the same value of CS_3, CS_4, and CS_5. This means the change in the turbulence level of wind profiles does not affect the correlation between structural loads and generated power when using the same controller. The variation in generated power and loads indicated by CS_2 and CS_1, in the other hand, increase about

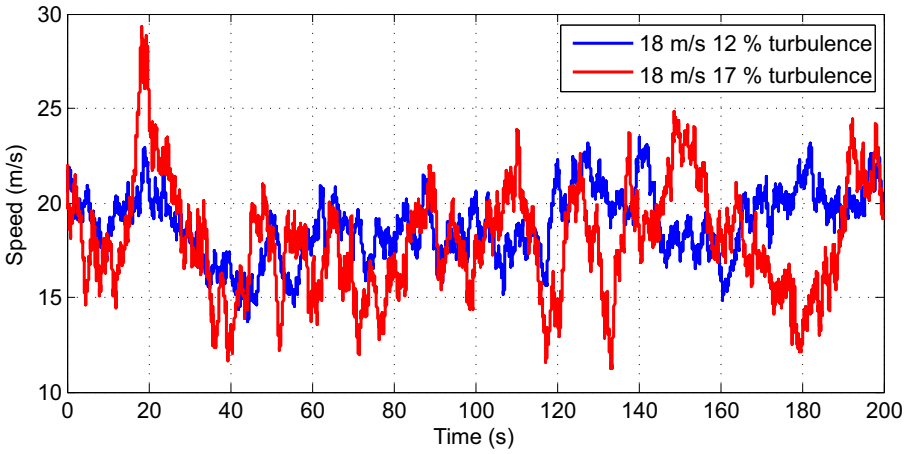

Figure 3.8: Hub height wind profiles with the same mean speed and different turbulence levels [DNS20]

25 % when the wind turbulence level raises from 12 % to 17 %. Each controller is characterized by the relation between loads and power produced or the angles between corresponding ellipse axes and coordinate axes. The control performance levels depend on both control approach and wind characteristics.

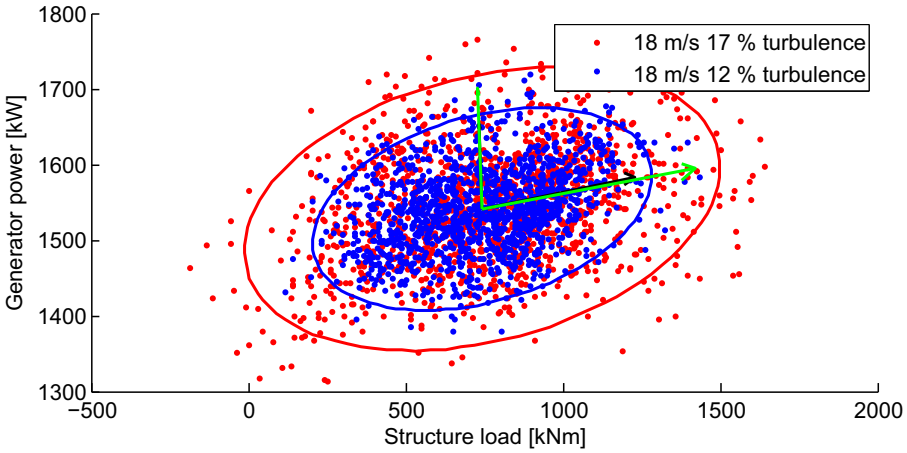

Figure 3.9: Illustration of the effects of the wind turbulence level on control performances using new measures [DNS20]

Wind speed region 2

In wind speed region 2 which is below rated speed, the control objectives are to maximize extracted power from the wind while keeping the structural loads smallest possible. Typically, the control design goals are realized by a torque controller

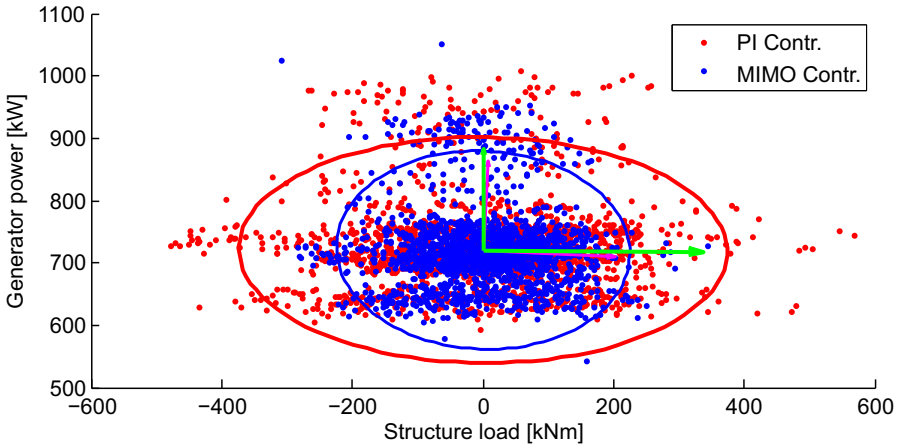

Figure 3.10: Comparison performances of two controllers in wind speed region 2 using new measures [DNS20]

to govern the rotor speed to reach optimal value depending on wind speed. The blade angles are kept constant at a predefined optimal value. To better mitigate structural loads, a MIMO controller is used combined with existing torque controller to add damping into the blades and tower bending modes. The additive controller modifies the blade angles around optimal value to reduce the blades and tower variations. The modification may affect the overall optimum tip-speed-ratio thus reducing the extracted power, however the mean values of loads (m_x) and power (m_y) are remained the same. This trade-off is shown in fig. 3.10. The magnitude of the ellipse in vertical direction represent variations of generator power, and in horizontal direction represent those related to structural loads. From the simulation results in fig 3.10, a reduction of 32 % in structural load (CS_1) exchange for 10 % decrease in power production (CS_2) can be observed. It is also can be detected that the produced loads and power are uncorrelated in this scenario for both control approaches due to CS_5 equal to zero.

Wind speed region 3

In wind speed region 3 which is above rated speed, the rotor speed is regulated to the design rated value by the PI controller to avoid mechanical stress larger than that designed by governing the blade angles, while the generator torque is held constant. In this situation, the MIMO controller has much better speed regulation performance than classical PI controller (80 % smaller CS_2 rotor speed variation) (fig. 3.11). In addition, by applying the MIMO controller, the structural loads that the turbine has to withstand are also reduced by 27 % indicated by reduction in CS_1.

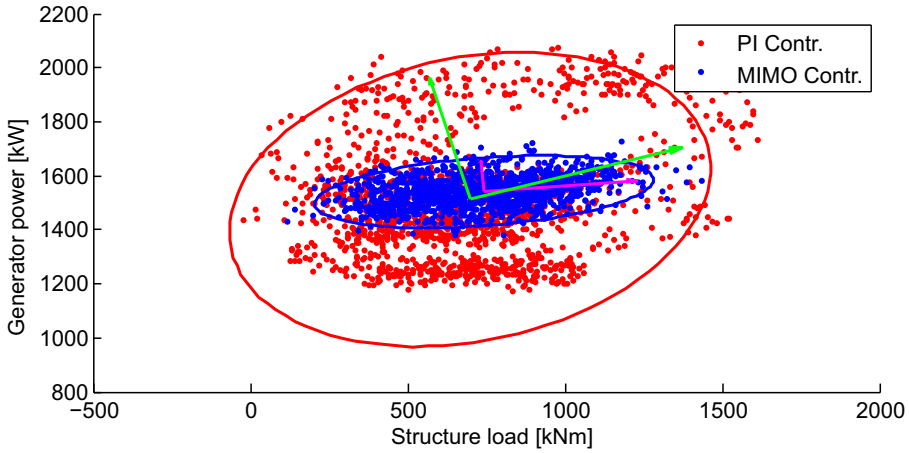

Figure 3.11: Comparison performances of two controllers in wind speed region 3 using new measures [DNS20]

Controller parameter design

For an illustration of using the new measures for designing controller in wind speed region 3, the weighting matrix Q of the MIMO controller is tuned and compared to determine the best parameters. For example, three combinations of controller parameters are used. The element of the weighting matrix Q corresponding to the rotor speed regulation performance is chosen constantly at 5, the element corresponding to structural load (in this case is blade bending moments) is varied at increasing values 10, 15, and 20. So three combinations of weightings are 5-10, 5-15, and 5-20.

The results are shown in fig. 3.12 and table 3.3. It can be seen that CS_3, CS_4, and CS_5 do not change when varying Q, which means that the correlation between structural loads and power production remain the same for all combinations. However, CS_1 and CS_2, representing structural load mitigation and rotor speed regulation performances, are changing depending on the value of the weighting matrix Q. By increasing the coefficient from 10 to 15, CS_1 and CS_2 decrease, the control performance for both criteria are improved. When continuously increase the coefficient from 15 to 20, CS_1 increases, the load mitigation performance is reduced while CS_2 nearly unchanged. It can be observed from the new measures that the best parameter combination for the MIMO controller in this situation is 5-15.

3.4.2 Conclusions

In this section, new measures are introduced to characterize and therefore also to compare control approaches applied to wind turbine control systems. The measures are able to describe the different and conflicting control goals of wind turbines

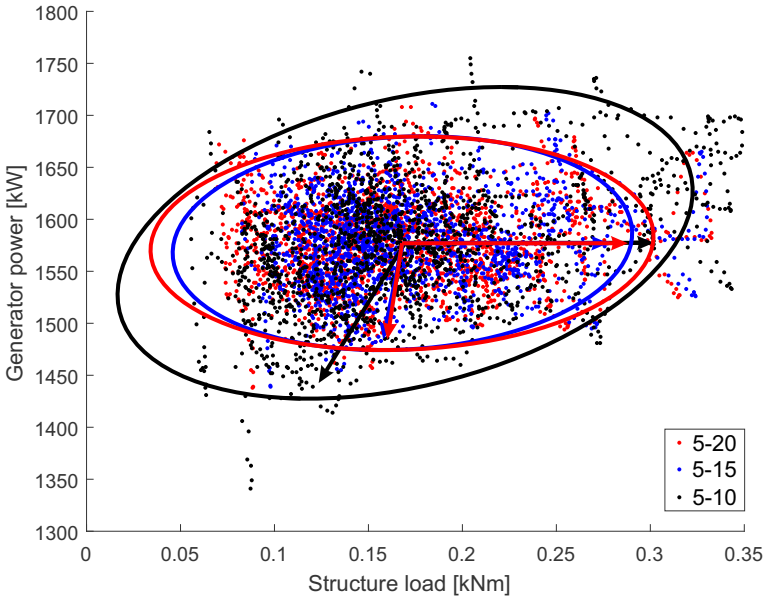

Figure 3.12: Comparison results of a MIMO controller with different weightings (5-20, 5-15, and 5-10) using new measures [DNS20]

Table 3.3: Comparison results of a MIMO controller with different weightings (5-20, 5-15, and 5-10) using new measures [DNS20]

CS measures	CS_1	CS_2	CS_3	CS_4	CS_5
Variables	σ_x	σ_y	m_x	m_y	α
5-20	0.134	102.7	0.168	1577	1.57
5-15	0.122	102.8	0.168	1577	1.57
5-10	0.144	149.9	0.169	1577	1.57

by graphical and numerical representations. Five measures are introduced, CS_1 denotes the strength of force variation representing structural loads, CS_2 denotes power variation representing power production in region 2 and the accuracy of power regulation in region 3, CS_3 and CS_4 denote the mean values of loads and generated power, finally CS_5 denotes the relationship between loads and power as a measure for the sensitivity of controllers. All measures are visualized graphically in one figure providing quick evaluation and comparison of control performances.

As illustrative examples, two different controllers are applied to express the measure options introduced. Now for the first time, it is possible to qualify control approaches regarding both conflict goals structural load reduction and control performance improvement. The measures can help to evaluate different performance dimensions of controllers, to analyze the effects of various aspects to the system behaviors, and give new design criteria for tuning controllers.

4 Robust disturbance observer-based control for wind turbines for efficiency and load mitigation

The figures, tables, and content in this chapter are based on the submitted journal paper [DS20d] and conference proceedings [DNS18, DS19, DS20b].

Commercial wind turbines today are becoming larger due to growing power output demands and efficiency requirements. The current largest turbine can produce 216.000 kWh per day with a height of about 190 meters from the ground to the blade tip. Wind turbines are constantly affected by wind varying in space and time, and gravity. Forces applied to turbines not only make the turbines to rotate, producing electricity, but also make elastic typically undamped turbine structures such as blades and tower deflect. These variations make the wind turbine structure become weakened and reduce its lifetime. The larger the wind turbine, the stronger the variation leading to the severity of structural load problems.

To reduce the structural load, wind forces affecting the wind turbines are controlled by modifying the pitch angle of blades collectively (CPC - Collective Pitch Control), or individually (IPC - Individual Pitch Control). However, this modification also affects the power production performance of the turbines resulting in requirements of a multi-objective control algorithm. The control system has to balance between maximizing power production in wind speed region 2 (between cut-in and rated wind speed), regulating power production in wind speed region 3 (above-rated wind speed), and mitigating structural load. Related control approaches need to be robust and able to reduce the effects of unknown variable wind speed disturbances and modeling errors.

Employment of advanced and reliable control methods which are robust against wind speed variation and model uncertainties can significantly reduce the cost of producing power. From the control point of view, this can be achieved by operating wind turbines optimally during low wind speed regime by tracking the wind speed in order to extract as much power as possible. Conversely, in high wind speed regime the objective changes from power extraction maximization to the limitation of extracting power at the rated value; hence, avoiding fatal damage that could result from exceeding mechanical and electrical limits. In both regions, controllers also have to minimize the structural loads while maintaining other objectives. The reduction of structural loads could increase the expected lifetime of wind turbines, but it could also enable the use of lighter components, which would lower the cost of wind energy and enable further increase in wind turbine dimensions and rated power. So load mitigation is attractive, promise and therefore has to be investigated.

Large wind turbines often have variable-speed configuration due to the ability to optimally operate over a wide range of wind speed. The amount of extractable wind power is strongly related to the turbine operating point defined by wind speed,

rotor rotational speed, and blade pitch angle. The wind speed varies stochastically in nature, so to make wind turbines operate at the optimal point, the rotor speed and blade pitch angles need to be controlled accordingly by Maximum Power Point Tracking (MPPT) control methods [AYTS12, TB16].

The MPPT methods determine optimal operating point using the information of wind speed, output power, or the characteristic curve of the wind turbine [AYTS12]. Typical MPPT control algorithms applied to wind turbines are Tip-Speed-Ratio (TSR) control, Power Signal Feedback (PSF), Hill-Climb Searching (HCS), Optimal Torque Control (OTC), and soft computing techniques. Both the TSR and PSF control methods require prior knowledge of wind turbine parameters and feedback measurements. The HCS control method is based on an iterative search of optimum power point using power and rotational speed measurements or converter duty cycles. The tip-speed-control method requires knowledge of optimum tip speed ratio λ_{opt} and the measurement of effective wind speed to give accurate results. The error between the actual torque and the reference torque defined by maximum power point at particular wind speed is used to modify the generator torque in OTC methods. Soft computing methods including Fuzzy Logic Controller (FLC) and Artificial Neural Network (ANN) on the other hand do not require prior knowledge of wind turbine parameters [TB16].

Most of the proposed methods for region 2 only focus on power maximization without considering mitigation of structural loads which can help to extended lifetime and reduced failure rate, especially in large wind turbines [NS16]. In [SZW06], an Individual Pitch Controller (IPC) is designed to mitigate structural load in both the partial load region and in high wind speed region. A negligible drop in energy capture and significantly reduced tower side-side fatigue damage was observed in high wind speed region, but no noticeable reduction in the part-load region can be realized compared with standard baseline controller. Disturbance Tracking Control (DTC) theory is used in combination with IPC to reduce fatigue damage in [Sto09]. The blade damage equivalent load is claimed an 11 % reduction while the power production remains identical compared to a conventional controller. However, the method uses the linearized model of nonlinear wind turbine so that the control performance will be deteriorated when the turbine operates outside the designed wind speed. In [SSU+13] a model predictive controller is applied for both below and above-rated region. Although a significant reduction in extreme loads could be obtained in the above-rated region, the MPC controller shows limited benefits in the below-rated region. An algorithm to avoid a wind turbine operating at the tower resonance frequency is proposed in [MSC15]. Simulation results show a significant reduction in tower fatigue damage can be achieved with a slight sacrifice in the energy captured.

Wind turbines are complex systems having many relevant variables hard or expensive to be measured. To obtain the value of unmeasured outputs for control purposes,

observers are commonly used. In [WB03], [SB01], [BLSH07], and [YGX+09] the authors apply LQG approach to design observer-based controller for wind turbines in order to regulate the rotor speed and reduce structural loads. The LQG full-state feedback approach has been tested in a real turbine (the Controls Advanced Research Turbine (CART) located in the National Wind Technology Center, Colorado, USA) in [WFB06]. In [SPJ11] the authors use an observer and a fuzzy controller for stabilizing the uncertain nonlinear wind turbines. Sliding mode control approach is applied in [CCC+12] combined with an observer to optimize the energy harvesting task.

Existing observer-based control approaches applied to wind turbines usually require to design observers and controllers separately in two steps even considering the separation principle. Although the observer design does not affect system stability, it can introduce variation in control performance so needed to be optimized. A precise system model is required for observer-based control synthesis. Modeling errors due to unconsidered effects like nonlinearities, unmodeled dynamics, and the variation in operating conditions might degrade the performance of the system or even make the system unstable.

Disturbance Accommodating Control (DAC) [Joh76] is an effective and widely applied technique to mitigate the effects of wind variation on the wind turbines [NS16]. The method introduces an additional feed-forward controller to compensate effects of changing wind speed and unknown disturbances in combination with a regular feedback controller. Often a predefined disturbance model is used in combination with general state-space system model to estimate the unknown inputs by an extended observer. The gain matrix of the disturbance observer needs to be designed carefully because of the trade-off between the error of disturbance estimation and the error caused by the model uncertainties. In addition, it is a challenge to define a suitable feed-forward disturbance rejection control gain matrix to guarantee system stability and totally cancel the disturbance effects.

In literature, disturbance observers are often designed using an extended system model and classical design methods such as pole placement [IHS14, IHS15] or Linear Quadratic Regulator (LQR) [GD13]. However, tuning methods for a precise disturbance estimation and about effects of uncertainties on the estimation quality depending on the dynamics of the disturbances are not discussed.

The disturbance rejection controller is typically considered as feed-forward and is calculated separately. The effects of state and disturbance estimation quality, system robustness, and overall system optimality are not fully considered. The feed-forward gain matrix can be found by using Moore-Penrose Pseudoinverse [GD13]. This method does not guarantee to find a non-zero matrix, especially with the presence of the actuator dynamics. The disturbance effects are not totally canceled by using this method leading to the steady-state error. In [WWJ16, WWB17] the Kronecker Product is used to find the disturbance rejection gain matrix which completely

cancels out the effects of disturbances, however, the steady-state error still exists due to the error in the disturbance estimation caused by the incorrect assumed wind disturbance model. Instead of calculating the disturbance rejection gain matrix individually, in [NS15] the feedback and feed-forward gain matrices are calculated simultaneously by using the extended system model including the disturbance model for the LQR synthesis procedure. The method considers the overall system stability, however, an assumption about the connection between unknown input and system states is needed to guarantee the exosystem controllability. In [DNS18], an extra integral loop is used in combination with the DAC to eliminate the rotor speed regulation steady-state error with the presence of the model uncertainties.

It can be observed that most of the existing solutions face the problem of modeling errors due to the use of linearized and reduced-order models. The aerodynamics of wind turbines are nonlinear in nature, the control input gains vary with blade pitch angle, rotor speed, and wind speed. When the turbines operate at continuous changing wind speed, the gains may defer from that of the linear model used for control design leading to poor performance or even unstable closed-loop behavior [Wri04].

In this section, robust multi-objective control strategies are proposed to regulate power production and mitigate undesirable structural loads at the same time. Unlike traditional approaches such as LQG and pole-placement, the proposed approach determines the optimal observers and controllers simultaneously considering model errors and uncertainties to ensure system robustness by minimizing the H_∞ norm of the generalized system. A partial integral action is included in the design process to eliminate the rotor speed regulation steady-state error due to the model uncertainties. The closed-loop stability is ensured by providing constraint to the H_∞ norm of the closed-loop transfer function. The approach uses non-smooth H_∞ optimization with constraints [GA11] applied for wind turbines. Additional disturbance observer and disturbance rejection controller are considered and calculated to accommodate the effects of varying wind speed. The proposed method successfully reduces the structural load (tower bending moment) and regulates the rotor speed without steady-state error despite the presence of the model uncertainties. The method also has high robustness against the model errors caused by system nonlinearities.

4.1 Disturbance accommodating control

This section provides a review of DAC design methods for the wind turbine application. Open problems and limitations of the existing approaches are also discussed.

In the theory of DAC, external disturbance structures are assumed as known, a predefined internal model for the disturbances is used to generate the estimation

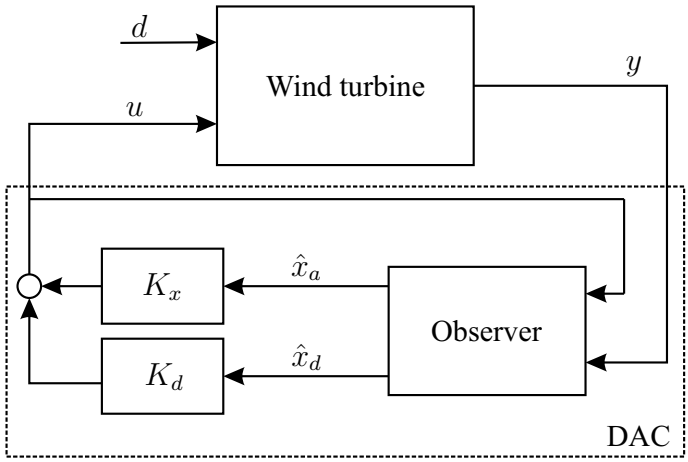

Figure 4.1: Disturbance accommodating control [DS20d]

[Joh76]. In the case of wind turbine control, the speed of wind reaching the blades is considered as the additive disturbance. The disturbance model is expressed as

$$\begin{aligned} \dot{x}_d &= D x_d \\ d &= H x_d, \end{aligned} \tag{4.1}$$

here x_d denotes the disturbance state, D and H denote the disturbance state space model. For stepwise constant uniform wind speed, they can be chosen as $D = 0$, $H = 1$ [WF08].

By expanding model (2.12) with (4.1) an extended system can be achieved as

$$\begin{aligned} \begin{bmatrix} \dot{x}_a \\ \dot{x}_d \end{bmatrix} &= \underbrace{\begin{bmatrix} A_a & B_{da}H \\ 0 & D \end{bmatrix}}_{A_e} \underbrace{\begin{bmatrix} x_a \\ x_d \end{bmatrix}}_{x_e} + \underbrace{\begin{bmatrix} B_a \\ 0 \end{bmatrix}}_{B_e} u \\ y &= \underbrace{\begin{bmatrix} C_a & 0 \end{bmatrix}}_{C_e} \begin{bmatrix} x_a \\ x_d \end{bmatrix}. \end{aligned} \tag{4.2}$$

System and disturbance states are estimated using a standard observer with the extended model

$$\begin{aligned} \begin{bmatrix} \dot{\hat{x}}_a \\ \dot{\hat{x}}_d \end{bmatrix} &= \begin{bmatrix} A_a & B_{da}H \\ 0 & D \end{bmatrix} \begin{bmatrix} \hat{x}_a \\ \hat{x}_d \end{bmatrix} + \begin{bmatrix} B_a \\ 0 \end{bmatrix} u + L(y - \hat{y}) \\ \hat{y} &= \begin{bmatrix} C_a & 0 \end{bmatrix} \begin{bmatrix} \hat{x}_a \\ \hat{x}_d \end{bmatrix}. \end{aligned} \tag{4.3}$$

The error e between the real and estimated states is expressed as

$$e = \begin{bmatrix} x_a - \hat{x}_a \\ x_d - \hat{x}_d \end{bmatrix}, \tag{4.4}$$

with the corresponding error dynamics

$$\dot{e} = (A_e - LC_e)e. \tag{4.5}$$

Assuming (A_e, C_e) as observable, the observer gain matrix L can be calculated by pole placement or LQR technique using the extended model (4.2) to make (4.5) stable, so the estimated error e converges to zero.

The estimated values are used to calculate the control variable

$$u = u_x + u_d = K_x\hat{x}_a + K_d\hat{x}_d, \tag{4.6}$$

where u_x is used for realizing control objectives such as speed regulation and structural load mitigation, u_d is used for canceling the effect of the wind disturbance d (fig. 4.1). Assuming (A_a, B_a) as controllable, the feedback controller gain matrix K_x can be defined via standard state feedback control design techniques like LQR as

$$K_x = R^{-1}B_a^T P, \tag{4.7}$$

with P obtained by solving the Riccati Equation

$$A_a P + PA_a^T + Q - PB_a R^{-1}B_a^T P = 0, \tag{4.8}$$

here Q and R are positive definite. The matrices Q and R are chosen to get the desired system dynamic responses.

The disturbance rejection controller gain matrix K_d is calculated separately to oppress the effects of the unknown inputs. The closed-loop system with the controller can be expressed as

$$\begin{aligned} \dot{x}_a &= (A_a + B_a K_x)x_a + (B_a K_d + B_{da}H)x_d \\ y &= C_a x_a. \end{aligned} \tag{4.9}$$

To oppress the effects of the disturbance on the system dynamic, K_d is designed to minimize the norm $\|B_a K_d + B_{da}H\|$. The disturbance rejection controller gain matrix K_d can be calculated using Moore-Penrose Pseudoinverse (†) as

$$K_d = -B_a^{\dagger}B_{da}H = -(B_a^T B_a)^{-1}B_a^T B_{da}H. \tag{4.10}$$

Generally, the norm $\|B_a K_d + B_{da}H\|$ is not equal to zero using K_d calculated from (4.10), thus the effects of disturbances are not completely canceled. In addition, when the actuator dynamics is considered, eq. (4.10) can not provide non-zero gain matrix of the disturbance rejection controller [GD13, WWB17].

The Kronecker product method described in [WWB17] can be used to find a non-zero disturbance rejection controller K_d that, under given conditions, totally cancels the disturbance effects. The method calculates the disturbance rejection gain matrix K_d by solving the regulation equation as

$$\underbrace{\begin{bmatrix} A_a & B_a \\ C_a & 0 \end{bmatrix}}_{F} \begin{bmatrix} S_1 \\ S_2 \end{bmatrix} - \begin{bmatrix} S_1 \\ 0 \end{bmatrix} D = - \underbrace{\begin{bmatrix} B_{da} H \\ 0 \end{bmatrix}}_{J}. \tag{4.11}$$

The solutions S_1 and S_2 of (4.11) can be found using the Kronecker product as

$$\begin{bmatrix} S_1 \\ S_2 \end{bmatrix} = (I \otimes F + D \otimes I)^{-1}(-J), \tag{4.12}$$

here $\otimes$ denotes the Kronecker product of two matrices.

The disturbance rejection gain matrix K_d is computed as

$$K_d = S_2 - K_x S_1, \tag{4.13}$$

this controller guarantees zero steady-state error if the system and disturbance models are completely precise. The condition to find a non-zero K_d is defined as

$$-J \in col(I \otimes F + D \otimes I), \tag{4.14}$$

here $col()$ denotes the column span space of a matrix. If $(I \otimes F + D \otimes I)$ has full column rank, the solution is unique [WWB17].

The overall disturbance accommodating controller including the observer, feedback controller K_x, and disturbance rejection controller K_d can be considered as a dynamic controller (fig. 4.1). Replacing the control variable u from (4.6), (4.3) can be rewritten as

$$\begin{bmatrix} \dot{\hat{x}}_a \\ \dot{\hat{x}}_d \end{bmatrix} = \begin{bmatrix} A_a & B_{da} H \\ 0 & D \end{bmatrix} \begin{bmatrix} \hat{x}_a \\ \hat{x}_d \end{bmatrix} + \begin{bmatrix} B_a \\ 0 \end{bmatrix} \begin{bmatrix} K_x & K_d \end{bmatrix} \begin{bmatrix} \hat{x}_a \\ \hat{x}_d \end{bmatrix} - \underbrace{\begin{bmatrix} L_1 \\ L_2 \end{bmatrix}}_{L} \begin{bmatrix} C_a & 0 \end{bmatrix} \begin{bmatrix} \hat{x}_a \\ \hat{x}_d \end{bmatrix} + Ly, \tag{4.15}$$

here L_1 denotes the observer gain matrix for system states, L_2 observer gain matrix for disturbances.

The DAC dynamic controller defined by L, K_x, and K_d is described as

$$\begin{aligned} \begin{bmatrix} \dot{\hat{x}}_a \\ \dot{\hat{x}}_d \end{bmatrix} &= \begin{bmatrix} A_a + B_a K_x - L_1 C_a & B_{da} H + B_a K_d \\ -L_2 C_a & D \end{bmatrix} \begin{bmatrix} \hat{x}_a \\ \hat{x}_d \end{bmatrix} + Ly \\ u &= \begin{bmatrix} K_x & K_d \end{bmatrix} \begin{bmatrix} \hat{x}_a \\ \hat{x}_d \end{bmatrix}. \end{aligned} \tag{4.16}$$

Existing approaches to design DAC have following problems and limitations:

- Observer gain (L), state controller gain (K_x), and disturbance rejection gain (K_d) are calculated separately, the effects of state and disturbance estimation quality, and overall system optimality are not fully considered [WWB17, DNS18].
- Disturbance rejection controller K_d is designed as a feed-forward controller. System stability when adding the disturbance rejection controller is not fully considered [GD13].
- Precise turbine and wind disturbance models are required. System robustness regarding inaccurate models is not considered [GD13, IHS15, WWB17].

Existing all-in-one approaches with the combination of Proportional Integral Observer (PIO) [SYM95b, LS14] and output control [Dav72] solve all problems mentioned before but are very sensitive to measurement uncertainties as well as noise. The observer and controller gains are designed separately, assumptions related to the connection between unknown inputs and system states are needed to guarantee the exosystem controllability [DNS18].

In wind turbine applications, the disturbance model may not accurate due to uncertainties and stochastic variation of wind disturbance. Also, the use of linearized reduced order models leads to inaccurate turbine models, especially when the turbine operates outside the given operating conditions. So it is necessary to develop a method to define robust DAC for wind turbines with respect to model and measurement uncertainties.

4.2 Combined PIO and DAC approach

Disturbance Accommodating Control (DAC) [Joh76] is an effective technique to attenuate disturbances therefore also to mitigate the effects of wind variation on the wind turbines, and the wind shear effect [WWJ16]. The technique requires an accurate system model which is difficult to obtain and even may be nonlinear but not suitable for control design. To acquire a linear model for controller synthesis, it is required to linearize the nonlinear model at an operating point. The model received after linearization does not exactly represent the real system behavior if the system is not working at the linearization point. In addition, the nonlinear model itself only formulates the dominant part of system dynamics, so typically reduced order models are used to design the controller. Unmodeled dynamics affect the control performance, so should be considered during design process [GD12].

Various robust nonlinear control schemes have been applied to wind turbines, such as gain scheduled control in [BDBM10], sliding mode control in [YL10], or LMI-based control [SEN+09]. Most of the researches require nonlinear model of the

turbines and do not consider structural loads. Robust control for nonlinear systems with uncertainties using Proportional Integral Observer (PIO) was introduced in [SLQ+07]. Proportional Integral Observers are used for estimate uncertainties of the systems including nonlinearities and unmodeled dynamics.

In this section a suitable control algorithm is proposed to regulate the generator power, and to reduce fatigue loads on the blades and the tower during high wind speed regime without assuming exact knowledge about the nonlinear system or unmodeled dynamics. The idea of the contribution is to combine an easy to get real model approach with a robust model-based control considering load mitigation effects.

4.2.1 Proportional-Integral Observer

The Proportional-Integral Observer PIO applied and developed in [SYM95b] is used and briefly introduced here. Assuming that the nonlinear model (2.7) can be expressed as a combination of linear and additive nonlinear part

$$\begin{aligned} \dot{x} &= Ax + Bu + Nf \\ y &= Cx, \end{aligned} \tag{4.17}$$

with the state vector $x \in \mathbb{R}^n$, the input vector $u \in \mathbb{R}^l$, the measurement vector $y \in \mathbb{R}^m$, unmodeled dynamics and nonlinearity $f(x,t) \in \mathbb{R}^r$ assumed as additive input. Here, the information about the dynamics of f is assumed as unknown. The matrix N denotes the location of unknown inputs acting to the system assumed as known. The aim is, based on the given information of the system model, the matrices $A \in \mathbb{R}^{n\times n}, B \in \mathbb{R}^{n\times l}, C \in \mathbb{R}^{n\times n}$, and $N \in \mathbb{R}^{n\times r}$, to estimate the system states and the effects of the nonlinearity and unmodeled dynamics as unknown inputs. The system is assumed as controllable and observable for the existence of the controller and observer. The condition is satisfied by choosing control variables and measured outputs [Wri04].

The basic idea is to extend the system states with an additional state to express the nonlinearity and unmodeled dynamics. Without exact knowledge about the dynamics of unknown input f and assuming that f is varying slowly so that the dynamics can be assumed as piecewise constant, the dynamics f is expressed as

$$\dot{f} = \Theta f \leq \epsilon, \tag{4.18}$$

where ϵ denotes a slow and bonded change rate and is a very small number. If the unknown dynamics f is assumed as piecewise constant, $\Theta = 0$ [SYM95a].

The extended system can be described by

$$\begin{aligned}\begin{bmatrix}\dot{x}\\ \dot{f}\end{bmatrix} &= \underbrace{\begin{bmatrix}A & N\\ 0 & 0\end{bmatrix}}_{A_p}\underbrace{\begin{bmatrix}x\\ f\end{bmatrix}}_{x_p} + \underbrace{\begin{bmatrix}B\\ 0\end{bmatrix}}_{B_p} u\\ y &= \underbrace{\begin{bmatrix}C & 0\end{bmatrix}}_{C_p}\begin{bmatrix}x\\ f\end{bmatrix}.\end{aligned} \tag{4.19}$$

Assuming observability of (A_p, C_p), states x and unknown input f are estimated as

$$\begin{bmatrix}\dot{\hat{x}}\\ \dot{\hat{f}}\end{bmatrix} = \begin{bmatrix}A & N\\ 0 & 0\end{bmatrix}\begin{bmatrix}\hat{x}\\ \hat{f}\end{bmatrix} + \begin{bmatrix}B\\ 0\end{bmatrix} u + \begin{bmatrix}L_1\\ L_2\end{bmatrix}(y - \hat{y}). \tag{4.20}$$

This extended system can also be interpreted by adding an integral part to a classical Luenberger observer shown in Fig. 4.2 where L_1 is the original Luenberger gain, L_2 is an additional integral gain of the observer.

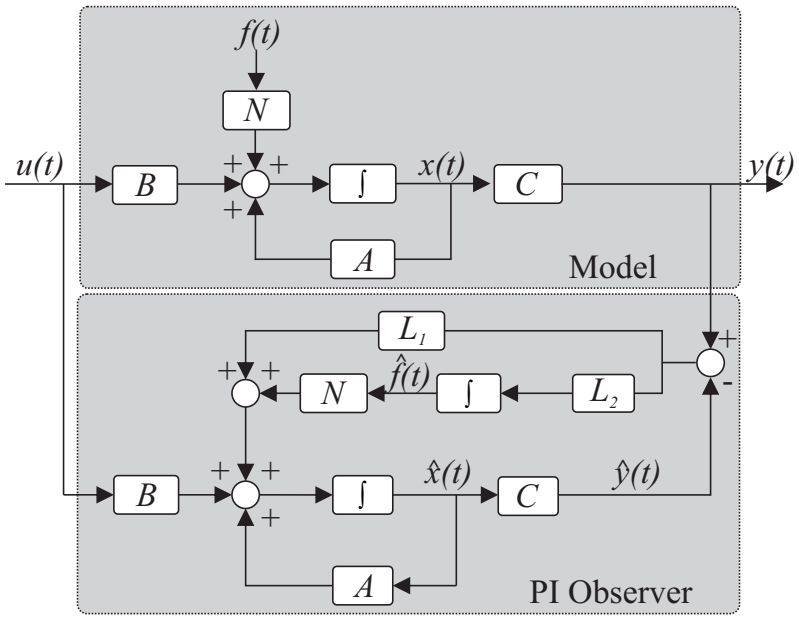

Figure 4.2: Proportional-Integral Observer PIO [SYM95a]

Based on (4.19) and (4.20), considering the estimation errors as $e = \hat{x} - x$ and $f_e = \hat{f} - f$, the error dynamics of the extended system becomes

$$\begin{bmatrix}\dot{e}\\ \dot{f}_e\end{bmatrix} = \underbrace{\begin{bmatrix}A - L_1C & N\\ -L_2C & 0\end{bmatrix}}_{A_{p,obs}}\begin{bmatrix}\hat{e}\\ \hat{f}_e\end{bmatrix} + \begin{bmatrix}L_1\\ L_2\end{bmatrix}(y - \hat{y}). \tag{4.21}$$

For a suitable observer design, the feedback matrix L has to be chosen in such a way that the estimation errors tend to zero ($e \to 0, f_e \to 0$). The error dynamics is affected by the term f. The feedback matrices L_1 and L_2 are required to stabilize the extended system described by the matrix $A_{p,obs}$, and to minimize the influence from the unknown inputs f to the estimations e and f_e. The two requirements

- $Re(\lambda_i) < 0$, for all the eigenvalues of matrix $A_{p,obs}$, and
- $\|L_2\|_F \gg \|L_1\|_F$,

for the PIO gain matrices design have to be fulfilled, $\|.\|_F$ denotes the Frobenius norm.

These requirements can be realized by using LQR method with suitable weighting matrices

$$Q_{obs} = \begin{bmatrix} I_n & 0 \\ 0 & qI_r \end{bmatrix}, R_{obs} = I_m, \tag{4.22}$$

with q as scalar design parameter so that $\|L_2\|_F \gg \|L_1\|_F$ with $q \gg 1$ expressing "high-gain" [YS14].

4.2.2 Disturbance accommodating control for WTs

In the theory of DAC, external disturbance structures are assumed as known, so a predefined internal model for the disturbances is required [Joh76]. In case of wind turbine control, the speed of wind reaching the blades is considered as additive disturbance. Because of the vertical wind shear, the wind speed affecting WT baldes varies periodically with 1P frequency depending on the rotor speed. Combining sinusoidal periodically and uniform stepwise waveform, a suitable wind disturbance model can be expressed as

$$\begin{aligned} \dot{z} &= Dz \\ d &= Hz, \end{aligned} \tag{4.23}$$

$$D = \begin{bmatrix} 0 & 1 & 0 \\ -\Omega^2 & 0 & 0 \\ 0 & 0 & 0 \end{bmatrix}, H = \begin{bmatrix} 1 & 0 & 0 \\ 0 & 0 & 1 \end{bmatrix}, d = \begin{bmatrix} d_s \\ d_u \end{bmatrix}, \tag{4.24}$$

with z as wind disturbance state, Ω as rotor speed, d_s and d_u as sinusoidal and uniform wind components.

By expanding the model (2.9) with (4.23) an extended system can be achieved as a base for a standard corresponding observer design

$$\begin{bmatrix}\dot{\hat{x}}\\ \dot{\hat{z}}\end{bmatrix} = \begin{bmatrix}A & B_dH\\ 0 & D\end{bmatrix}\begin{bmatrix}\hat{x}\\ \hat{z}\end{bmatrix} + \begin{bmatrix}B\\ 0\end{bmatrix}u + L_{dac}(y-\hat{y}). \tag{4.25}$$

Observer gain matrix L_{dac} can be calculated by pole placement or LQR technique. The observer provides a real-time estimation of the wind disturbance state, so that the disturbance can be compensated by a suitable controller.

4.2.3 Combined PIO and DAC approach

Combining (2.9) and (4.17), a wind turbine model with nonlinearity, unmodeled dynamics, and wind disturbance

$$\begin{aligned}\dot{x} &= Ax + Bu + Nf + B_dd\\ y &= Cx,\end{aligned} \tag{4.26}$$

can be obtained as

$$\begin{bmatrix}\dot{x}\\ \dot{f}\\ \dot{z}\end{bmatrix} = \underbrace{\begin{bmatrix}A & N & B_dH\\ 0 & 0 & 0\\ 0 & 0 & D\end{bmatrix}}_{A_{pe}}\underbrace{\begin{bmatrix}x\\ f\\ z\end{bmatrix}}_{x_{pe}} + \underbrace{\begin{bmatrix}B\\ 0\\ 0\end{bmatrix}}_{B_{pe}}u. \tag{4.27}$$

The corresponding observer equation is

$$\dot{\hat{x}}_{pe} = A_{pe}\hat{x}_{pe} + B_{pe}u + L_{pe}(y-\hat{y}). \tag{4.28}$$

The gain matrix L_{pe} can be obtained with the method described in section 4.2.1. Note that the q parameter in this case corresponding to both f and d. However f and d can be tuned separately by using the matrix N. It can be seen from fig. 4.2 that increasing N is equivalent to the increase of L_2. To guarantee the condition $\|L_2\|_F \gg \|L_1\|_F$, letting $N := pN$, a scalar parameter p is used to adjust the design model for numerical reasons.

The complete PIO-DAC combined control approach is shown in fig. 4.3 using the estimations $\hat{x}$, $\hat{f}$, and $\hat{d}$ realized from the observer (4.28). The state feedback controllers may have the problem of not zero steady control error, hence an additional integral loop is included to guarantee the accurate regulation. The integral gain is obtained from traditional PI controllers tuning methods for rotor speed regulation [WF08].

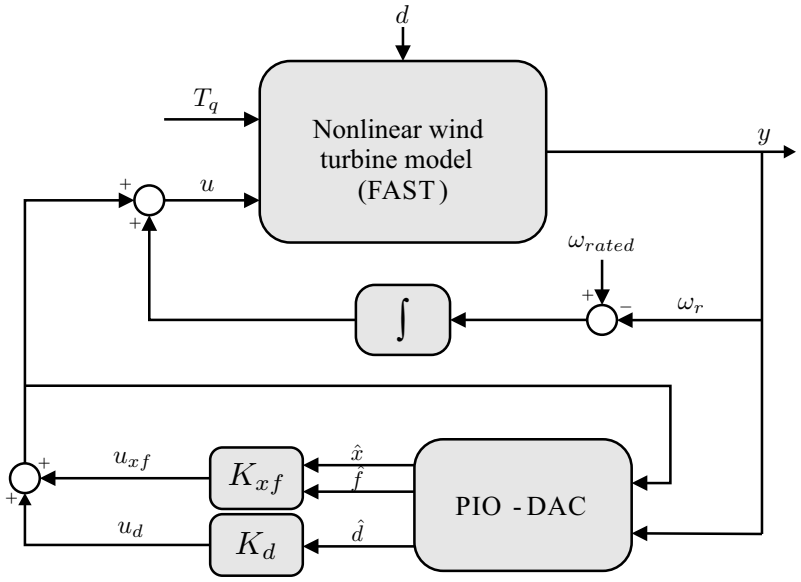

Figure 4.3: PIO-DAC combined control approach [DNS18]

The control variable is composed by

$$u = u_{xf} + u_d = u_x + u_f + u_d, \tag{4.29}$$

where u_x is used for realizing control objectives (i.e. power regulation and load mitigation), u_f for canceling the effect of nonlinearities and unmodeled dynamics f, and u_d is used for canceling the effect of the wind disturbance d. The control variables u_x and u_f are obtained from the extended model (4.19) by using standard pole placement or LQR method. To avoid uncontrollability of the exosystem (4.19), it is assumed that the nonlinearity and unmodeled dynamics f is connected to the system states

$$\dot{f} = Fx, \tag{4.30}$$

where F couples the system states to the nonlinearity and unmodeled dynamics. The F matrix of order $(r \times n)$ contains elements with small values. The plant model (4.19) is expressed as

$$\begin{bmatrix} \dot{x} \\ \dot{f} \end{bmatrix} = \underbrace{\begin{bmatrix} A & N \\ F & 0 \end{bmatrix}}_{A_c} \underbrace{\begin{bmatrix} x \\ f \end{bmatrix}}_{x_c} + \underbrace{\begin{bmatrix} B \\ 0 \end{bmatrix}}_{B_c} u. \tag{4.31}$$

The sytem (4.31) is controllable if

$$rank\left(\begin{bmatrix} B_c & A_cB_c & \dots & A_c^{n+r-1}B_c \end{bmatrix}\right) = n + r. \tag{4.32}$$

Assuming the original system (A, B) (4.26) as controllable, the condition (4.32) is equivalent to $rank(F) = r$. The control variable u_{xf} is calculated as

$$u_{xf} = u_x + u_f = K_{xf} \underbrace{\begin{bmatrix} \hat{x} \\ \hat{f} \end{bmatrix}}_{\hat{x}_c} \tag{4.33}$$

using $K_{xf} = R_c^{-1} B_c^T P_c$, with P_c obtained by solving the Riccati Equation

$$A_c P_c + P_c A_c^T + Q_c - P_c B_c R_c^{-1} B_c^T P_c = 0, \tag{4.34}$$

with Q_c and R_c as positive definite. The matrices Q_c and R_c are chosen to get the desired system dynamic responses, so comprehensive control signal (4.29) becomes

$$u = u_{xf} + u_d = \begin{bmatrix} K_{xf} & K_d \end{bmatrix} \begin{bmatrix} \hat{x}_c \\ \hat{z} \end{bmatrix}. \tag{4.35}$$

The plant model (4.26) can be rewritten using (4.31) as

$$\dot{x}_c = A_c x_c + B_c u + \underbrace{\begin{bmatrix} B_d \\ 0 \end{bmatrix}}_{B_{dc}} d. \tag{4.36}$$

Applying control input (4.35) to (4.36) considering the wind model (4.23)

$$\dot{x}_c = (A_c + B_c K_{xf})\hat{x}_c + (B_c K_d + B_{dc} H)\hat{z}, \tag{4.37}$$

is obtained.

To accommodate the disturbance term z, the norm $\|B_c K_d + B_{dc} H\|$ must be minimized. Here Moore-Penrose Pseudoinverse (†) is employed to get the feedback matrix

$$K_d = -B_c^{\dagger} B_{dc} H = -(B_c^T B_c)^{-1} B_c^T B_{dc} H. \tag{4.38}$$

4.2.4 Results and discussions

The results are obtained using the wind turbine model and simulation tool described in Section 2.2. Note that despite using the reduced order linear model in the control design process, a full order nonlinear model is employed by enabling all DOFs of the FAST code. The simulations are realized for the proposed PIO-DAC combined approach (PDAC) and a PI controller given in [WF08] as a baseline with step (fig. 4.4.a) and stochastic wind profiles (fig. 4.6.a).

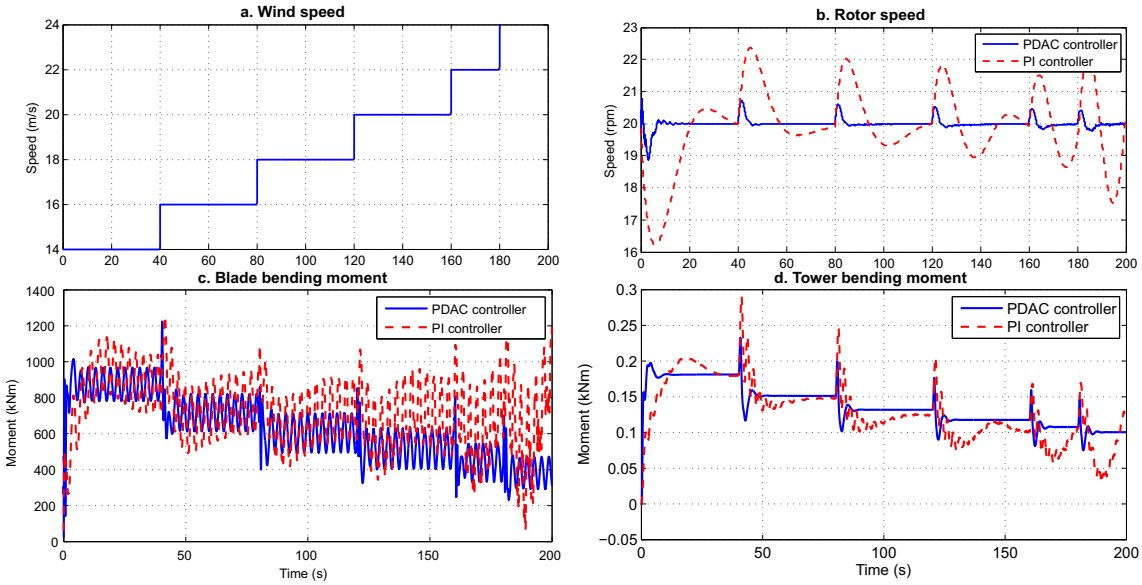

Figure 4.4: Step wind profile responses - region 3 control [DNS18]

Step wind responses

In fig. 4.4.b the WT rotor speed respond of step wind profile is shown. From fig. 4.4.b it can be detected that the proposed approach (PDAC) has better response over a wide range of wind speed (from 14 m/s to 24 m/s). The model used for design controllers is a reduced order model and linearized at the wind speed of 18 m/s. Because of the umodeled dynamics caused by reduced order, the speed regulation performance of the PI controller is poor with high overshoot and long settling time. In addition, the response of the PI controller shows stronger variation in wind speed region that differs from operation point (18 m/s) because of the nonlinearity of wind turbines. On the other hand, the proposed PDAC controller has much more lower overshoot and faster settling time despite of using reduced order model. The control performance of proposed approach is also robust against the change of wind speed compare to the PI controller.

The blade flap-wise and tower fore-aft bending moments of the turbine are shown in fig. 4.4.c and fig. 4.4.d respectively. The structural loads (blade and tower bending moments) are reduced by applying the proposed controller indicating by reduction of vibration amplitudes. To clarify the above statement, the blade and tower fatigue damage equivalent loads (DELs) [Hay12] are calculated. The results (fig. 4.5) indicate that a significant reduction of the tower load (29 %) and slight mitigation of blade loads (6 %) can be obtained using the proposed PIO-DAC combined controller (PDAC) compared to that of the traditional PI controller.

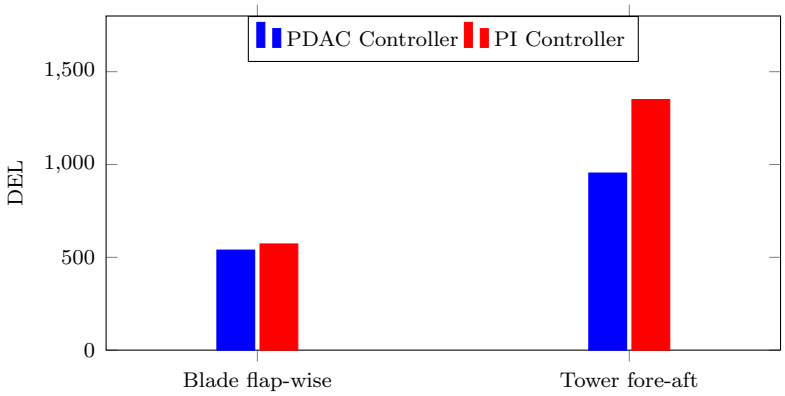

Figure 4.5: Damage equivalent load results - region 3 control [DNS18]

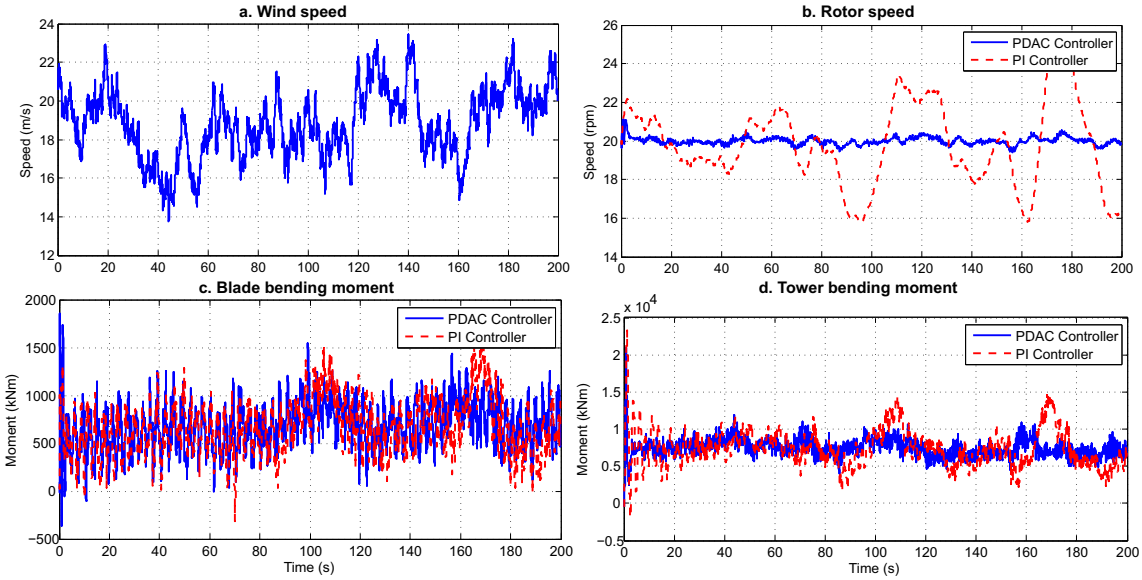

Figure 4.6: Stochastic wind profile responses - region 3 control [DNS18]

Stochastic wind responses

The stochastic wind profile used is generated using IEC von Karman wind turbulence model by TurbSim [JBJ09]. The wind has a mean value of 18 m/s, the linear vertical wind shear power law exponent of 0.2, and the turbulence intensity is 17 % (fig. 4.6.a).

The rotor speed response of the stochastic wind profile is shown in fig. 4.6.b. The combined PIO-DAC based controller has better speed regulation performance than PI controller in case of stochastic wind profile with much more lower speed variation (fig. 4.6.b). The load mitigation capacity is also improved in parallel (fig. 4.6.c, fig. 4.6.d) by using the proposed controller. The tower bending moment loads of proposed and PI controller are compared in fig. 4.6.d. Significant reduction in tower

bending moment can be detected using proposed MIMO controller. The deviations of blades bending moment also slightly mitigate in comparison with PI controller (fig. 4.6.c).

The relation between generated power (correlated to rotor speed) and structural loads is illustrated in fig. 4.7. In fig. 4.7, each point represents the bending moment of the blades or tower and the generated power at certain wind speed and controller. Thus for a arbitrary wind profile and a control system, an unique distribution is acquired. Here, the blue denotes results from full state feedback controller, and the red represents those of PI controller. It can be obtained that the distribution area representing the output of the proposed approach is "inside" the area representing the PI controller responses, so the PDAC controller produces smaller variation in both power generated and structural loads. Using proposed PDAC controller better results are obtained, so better mitigation of structural loads while maintaining regulation power can be concluded compared to the conventional PI controller.

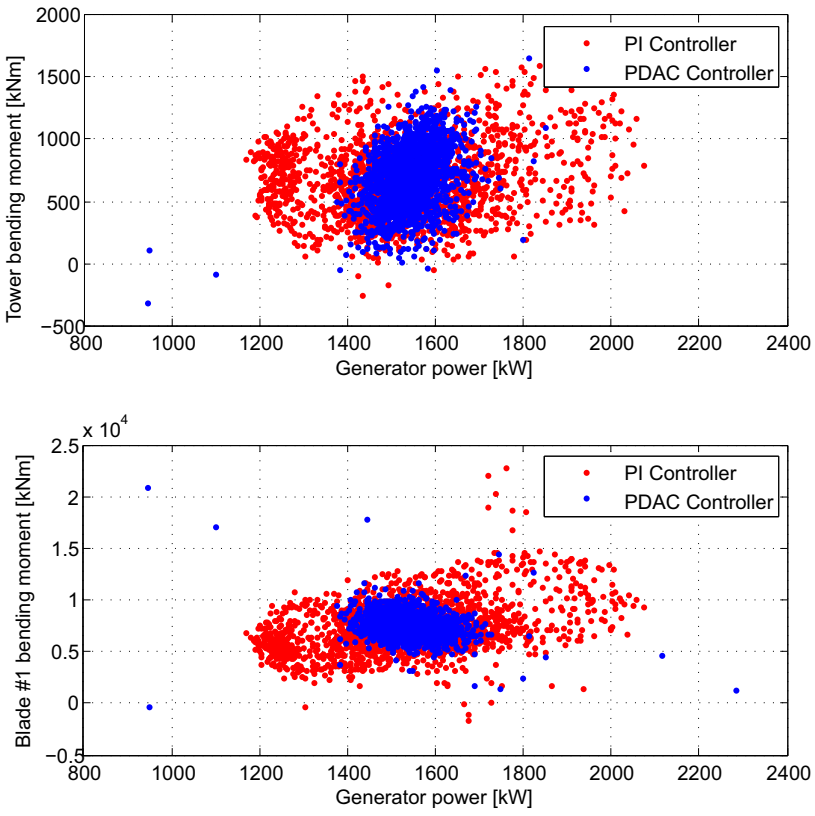

Figure 4.7: Power - Structural loads relationship [DNS18]

4.2.5 Conclusions

An observer-based control approach to mitigate structural loads and regulate the rotor speed for nonlinear wind turbines in the high wind speed region is proposed. The combination of PIO and DAC approaches are applied for the first time for wind turbine control in combination with load mitigation. The PIO is used to estimate the nonlinearity and unmodeled dynamics of the system, so the controller accommodates related effects to achieve high robustness. An additional state for wind disturbance is also included and considered using DAC. The simulation results show that the proposed scheme has better performance and robustness compared to the classical PI controller with respect to both objectives.

4.3 Robust disturbance observer-based control

The DAC design methods described in section 4.1 and 4.2.3 are used to calculate the observer, state controller, and disturbance controller gains separately. The overall system stability, robustness, and optimality are not fully considered. This section proposes a novel scheme to simultaneously compute the robust disturbance accommodating control (RDAC) parameters (L, K_x, and K_d) off-line. The idea is using the mixed-sensitivity H_∞ norm of the closed-loop transfer function as the cost function to optimize the DAC parameters.

4.3.1 Robust H_∞ control background

The H_∞ problem can be formulated as the task to minimizing the H_∞ norm $\| \, . \, \|_\infty$ of the close-loop transfer function G_{zd} from the unknown inputs d to the controlled outputs z as

$$R^* = \underset{R \in \mathcal{R}}{argmin} \parallel G_{zd}(P, R) \parallel_\infty, \tag{4.39}$$

where P denotes generalized plant, R controller, $\mathcal{R}$ a space of controllers that stabilize P, and R^* denotes the optimized controller (fig 4.8). By using the optimized controller, the effect of unknown inputs or disturbances to the outputs is minimized increasing the system robustness. This optimization is equivalent to the minimization of the norm of the sensitivity function $S = (I + OR)^{-1}$, where O denotes the transfer function of the plant. The H_∞ control design can be solved by using Algebraic Riccati Equations (AREs) [DGKF89], or Linear Matrix Inequality (LMI) [GA94] by convex optimization approaches.

There is a trade-off between performance and robustness against uncertainties of the H_∞ controller [SP07]. The trade-off can be solved by introducing weighting

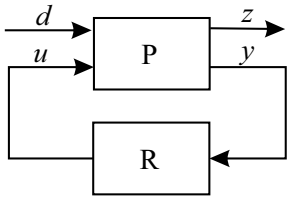

Figure 4.8: Standard H_∞ problem [DS20d]

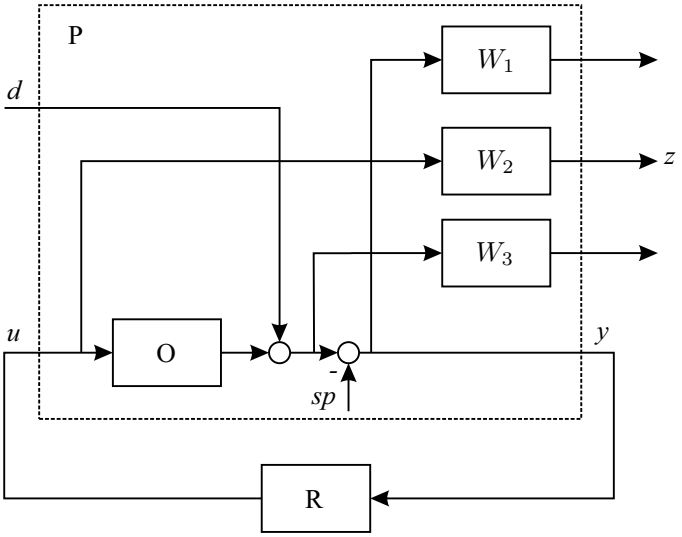

Figure 4.9: Mixed-sensitivity H_∞ control [DS20d]

functions W_1, W_2, and W_3 to the original plant O to design the system dynamics at different frequency ranges (fig. 4.9). The standard H_∞ problem is represented as the mixed-sensitivity loop shaping, which not only shapes the sensitivity function S but also the RS function, and the complementary sensitivity function T. The weighting functions are introduced to determine the desired shape of the above corresponding transfer functions. The optimization problem (4.39) now is extended as

$$R^* = \underset{R \in \mathcal{R}}{argmin} \left\| \begin{matrix} W_1 S \\ W_2 RS \\ W_3 T \end{matrix} \right\|_\infty . \tag{4.40}$$

In general, W_1 can be selected as a low-pass filter to make S small inside the desired bandwidth, and large in the high-frequency region to ensure the stability margin with the multiplicative uncertainty. To improve the system robustness against additive uncertainty and reduce the controller activity in the high-frequency regime, W_2 can be chosen as a high-pass filter.

4.3.2 Robust DAC approach

As presented in the previous section, the mixed-sensitivity H_∞ norm of the closed-loop transfer function is a good indicator for both system performance and robustness. The norm is used as the cost function to find the optimal robust DAC (RDAC). Unlike the standard H_∞ control finding the full order controller, the proposed RDAC approach finds parameters of a "structured controller" [AN17] having the DAC structure (4.16). Non-smooth H_∞ synthesis proposed in [AN06] is used to define the controller parameters with structural constraints. As a novelty, an additional disturbance observer and disturbance rejection controller are introduced to improve the disturbance accommodating performance.

The problem to find the robust disturbance accommodating controller (RDAC) is formulated as

$$RDAC = DAC^* = \underset{DAC \in \mathcal{DAC}}{argmin} \parallel G_{zd}(P, DAC) \parallel_\infty, \tag{4.41}$$

where DAC denotes a controller having DAC structure (4.16), $\mathcal{DAC}$ a space of DAC controllers that stabilize P, and DAC^* denotes the optimized controller defined by the optimal values of L, K_x, and K_d. With structural constraints, the problem (4.41) is non-convex and can not be solved by traditional H_∞ synthesis approaches such as AREs or LMI. The problem (4.41) can be solved using optimization methods such as gradient descent or genetic algorithms. However, the difficulty is to find DAC controllers that guarantee system stability.

To find a DAC controller stabilizing the closed-loop system, a stability constraint is added to the original optimization problem. Assuming full controllability and observability, a linear time-invariant system is Lyapunov stable if and only if its H_∞ norm is finite [DV75], so the stability constraint is fulfilled by

$$\parallel C_a(sI - \mathcal{A}(DAC))^{-1}B_a \parallel_\infty < +\infty, \tag{4.42}$$

where $\mathcal{A}(DAC)$ denotes the closed-loop system matrix depending on the controller DAC.

The task to define robust and optimal DAC controller is formulated as an optimization problem as

$$\begin{aligned} RDAC = DAC^* = argmin \parallel G_{zd}(DAC) \parallel_\infty \\ s.t. \parallel C_a(sI - \mathcal{A}(DAC))^{-1}B_a \parallel_\infty < +\infty. \end{aligned} \tag{4.43}$$

The additional constraint (4.42) guarantees asymptotic stability of the controlled system when finding the optimal parameters for the DAC controller. Note that (4.43) must be initialized with a stabilizing controller. The H_∞ norms in (4.43) are calculated from the system closed-loop state-space model using a bisection algorithm

[BBK89]. The problem (4.43) is non-smooth and non-convex and can be solved using global optimization approaches such as Genetic algorithm (GA). In [AN06] a nonsmooth optimization algorithm is proposed to solve (4.43) with a reasonable balance between computing time and effectiveness. The method uses the Clarke sub-differential and a modified multi-start steepest descent algorithm to minimize the H_∞ norms [AN06]. The procedure to calculate RDAC controller parameters is shown in fig. 4.10.

By solving (4.43), the optimal parameters L, K_x, and K_d of the DAC controller are defined (fig. 4.10). The obtained RDAC controller is robust with respect to the minimization of mixed-sensitivity H_∞ norm of the closed-loop transfer function. The inaccuracies of system and disturbance models are considered as additive and multiplicative uncertainties. Suitable system performance and robustness can be achieved by designing the shape of weighting functions. With additional disturbance observer and disturbance rejection controller, the computed RDAC controller also can accommodate the effects of varying wind disturbance and can be realized as a standard DAC controller.

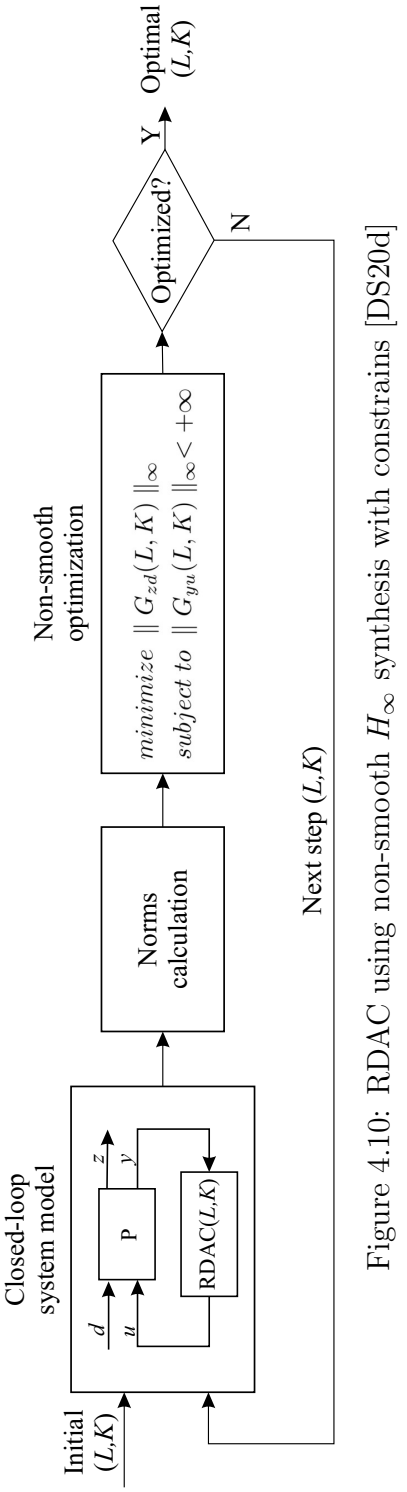

Figure 4.10: RDAC using non-smooth H_∞ synthesis with constrains [DS20d]

4.4 Robust DAC for wind turbine region 3 control

The proposed RDAC approach is applied to the 1.5 MW baseline wind turbine region 3 control as shown in fig. 4.11. The blade pitch actuator dynamics are considered by including the actuator transfer function into the generalized plant P. The wind turbine model has the pitch angle β as the control input, the hub-height wind speed d as disturbance, the rotor speed ω and tower fore-aft bending moment ζ as measured outputs. Above-rated wind speed region is considered, in this region the goals are to regulate the rotor speed at rated value and reduce the tower fore-aft bending moment (structural load). The designed controller also have to be robust against the wind disturbances and model uncertainties.

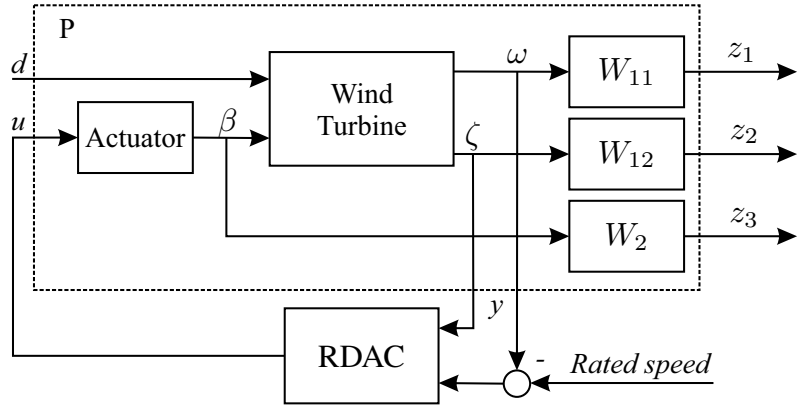

Figure 4.11: RDAC for wind turbine region 3 control [DS20d]

The generalized plant P of the wind turbine and actuator is expressed by

$$P : \begin{cases} \dot{x}_a &= A_a x_a + B_a u + B_{da} d \\ y &= C_a x_a \\ z &= W C_z x_a, \end{cases} \tag{4.44}$$

here W denotes the weighting function matrix and C_z the exogenous output matrix.

Weighting functions W_{11}, W_{12}, and W_2 are defined to obtain the desired performance and robustness. The exogenous output z with weighting functions are described as

$$\underbrace{\begin{bmatrix} z_1 \\ z_2 \\ z_3 \end{bmatrix}}_{z} = \underbrace{\begin{bmatrix} W_{11} & 0 & 0 \\ 0 & W_{12} & 0 \\ 0 & 0 & W_2 \end{bmatrix}}_{W} \begin{bmatrix} \omega \\ \zeta \\ \beta \end{bmatrix} = W C_z x_a. \tag{4.45}$$

The function W_{11} is chosen as low-pass filter effecting the rotor speed response and robustness against wind disturbances. To reduce the tower fore-aft bending

moment variation which mainly happens at the tower fore-aft frequency T_{fa} (6.55 rad/s), W_{12} is chosen as an inverted notch filter centered at the T_{fa} frequency (fig. 4.12). Finally, W_2 is chosen as a high-pass filter to reduce the controller activity in the high-frequency regime, and improve the robustness. The detailed values of the weighting functions are

$$\begin{aligned} W_{11} &= \frac{0.045s + 0.125}{s + 0.025}, W_2 = \frac{10s + 10}{0.01s + 1}, \\ W_{12} &= \frac{11.11s^2 + 11.11s + 72.82}{s^2 + 0.1s + 6.55}. \end{aligned} \tag{4.46}$$

The weighting functions can be adapted to the desired objectives and actual wind dynamics for optimal situation-based operation.

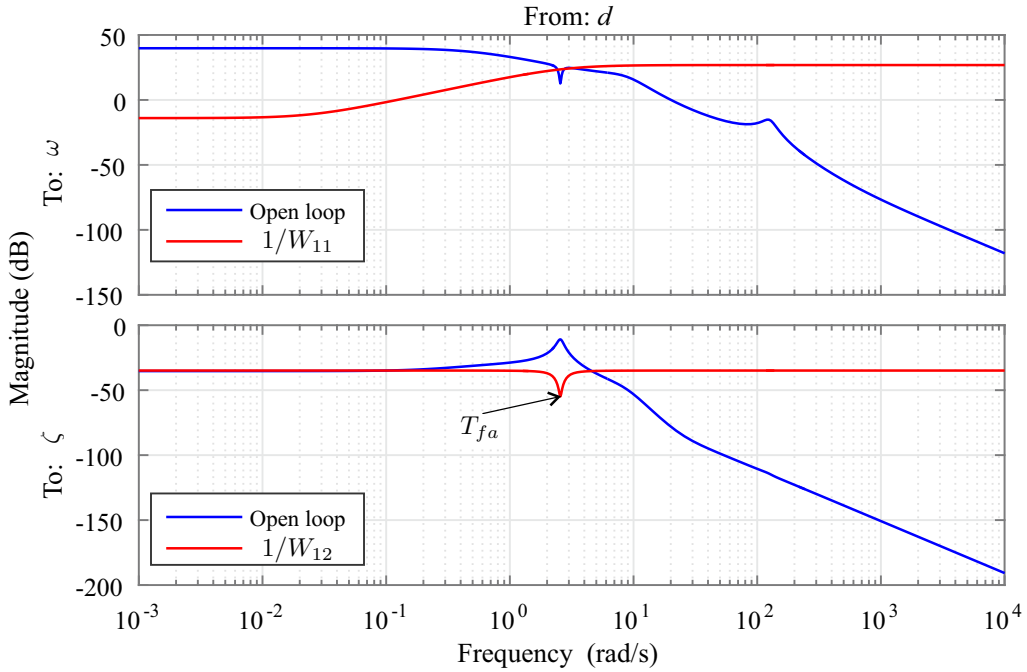

Figure 4.12: Open loop and weighting functions Bode plot [DS20d]

For a zero steady-state tracking error of the rotor speed regulation, in this work partial integral action is included in DAC controller. The additional integral state of the rotor speed measured output x_i is included into the controller

$$\begin{aligned} \dot{x}_i &= C_i y \\ u &= K_x \hat{x}_a + K_d \hat{x}_d + K_i x_i, \end{aligned} \tag{4.47}$$

where the matrix C_i defines the location of the measured rotor speed in the outputs, K_i denotes the integral gain.

From (4.3) and (4.47), the DAC dynamic controller with partial integral action is described as

$$\begin{aligned}\begin{bmatrix}\dot{\hat{x}}_a\\ \dot{\hat{x}}_d\\ \dot{x}_i\end{bmatrix} &= \underbrace{\begin{bmatrix}A_a + B_aK_x - L_1C_a & B_{da}H + B_aK_d & B_aK_i\\ -L_2C_a & D & 0\\ 0 & 0 & 0\end{bmatrix}}_{A_r}\underbrace{\begin{bmatrix}\hat{x}_a\\ \hat{x}_d\\ x_i\end{bmatrix}}_{x_r} + \underbrace{\begin{bmatrix}L_1\\ L_2\\ C_i\end{bmatrix}}_{B_r} y,\\ u &= \underbrace{\begin{bmatrix}K_x & K_d & K_i\end{bmatrix}}_{C_r}\begin{bmatrix}\hat{x}_a\\ \hat{x}_d\\ x_i\end{bmatrix}.\end{aligned} \tag{4.48}$$

The DAC controller (4.48) is considered as a "structured controller" [AN17]. The controller depends smoothly on the matrices K_x, K_d, K_i, and L

$$DAC = DAC(L, K_x, K_d, K_i). \tag{4.49}$$

The existence condition for a controller DAC stabilizing P are the full controllability and observability of the extended system (4.2). The robust disturbance accommodating controller RDAC is obtained by finding optimal gain matrices $K = [K_x\ K_dH\ K_i]$ and $L = [L_1\ L_2]^T$ by solving the optimization problem (4.43) using non-smooth H_∞ synthesis [AN06]. To formulate the cost function and constraint in (4.43), the H_∞ norms of close-loop transfer functions need to be calculated.

The DAC controller (4.48) can be described as

$$DAC(L, K) : \begin{cases}\dot{x}_r &= A_rx_r + B_ry\\ u &= C_rx_r,\end{cases} \tag{4.50}$$

here $A_r(L, K), B_r(L)$, and $C_r(K)$ as defined in (4.48).

Using (4.44) and (4.50) the closed-loop system is described as

$$\begin{bmatrix}\dot{x_a}\\ \dot{x_r}\\ y\\ z\end{bmatrix} = \begin{bmatrix}A_a & B_aC_r & B_{da}\\ B_rC_a & A_r & 0\\ C_a & 0 & 0\\ WC_z & 0 & 0\end{bmatrix}\begin{bmatrix}x_a\\ x_r\\ d\end{bmatrix}. \tag{4.51}$$

The behavior of closed-loop system (4.51) for a given weighting matrix W only depends on the controller matrices (A_r, B_r, C_r). The controller is based on the DAC structure (4.48) and determined by K and L gain matrices. Closed-loop transfer functions are derived from (4.51), the H_∞ norms of the close-loop system then is calculated [BBK89, BS90] to formulate the optimization problem (4.43). The optimal parameter K^* and L^* for the RDAC controller are obtained by solving (4.43) using the nonsmooth H_∞ synthesis algorithm implemented in the MATLAB function hinfstruct [GA11].

4.4.1 Results and discussions

A high fidelity simulation software, FAST [JBJ05], is used for illustration of the proposed method. The full-order 1.5 MW WindPACT nonlinear wind turbine model is used for simulation; the linearized reduced order model is used for designing the controller. This combination allows the representation of modeling errors due to the fact the controller is controlling the nonlinear system, but the related design is based on the related linearized model. The control objectives are to regulate the rotor speed at rated value 20.463 rpm (rated generator speed 1800 rpm) and to reduce the tower fore-aft bending moment variation. The standard load case for fatigue and normal power production is based on IEC 61400-1 DLC 1.2 [IEC05]. The proposed RDAC controller is examined and compared with the standard DAC controller designed by Kronecker product method described in section 4.1 using two scenarios based on step and stochastic wind profile.

Step wind profile results

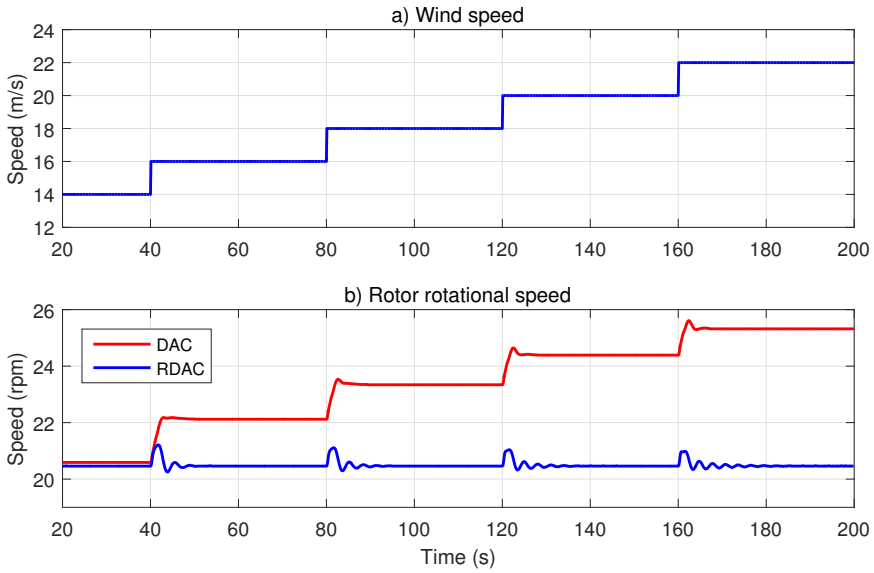

Figure 4.13: Robust DAC responses of step wind profile - region 3 control [DS20d]

A step wind profile varying from 14 m/s to 22 m/s is used (fig. 4.13.a) for assessing the effects of changing operation point (wind speed) and the steady-state error. The model used for controller design is linearized at the wind speed of 18 m/s. When the turbine operates at the wind speed differ from the selected linearized point, the model is not precise due to the nonlinearity nature of wind turbines. The results for the rotor speed responses of the proposed method (RDAC) and the standard DAC solved via Kronecker Product (DAC) are shown in fig. 4.13.b. It can be seen that

the standard DAC method cannot provide zero steady-state error due to the model mismatch caused by unmodeled dynamics and nonlinearities of the wind turbine (model used for simulation). On the other hand, the proposed method successfully regulates the rotor speed at the rated value without static error and shows strong robustness against the changing wind speed.

To eliminate the static error of the standard DAC, an additional integral control loop of the rotor speed, which is required to tunned separately, is used in combination with the standard DAC (fig. 4.14). The results of DAC with integral action method (DACI) is compared to that of RDAC (fig. 4.15). Note that the proposed RDAC method also has the partial integral action, the integral gain K_i in this case is optimized with other parameters. It can be observed from the figure, the RDAC method shows better rotor speed regulation performance with respect to lower overshot and settling time than that of the standard DAC with the integral loop (DACI).

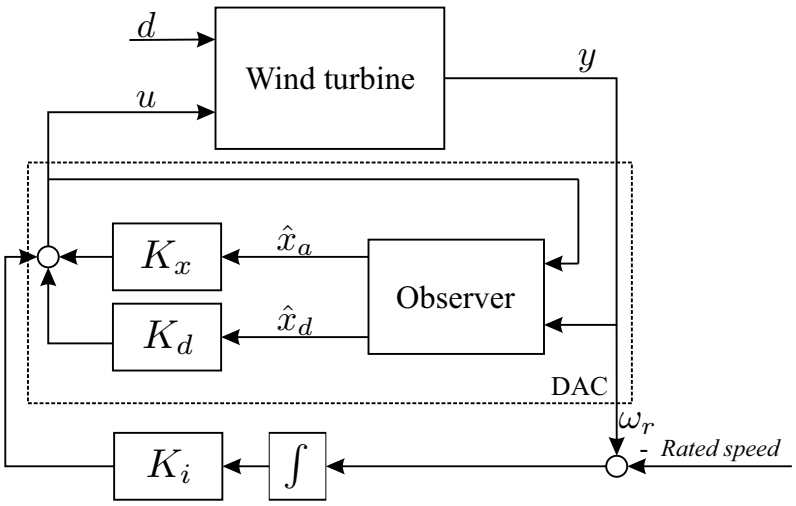

Figure 4.14: Disturbance accommodating control with integral action - DACI [DS20d]

Stochastic wind profile results

For more realistic working conditions and the investigation of wind disturbances rejection ability of the controllers (RDAC and DACI), stochastic wind profiles with different mean wind speed and turbulence intensity (TI) is used (fig. 4.16). The wind is generated using the von Karman wind turbulence model by TurbSim [JBJ09] followed the IEC 61400-1 standard [IEC05]. The wind profiles are chosen to have the mean speed of 18 m/s, 16 m/s, 14 m/s and the turbulence level of A, B, and C respectively. Here, turbulence level A correspond to the standard IEC categories of

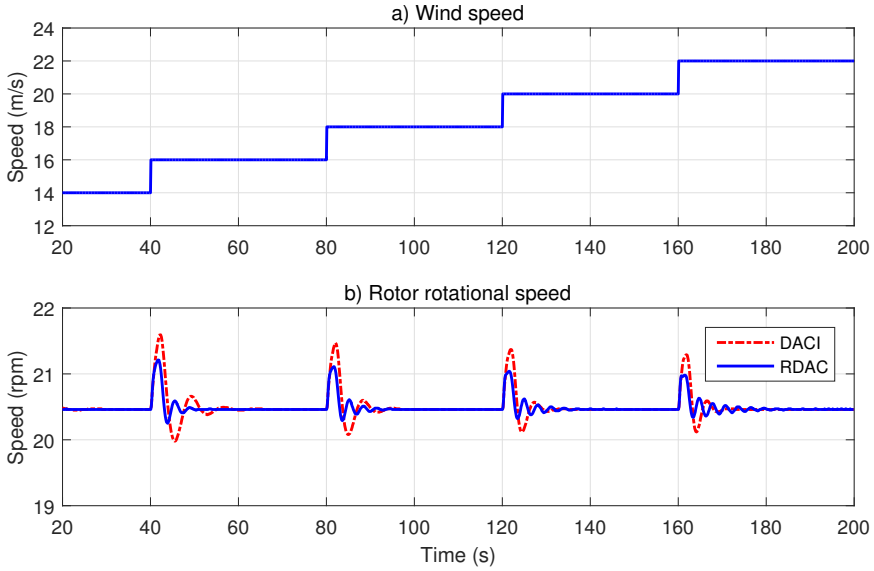

Figure 4.15: Robust DAC responses of step wind profile - with integral action [DS20d]

turbulence characteristics is the most turbulence level wind profile with the expected value of TI at 15 m/s is 16 % [JBJ09].

The simulation results for stochastic wind are shown in fig. 4.17. Lower speed variation of the proposed RDAC method is observed from fig. 4.17.b for all considered wind profiles. This means the proposed controller provides better rotor speed regulation performance than the standard DACI method. The tower structural load is also reduced by using the proposed controller indicated by lower tower bending moment variation amplitude compare to that of the DACI controller (fig. 4.17.c). The control variable (collective blade pitch angle) of two controllers are shown in fig. 4.17.d.

Quantitative evaluation of the results is realized using the mean square rotor speed regulation error and the tower fatigue damage [Sch96]. The cumulative fatigue damage of the tower is calculated from the tower bending moment time series using Miner's rule [Min45] and rainflow-counting algorithm (RFC) [ME68]. The cumulative damage results for different wind profiles are shown in fig. 4.18.b. The normalized mean square rotor speed regulation error and damage of the two controllers are shown in fig. 4.18.c. It can be seen that the RDAC method produces less regulation error and damage than the DACI method for all cases.

For a more clear illustration of the control performances respected to both speed regulation and structural load mitigation, a distribution diagram [DNS20] is shown in fig. 4.19. In the figure, each point represents the generated power (related to the rotor speed) and the tower bending moment at a certain point of time of

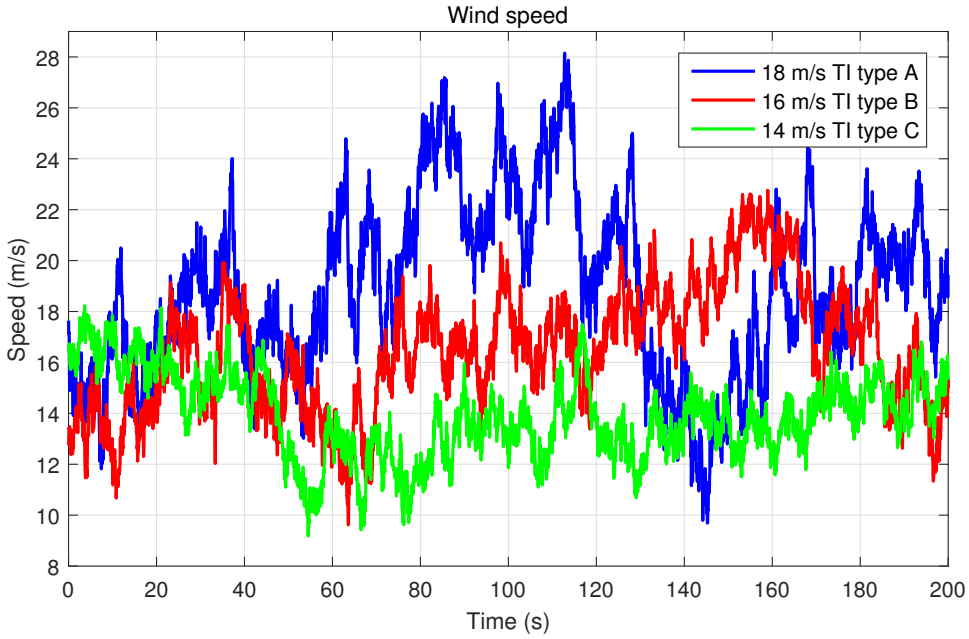

Figure 4.16: Stochastic wind profiles - region 3 control [DS20d]

each controller. The data distribution of each controller for all considered wind profiles is surrounded by an ellipse. The ellipse dimensions represent the standard variation of the generator power (proportion with rotor speed) and the structural load (tower bending moment). Lower dimensions mean better control performances in speed regulation and structural load reduction respectively. It can be seen that the ellipse representing the proposed controller has smaller dimensions than the ellipse representing the DACI controller.

4.5 Robust DAC for wind turbine region 2 control

The RDAC approach is applied in combination with a standard torque controller to region 2 wind turbine as shown in fig. 4.20 to reduce the tower bending moment. The maximization power production objective is realized by the torque controller as described in section 2.1. The torque controller will adjust the rotor speed ω to follow the wind speed d tracking the optimal tip-speed-ratio. To avoid conflicts in rotor speed control, RDAC does not affect the rotor speed, so no weighting function is given for the rotor speed output. On the other hand, the blade pitch angle β is used as a feedback to guarantee that β is regulated at the optimal value β^*.

The blade pitch actuator dynamics are considered by including the actuator transfer function into the generalized plant P. Due to the larger bandwidth of the pitch

actuator dynamics relative to the wind turbine dynamics, the actuator transfer function is chosen as first-order-lag (PT1) as

$$\frac{\beta}{u} = \frac{1}{s\tau_\beta + 1}, \tag{4.52}$$

where τ_β denotes the actuator lag time.

The turbine model (2.9) has the pitch angle β as the control input, the hub-height wind speed d as a disturbance or exogenous input, the rotor speed ω and tower fore-aft bending moment ζ as measured outputs. Combining (2.9) and (4.52), the generalized plant P (fig. 4.20) including actuator dynamics and additional measured output β is described as

$$\begin{aligned} \begin{bmatrix} \dot{x} \\ \dot{\beta} \end{bmatrix} &= \underbrace{\begin{bmatrix} A & B \\ 0 & -1/\tau_\beta \end{bmatrix}}_{A_p} \underbrace{\begin{bmatrix} x \\ \beta \end{bmatrix}}_{x_p} + \underbrace{\begin{bmatrix} 0 \\ 1/\tau_\beta \end{bmatrix}}_{B_p} u + \underbrace{\begin{bmatrix} B_d \\ 0 \end{bmatrix}}_{B_{dp}} d \\ \underbrace{\begin{bmatrix} y \\ \beta \end{bmatrix}}_{y_p} &= \underbrace{\begin{bmatrix} C & 0 \\ 0 & I \end{bmatrix}}_{C_p} \begin{bmatrix} x \\ \beta \end{bmatrix}, \end{aligned} \tag{4.53}$$

where x_p, y_p denote the states and measured outputs of P.

The goals are to regulate β at the optimal value and reduce the tower fore-aft bending moment ζ (structural load). These goals are realized by introduced and designed weighting functions W_1 for ζ and W_2 for β. The designed controller also has to be robust against the wind disturbance and the model uncertainties. The exogenous output z with weighting functions are described as

$$\underbrace{\begin{bmatrix} z_1 \\ z_2 \end{bmatrix}}_{z} = \underbrace{\begin{bmatrix} W_1 & 0 \\ 0 & W_2 \end{bmatrix}}_{W} \begin{bmatrix} \zeta \\ \beta \end{bmatrix} = WC_z x_p, \tag{4.54}$$

where C_z denotes the exogenous output matrix.

The generalized plant P is formulated as

$$P: \begin{bmatrix} \dot{x_p} \\ y_p \\ z \end{bmatrix} = \begin{bmatrix} A_p & B_p & B_{dp} \\ C_p & 0 & 0 \\ WC_z & 0 & 0 \end{bmatrix} \begin{bmatrix} x_p \\ u \\ d \end{bmatrix}. \tag{4.55}$$

The generalized plant P is connected with RDAC controller to form the closed-loop system. The RDAC controller. Weighting functions W_1 and W_2 are designed to obtain the desired performance and robustness. The function W_1 is chosen as a low-pass filter effecting the tower vibration mode and robustness against wind

disturbances. To reduce the tower fore-aft variation which mainly happens at the tower fore-aft resonance frequency, an inverted notch filter centered at the resonance frequency also is included in W_1. The function W_2 is chosen as a high-pass filter to reduce the controller activity in the high-frequency regime, and improve the robustness. The procedure to determine the optimal control parameters is the same with that of region 3 control described in the previous section.

4.5.1 Simulation results

The proposed method is validated using simulation software FAST in combination with MATLAB Simulink. A nonlinear reference WindPACT 1.5 MW onshore wind turbine model is used as the control plant [MH06]. The turbine cut-in, rated, and cut-out wind speed are 4, 12, and 25 m/s, respectively. Note that the control plant is the full-order nonlinear model while the controller is calculated based on a reduced-order linearized model. The linear model used for designing the controller is calculated numerically using a FAST built-in function. The linearization point is chosen as wind speed 8 m/s, pitch angle 2.6 deg, and rotor speed 14.8 rpm. The load case is based on the IEC 61400-1 DLC 1.2 standard for fatigue in normal power production condition. The proposed controller is examined in two scenarios step and stochastic wind profile.

Step wind profile

For assessing the system robustness to changing operating point, a step wind varying from 4 m/s to 10 m/s (fig. 4.21.a) is used, the wind shear power-law exponent is 0.2. The tower fore-aft bending moment responses of the baseline (in red) and the proposed controller (in blue) are shown in fig. 4.21.c. It can be seen that the tower variation is reduced significantly using RDAC helping to reduce the fatigue damage. Despite using fixed parameters, RDAC is able to robustly operate in a wide range of wind speed without significant degradation in performance.

The blade pitch angles are shown in fig. 4.21.b. For the baseline case, the angle is fixed at the optimal value (2.6 deg). The RDAC controller tries to perturb the pitch angle around the optimal value to reduce the structural load. It can be detected from fig. 4.21.d that this small perturbation does not affect much on power production. Generator power is nearly the same for the two approaches. The proposed approach successful reduces structural load without significant effects on power production.

Stochastic wind profile

For a more realistic operating condition, stochastic wind profiles with different mean wind speed and turbulence intensity (TI) is applied 4.22. The wind profiles are

generated using the IEC von Karman wind turbulence model. The wind profiles are chosen to have the mean speed of 6 m/s, 8 m/s, 10 m/s and the turbulence level of IEC type A [IEC05], 10 %, and 5 % respectively.

In this scenarios, the proposed RDAC approach is able to reduce the fluctuation of the tower compared to the baseline for all cases, as shown in fig. 4.23. The generator power of the two approaches has no obvious difference in these situations (fig. 4.23).

For quantitative evaluation, the normalized total power production and accumulated fatigue damage results of the two approaches are shown in fig. 4.24. The damage is calculated using the rain-flow counting (RFC) algorithm and Miner's rule. The power production and fatigue damage results are shown in fig. 4.24 have good agreement with the step wind case. A 14 % reduction in the accumulated damage is obtained using RDAC with the nearly same value of power production (under 0.1 % reduction).

4.6 Conclusions

A new method to design disturbance accommodating control (DAC) system with respect to model uncertainties and system stability for wind turbine power regulation and load reduction in both region 2 and 3 is introduced. The DAC including disturbance observer, feedback controller, and disturbance rejection controller is considered as a single dynamic controller. The parameters of the dynamic controller are computed by minimizing the mixed-sensitivity H_∞ norm of the generalized system with structure and stability constraints using the non-smooth optimization technique. Integral action is included in the dynamic controller instead of in the generalized plant for zero steady-state tracking error of the rotor speed. Simulation results for region 3 control show that the proposed method is able to regulate the rotor speed without steady-state error despite the presence of the model uncertainties. The proposed method provides better performance in both power production regulation, and structural load mitigation compared to the standard DAC controller designed by Kronecker Product method. The proposed method also shows high robustness against model errors caused by system nonlinearities and wind disturbances. In region 2, the simulation results show that RDAC can reduce the structural load by about 14 % without affecting the harvested power.

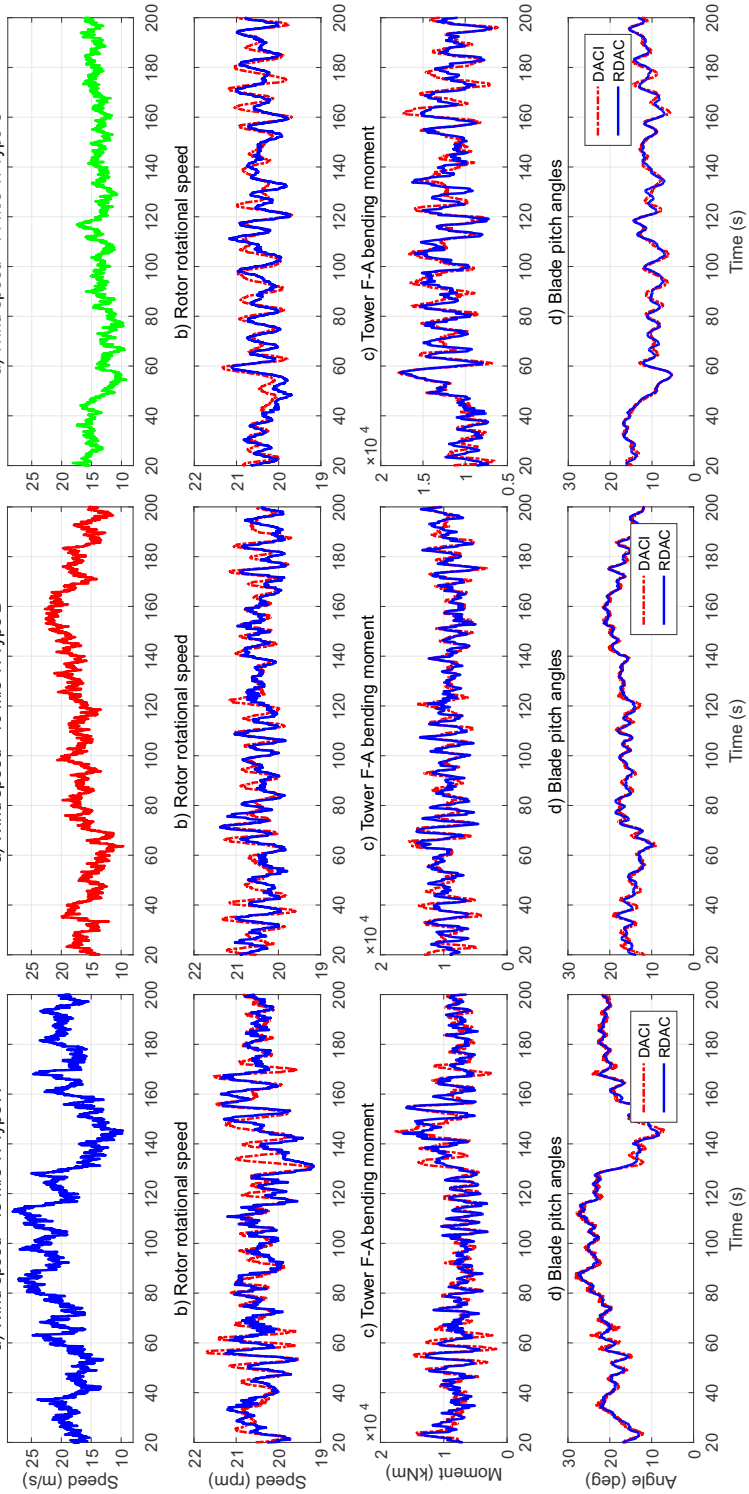

Figure 4.17: Responses of stochastic wind profiles - region 3 control [DS20d]

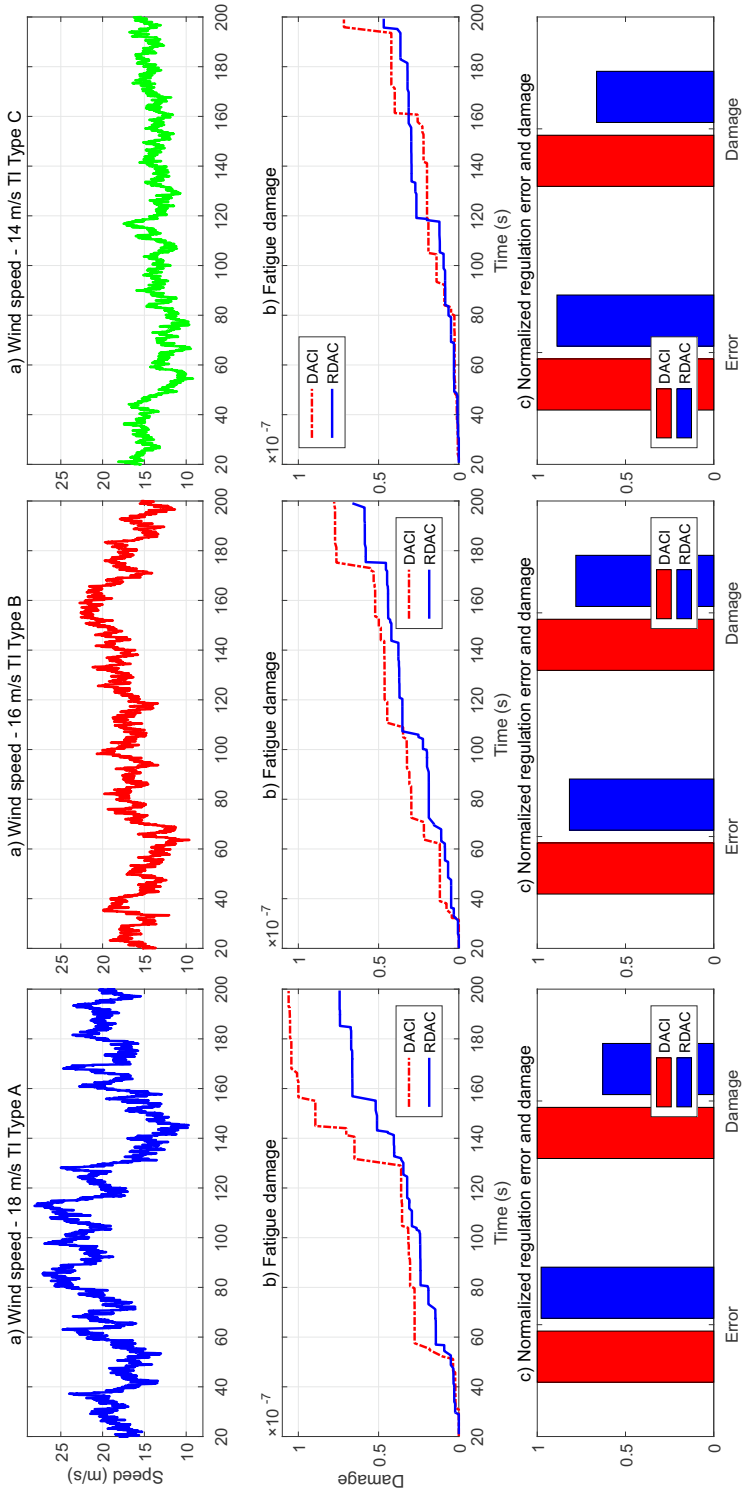

Figure 4.18: Regulation error and fatigue damage - region 3 control [DS20d]

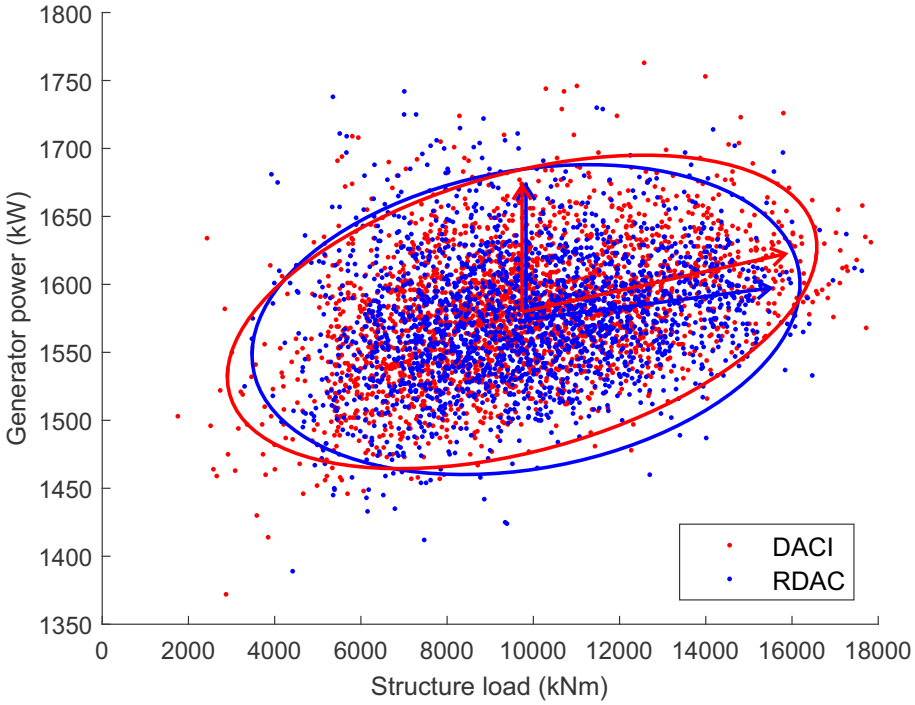

Figure 4.19: Generator power - structural load distribution diagram - region 3 control [DS20d]

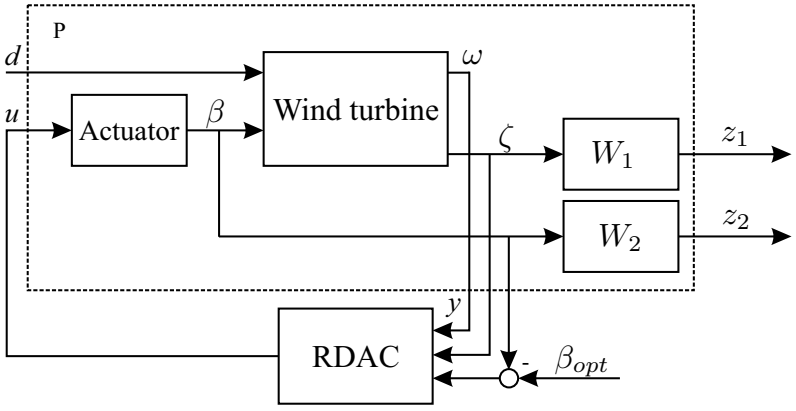

Figure 4.20: RDAC for wind turbine region 2 control

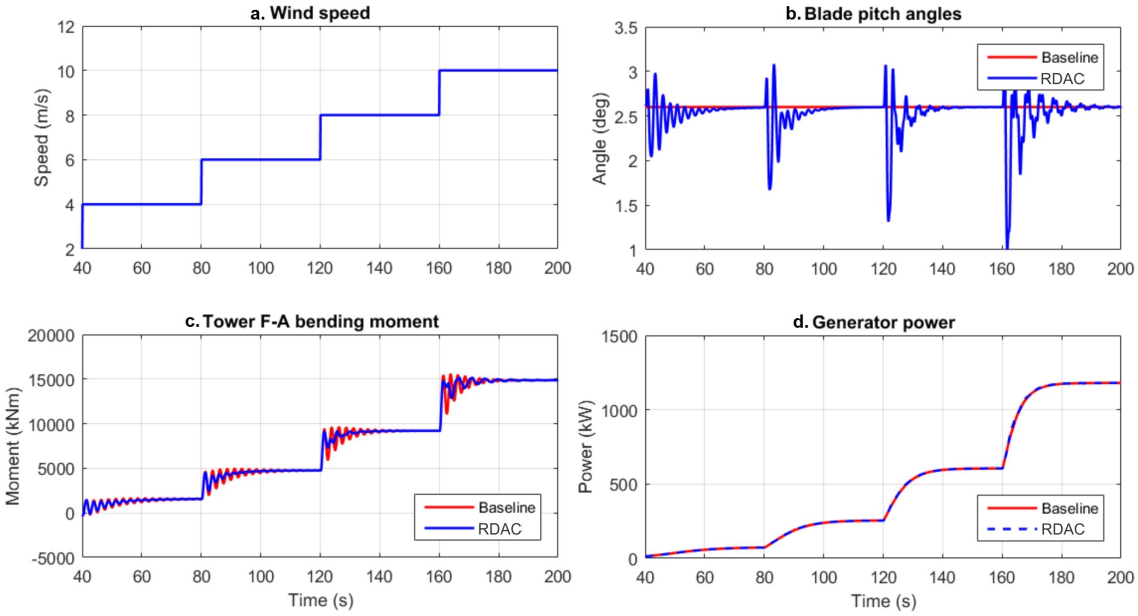

Figure 4.21: Step wind responses - region 2 control

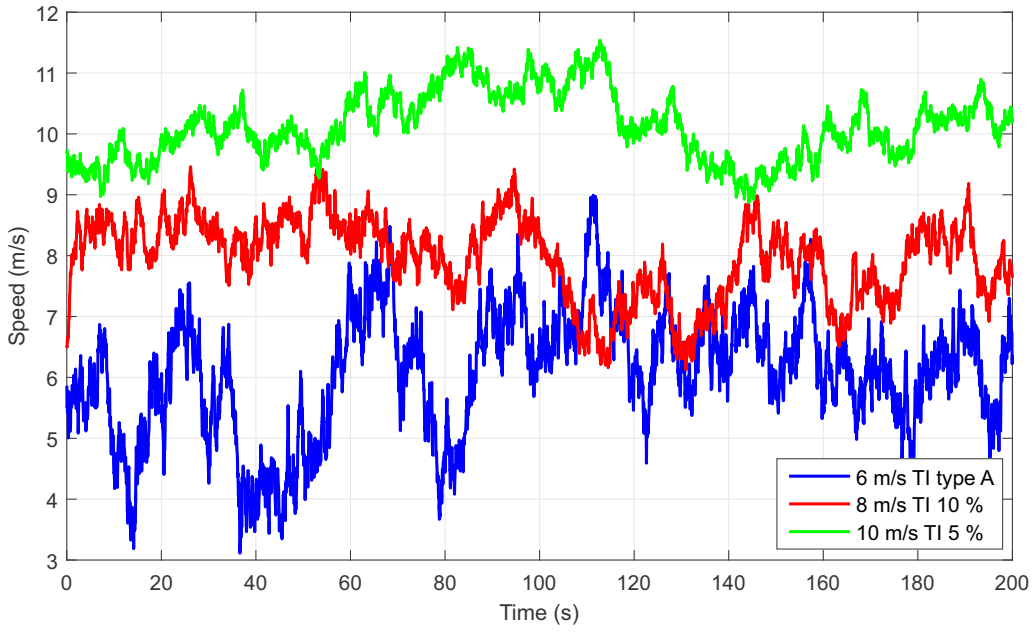

Figure 4.22: Stochastic wind profiles - region 2 control

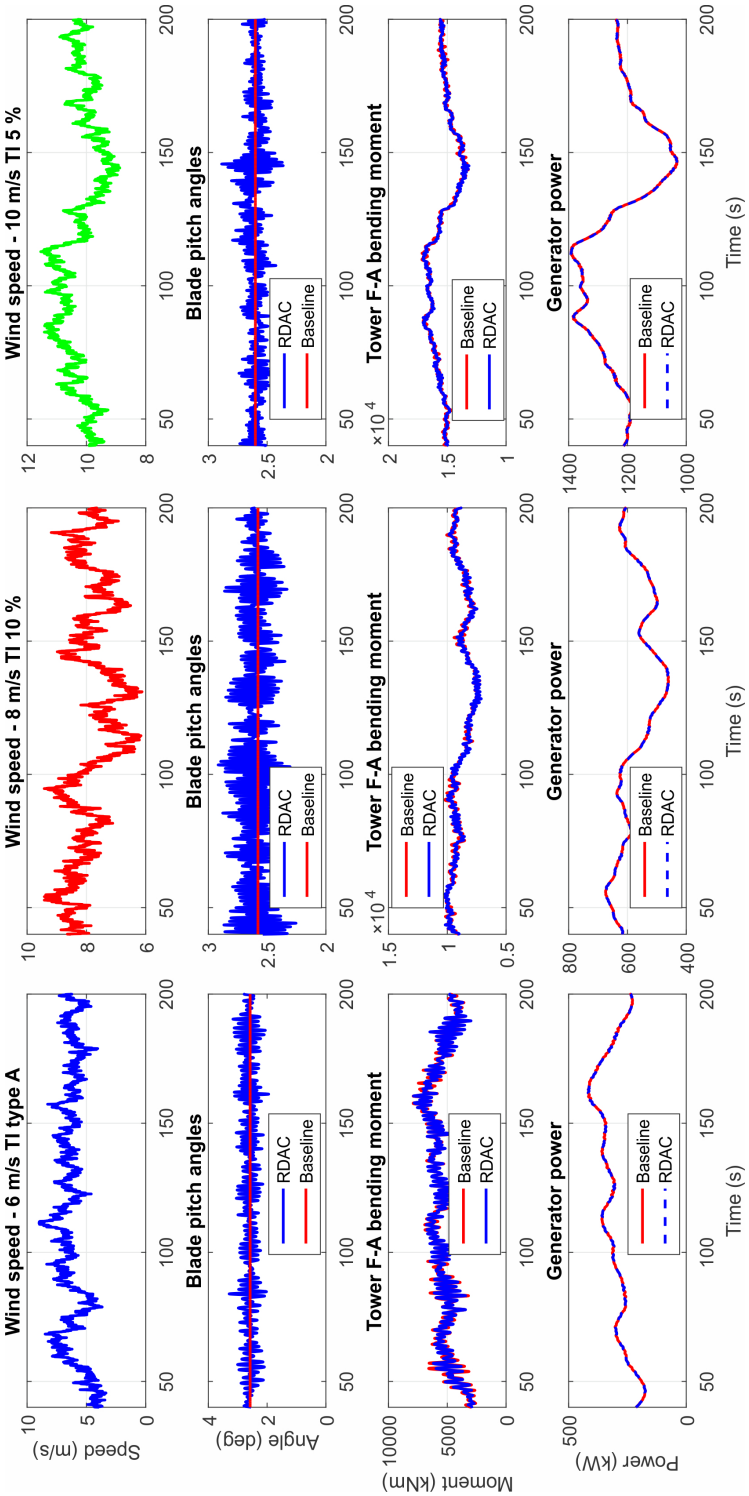

Figure 4.23: Stochastic wind profile responses- region 2 control

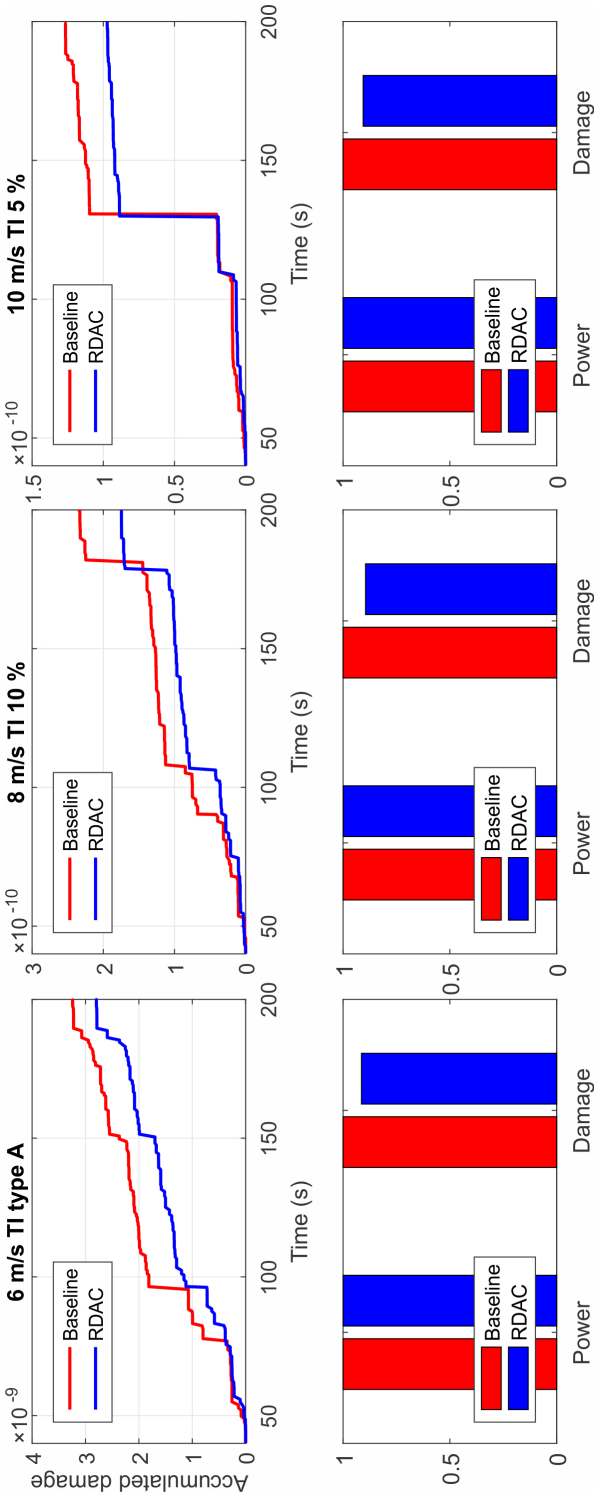

Figure 4.24: Power production and accumulated damage - stochastic wind

5 Wind turbine lifetime control using integrated PHM

The figures, tables, and content in this chapter are based on the conference proceeding [DS20c].

Wind power is one of the most promising sustainable energy sources to replace depleting traditional fossil energy. However, the production cost of wind energy still higher than that of conventional technologies ([Koo16]). To make wind energy more competitive, its Cost Of Energy (COE) needs to be reduced either by evolution in Wind Turbine (WT) design, applied material or optimal operation and maintenance. Recently, advanced MIMO control approaches are applied for WTs to maximize power production and reduce structural loads. Load mitigation helps to expand the turbine lifetime, reduce the maintenance cost, and allows to build larger WTs. However, load reduction often comes with the consequence of decreasing power production and increasing blade pitch activities. Balancing and optimizing this trade-off is challenging and still is an open problem.

The authors in [WB03] apply a LQG observer-based controller to regulate rotor speed and reduce structural loads. The trade-off between speed regulation and power production is defined by the corresponding rows of the weighting matrix Q. An adaptive controller is proposed in [MSC15] to maximize extracted power and reduce fatigue damage. The conflict between power maximization and load mitigation is considered by designing the parameters of an internal PI controller. An Individual Pitch Controller (IPC) to mitigate fatigue loading in both part-load and full-load region is employed in [SZW06]. The trade-off between competing objectives is balanced by designing weighting functions for the full-state feedback controller. The authors in [DS19] propose a robust observer-based control strategy for WT load mitigation. By designing the shape of performance channels, the level of load mitigation, speed regulation, and power production can be regulated.

Generally, weighting coefficients are used to balance the trade-off between load reduction, power extraction, and control energy. The design of weights is typically trial-and-error without a systematic procedure. To optimize the trade-off, in [NBDS19] a system health monitoring model is integrated into the control loop to provide the current system State Of Health (SoH) information. Depending on the actual health status indicated by accumulated damage level, more or less effort is put into load reduction capacity by switching between pre-calculated controllers. The proposed method can extend the service lifetime of WTs with a slight reduction in harvested power. However, due to the lack of Remaining Useful Lifetime (RUL) and future behavior information, the method can not guarantee the predefined lifetime.

The wind turbine is a complex system, a failure in one of the WT components may lead to un-schedule downtime increasing the Operation and Maintenance (O&M)

costs. To avoid an early failure of the system, the design lifetime of the components needs to be ensured. In this section, a novel adaptive lifetime control approach for wind turbines to reduce operation and maintenance costs is proposed. Lifetime controller uses the information of historical accumulated damage, predicted damage accumulate future behavior provided by a Prognostic and Health Management (PHM) model. The approach is based on a cascade structure with the outer loop utilizing structural health monitoring and prognosis techniques to determine suitable controller parameters and reference values of the inner loop. By continuously controlling the load mitigation level, the desired service lifetime can be achieved with maximum power generation possible providing the optimal balance between power generation and load mitigation. The trade-off between power production and load reduction is balanced to achieve predefined service lifetime using the knowledge of current system state-of-health and predicted future damage accumulation behavior. Unscheduled downtime is avoided by guaranteeing the predefined lifetime, hence reducing the maintenance cost.

5.1 Maintenance schedule and Lifetime control

Due to the degradation over time, WTs require regular maintenances to ensure performances and reliability. With the increasing size, the maintenance cost of WTs also increases significantly including the cost of unscheduled maintenances/repairs caused by components failure. So optimizing the maintenance and operation process helps to further reduce the cost of wind energy.

The maintenance schedule can be defined by corrective maintenance, preventive maintenance, and condition-based maintenance approaches [Dhi02]. Condition-Based Maintenance (CBM) strategies decide the maintenance action based on the actual system health status thus avoiding system breakdown and unnecessary maintenance actions reducing O&M cost [YWPH18]. The approaches use predicted RUL information to perform maintenance actions before faults appear. However, WTs operate at non-stationary workloads due to varying wind conditions may leading to the wrong prediction of system lifetime. The change in wind conditions results in the change in health degradation behavior and may lead to early failures or wasted lifetime (fig. 5.1). To guarantee the desired lifetime defined by maintenance schedules, the WT control system needs to be adapted with the actual health degradation dynamics obtained by PHM modules. This motivates lifetime control schemes to regulate the lifetime of WT components avoiding early failures. There are two main conditions for the feasibility of lifetime control schemes: i) the health degradation behavior can be affected by control systems; ii) RUL information can be calculated from measured data within a reasonable amount of time.

In the next sections, a novel lifetime control for WTs is developed using the IPMHC concept.

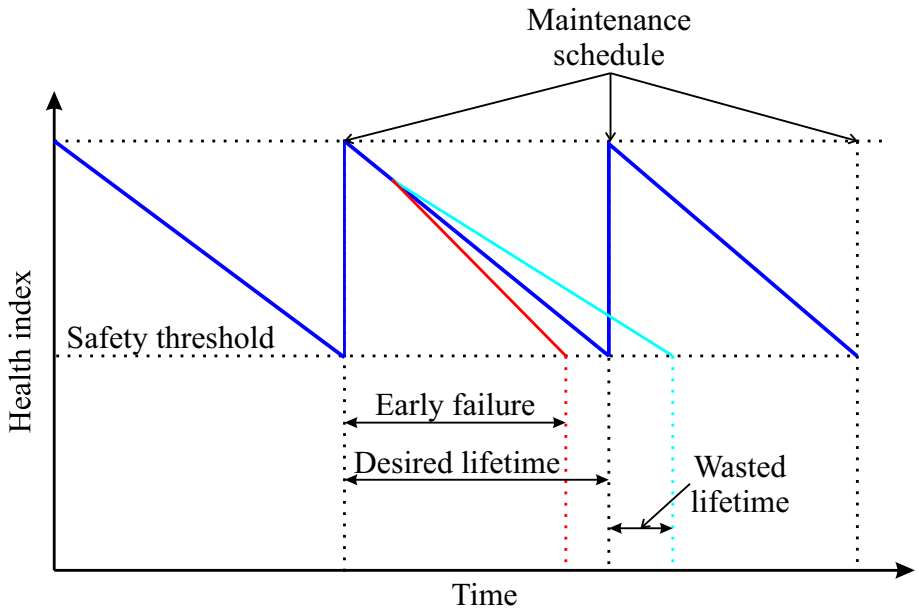

Figure 5.1: Maintenance schedule and desired lifetime

5.2 Health degradation control by load mitigation level

The load mitigation controllers presented in section 4 perturb the blade pitch angle around the optimal value β^* to reduce the WT tower vibration as an example of structural load. Structural load reduction required additional pitch activity lead to increasing fatigue damage of the actuators. When the blade pitch is controlled around the optimal value, the WT operates at sub-optimal conditions reducing the power production. The more efforts are put into load reduction, the more pitch activity required leads to more power contraction. This trade-off is illustrated in fig. 5.2.

In figure 5.2, the relationship between the accumulated fatigue damage and the pitch activity defined by the integration of the squared error of the real pitch angle and the optimal value is shown. In the figure, the evaluation of the results comparing load mitigation control (blue) with the baseline control (red) is given. The baseline control does not include the load reduction control loop. In this case, the blade pitch is constant at the optimal value, the power production is maximized by the MPPT controller, and the fatigue damage is the highest. The load reduction control results are shown for different controllers with varying load mitigation levels defined by weighting coefficients. It can be observed from the figure, the controller producing less damage shows higher pitch activity. In this case, the WT operates further from the optimal point, thus provides less energy. The maximum possible load mitigation level is limited by the actuator dynamics. The health degradation behaviors of the WT components can be controlled using different load mitigation levels by reconfiguring the load mitigation controllers.

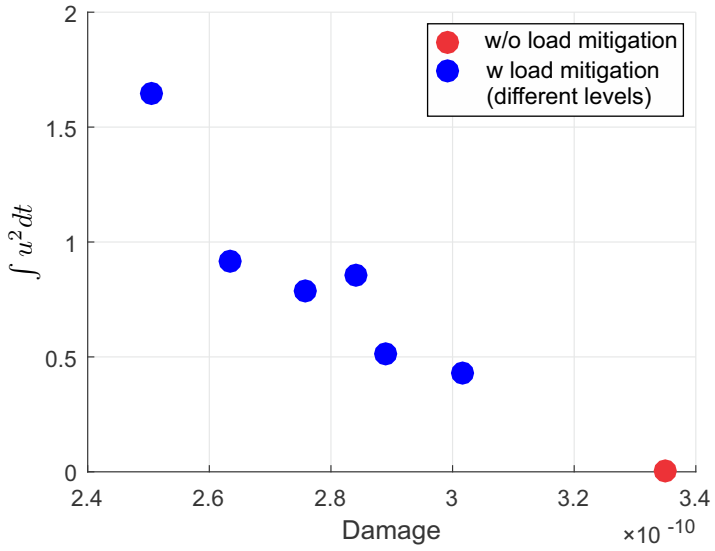

Figure 5.2: Pitch activity and fatigue damage with different weights [DS20c]

5.3 Health degradation control by power down-regulation

To supplementary reduce the structural load, beside the employment of load mitigation controllers, a tactical operation that can be adopted is to operate the WT at a down-scaled capacity, which has less power and fatigue damage produced. The goal of the approach is to keep the WT operate under a predefined damage threshold avoiding unscheduled downtime, see [FGO13].

In the full-load region, the tactic can be realized by regulating the generator power to below-rated value, as a result, the damage produced will be reduced accordingly. As mentioned in [NBDS19], when the generator is de-rated by 30 %, the structural load can be reduced by 36.6 %.

In the part-load region, the structural load can be reduced by tracking a sub-optimal power coefficient. In this case, the aerodynamic efficiency of the WT drops hence reduce power production and fatigue loading. Down-regulation is achieved through yaw or pitch control. For the load reduction purpose, down-regulation pitch control is typically done by increasing the pitch angle above the optimal value, see [HKE18].

Figure 5.3 shows the simulation results of the down-regulation strategy for the part-load region. The simulation is done using FAST software and WindPACT 1.5 MW reference WT, see [JBJ05]. A stochastic wind profile is used with the mean wind speed of 10 m/s and turbulence intensity of 5 % (fig. 5.3.a). In the optimal case represented in red, the blade pitch is kept at the optimal angle of 2.6 deg, the generator power is maximized (fig 5.3.b,d). In the down-regulation case denoted by blue, the blade pitch is increased to 5.2 deg, the WT operates at the sub-optimal

condition. The generator power structural load represented by the tower bending moment (fig. 5.3.c) is reduced with the exchange of power degradation. The health degradation behaviors of the WT components can be controlled using different down-regulation levels defined by the sub-optimal blade pitch angle reference.

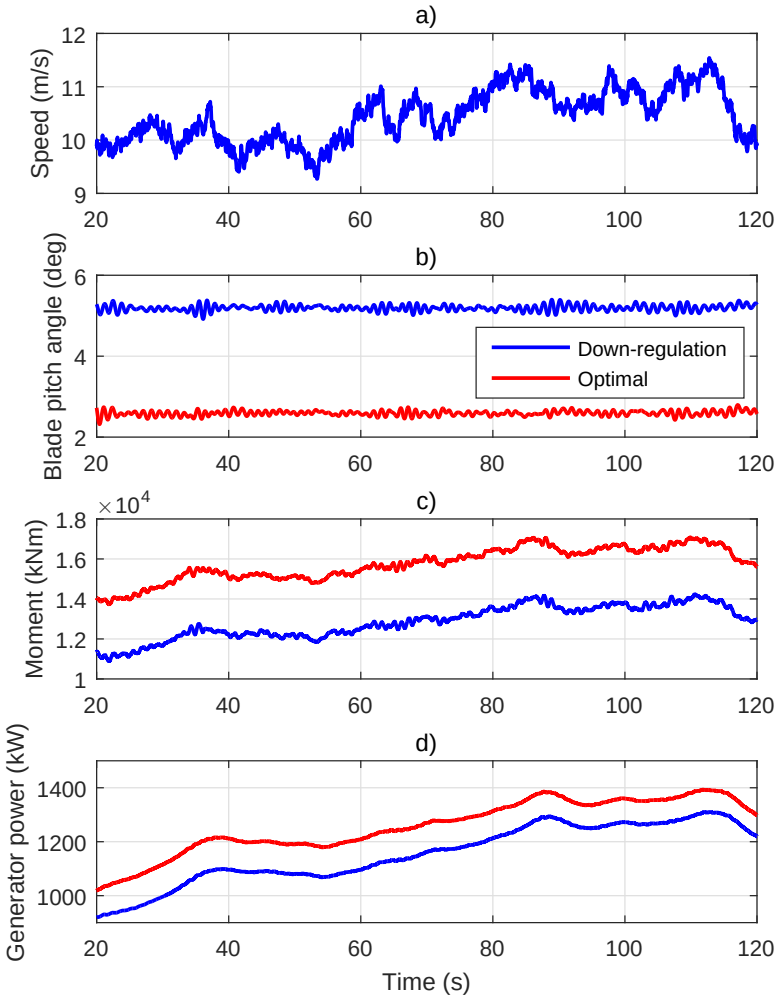

Figure 5.3: WT down-regulation: a) wind speed, b) blade pitch angle, c) tower bending moment, d) generator power [DS20c]

It can be detected that down-regulation techniques lead to significant deterioration in harvested wind energy. Due to this trade-off, the techniques are employed only in critical situations when the load mitigation controllers mentioned in the previous section can not guarantee the normal operation.

5.4 General concept of IPHMC

The general concept of Integrated PHM Control (IPHMC) applied for wind energy systems (WESs) is described in fig.5.4. The WESs could be wind turbines or wind farms with related controllers. The WEC control systems realize contradictory multiple objectives such as power production maximization, power reference tracking, structural load reduction for lifetime extension, or/and improving system reliability. The priority of each objective is vary depending on specific situations. For example, when the wind turbines/farms operate in a tough condition, such as strong wind turbulence intensity, it is more important to reduce structural load than maximize the instantaneous power harvested. The objective is to operate the turbine at reduced power without exceeding some damage thresholds resulting in unscheduled downtime [FGO13]. The trade-off needs to be optimized by control reconfiguration for each particular situation defined by the prognostic and diagnostic modules. In any case, system health-related information such as aging condition, accumulated damage, failure probability, and predicted RUL is an important aspect and needs to be considered.

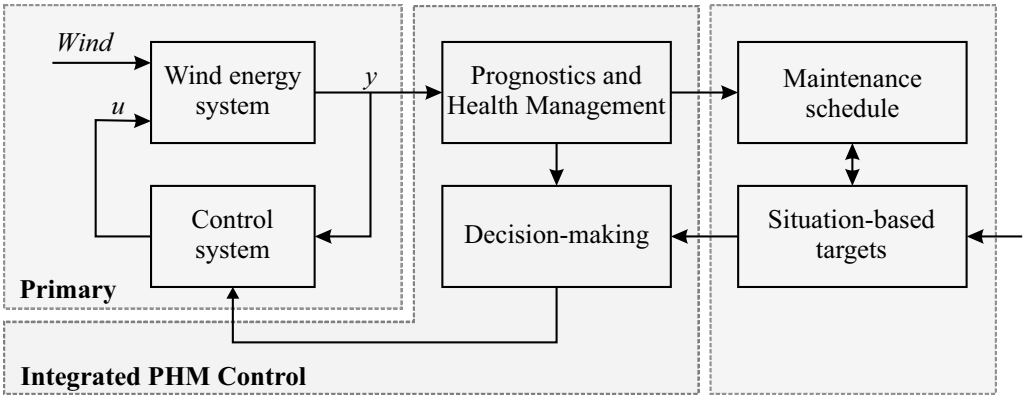

Figure 5.4: IPHMC concept for wind energy systems [DS20a]

Unlike traditional FTC approaches, the IPHMC framework allows adapting the control action even when the system is still in a non-faulty situation or before the fault appears [EPN12]. The idea is to not only control the physical states of the turbine (speed, power, bending moment, etc.) but also the health-related characteristics (fatigue damage, RUL, reliability, etc.) as indirect values obtained from the PHM modules [SR97]. The PHM module acts as a virtual sensor providing real-time feedback for the SoH control loop. Decisions are made using the heath status information and other requirements depending on each specific operating situation. The output of the decision-making module is the reconfiguring of controllers and/or reference values to accommodate the change of SoH, changing of control objectives depending on situations, or even stop the whole system. The maintenance schedule

of system components also could be considered to adapt the control law minimizing the overall cost.

5.5 Feedback lifetime control

The trade-off between structural load and power production can be balanced either by varying the load mitigation level of the MIMO controllers or by power down-regulation. The MIMO controllers are able to mitigate the structural load without a significant reduction in power generation. Still, MIMO controllers require additional pitch activity contributing to the actuator damage. Wind turbines operate in critical situations such as highly turbulent wind speed, or faulty conditions may produce extremely high damage exceeding the load mitigation capacity of controllers. In this situation, to further reduce the damage keeping the WT operates under safety limits, down-regulation needs to be applied with the exchange of power deterioration.

In this section, a novel adaptive scheme to optimal decides the load mitigation level guarantee a predefined desired lifetime is proposed. The decision-making process is based on the information of current and prognostic system SoH provided by a PHM module.

5.5.1 Lifetime prognosis

The accumulated fatigue damage D_k representing the structural load at the current time step T_k by RFC and Miner rule using the measured loading data (fig. 5.5). The time when the accumulated damage reaches a design limit D_d is considered as the WT service lifetime. The real service lifetime is expected to be larger than a design value L_d. The design lifetime is calculated based on normal working conditions plus some safety margins.

The future trend of the accumulated damage depends on the wind speed and control system configurations. Since the future wind speed is unknown and varies stochastically, it is difficult to predict the damage accumulation behavior or the actual WT lifetime. However, a potential range of the actual future lifetime can be obtained through Monte Carlo simulation. Simulations are repeated with wind profiles and controllers defined by mean wind speed, turbulence intensity, and load mitigation level. The wind profiles can be derived from previous measured data. For simplicity, the parameters for simulations are randomly sampled from possible values (table 5.1). From the simulation results, the worst and the best achievable lifetime L_w and L_b can be obtained. The average estimation lifetime L_e is calculated based on the average damage accumulation rate of the logged history data. The estimated lifetime is formulated as

$$L_e = \frac{T_k}{D_k} D_d. \tag{5.1}$$

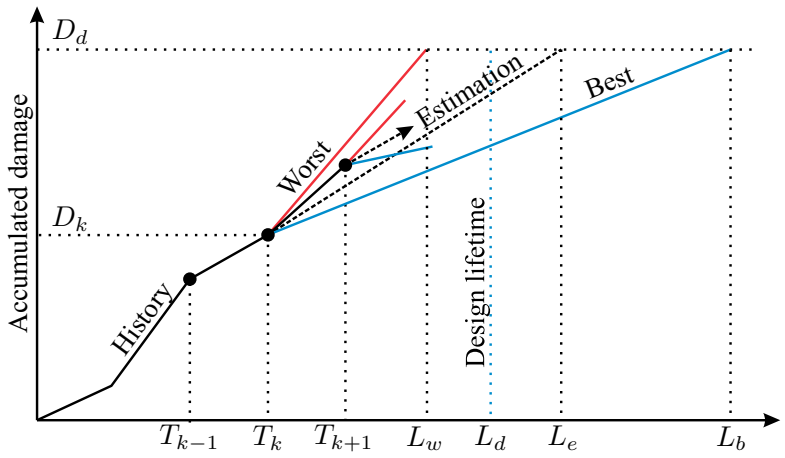

Figure 5.5: WT lifetime prognosis [DS20c]

The estimated remaining useful lifetime at current time step T_k is calculated as

$$RUL = L_e - T_k = T_k(\frac{D_d}{D_k} - 1). \tag{5.2}$$

Table 5.1: Parameter ranges [DS20c]

Mean speed (m/s)	Turbulence intensity (%)	Load mitigation level
4-12	0-18	0-max

5.5.2 Adaptive lifetime control algorithm

To avoid unwanted downtime that increases the O&M cost, it is important to ensure every component of WT can reach the design lifetime despite changing operating conditions. An adaptive algorithm is required to decide the optimal load mitigation level that guarantees the predefined lifetime while produces energy as much as possible. The adaptive algorithm is based on the design lifetime feasible coefficient (LFC) defined as

$$LFC = \frac{L_d - L_e}{L_b - L_e}. \tag{5.3}$$

Depending on the value of LFC, suitable actions are realized. The possible cases are:

1. $LFC < 0$: this is the desired case where the estimated lifetime L_e is larger than the design lifetime L_d. Load mitigation is not needed to ensure the design lifetime, so the load mitigation level can be reduced to optimize the power production and decrease the pitch activity.

2. $0 < LFC \leq 1$: the design lifetime L_d is larger than the estimated L_e and lower than the best value L_b. A higher level of load mitigation is required to make L_d lower than L_e. The load reduction level can be increased by increasing the weight element corresponded to the loading output and then re-design the controller. Down-regulation is not needed for this situation, the pitch angle reference is set to the optimal value.

3. $LFC > 1$: the best achievable lifetime L_b is lower than the design value L_d. The load mitigations controller are not able to guarantee the desired lifetime. To further reduce the load, down-regulation action is employed by increasing the pitch angle set-point.

The control structure is shown in fig. 5.6. The primary control system contains the MPPT controller and the RDAC load reduction controller. The MPPT controller controls the rotor speed to track the maximum power coefficient with the assumption that the blade pitch is at the optimal angle. If the blade pitch is not optimal, the MPPT controller tracks the sub-optimal power coefficient that produces less power and fatigue damage denoted as down-regulation. The load reduction controller regulates the pitch angle around the optimal value to mitigate the structural load. The load mitigation level can be adjusted by modifying the weighting functions in the controller design step.

To maximize power production with the constraint that the WTs must reach the design lifetime, the load mitigation level need to be controlled based on the estimated lifetime. Briefly speaking, a secondary control loop based on the information from the PHM system is used to control the system lifetime.

The measured values of wind speed and loading variable, here is the tower bending moment, are logged into the memory. The increased damage $\Delta D_k = D_k - D_{k-1}$ in the previous time interval from T_{k-1} to T_k at the current time step T_k is calculated from the logged data by RFC and Miner rule. Note that the damage is calculated at every time step, so only one step backward historical data is required avoiding the memory problem of the RFC algorithm. The time interval of the lifetime control loop is different and higher than that of the primary loop allowing real-time application. At every time step, the estimated, worst, and best lifetime is calculated based on the average, worst, and best damage accumulation rate obtained from the Monte Carlo simulations. From the prognosis data, the design lifetime feasible coefficient (LFC) is calculated. Based on the value of LFC, the secondary control loop can re-calculate parameters or modify the set-point of the primary controller regulating

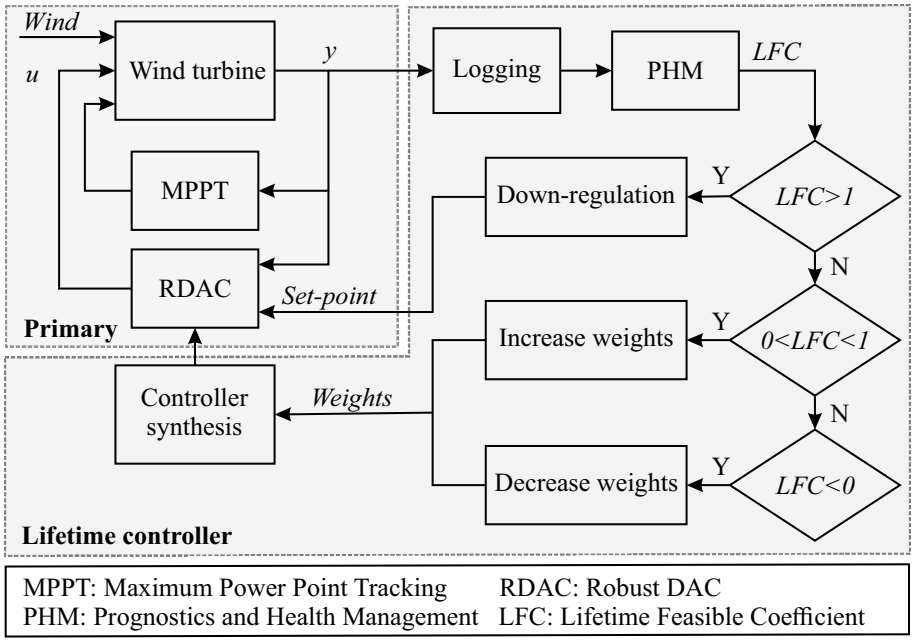

Figure 5.6: Proposed adaptive lifetime control scheme [DS20c]

WT lifetime. The load mitigation level of the primary loop is continuously adjusted to the optimal value using the lifetime feedback.

5.6 Simulation results

The proposed lifetime control scheme is illustrated by simulations using FAST software and WindPACT 1.5 MW reference WT. The wind profile used has 10 m/s mean speed and 5 % turbulence intensity (fig. 5.7). The objective of the lifetime controller is to generate power as much as possible while ensuring a predefined design lifetime. The time intervals of the primary and lifetime control loop are 0.001 s and 10 s, respectively. The goal is to regulate the actual lifetime to the desired value thus avoiding early failures and wasted lifetime. The desired lifetime for illustration purpose is a standard 10-minute period (600 s), the stochastic wind profile defined by mean wind speed and turbulence intensity is assumed unchanged in this period. The results can be extrapolated to obtain an arbitrary desired lifetime by accumulating 10-minute periods.

The results are shown in fig. 5.8 for maximizing power production, lifetime controlled, and maximizing load reduction cases. In the power maximization scenario, only MPPT controller is used without load reduction. The accumulated damage reaches the design damage before the design lifetime of 600 s leads to the risk of early failure. For maximizing load reduction case, an additional load reduction controller is used with the highest level of load mitigation. The WT lifetime, in

this case, is higher than the design lifetime with the payment of power reduction. The lifetime control case strikes an optimal balance between power production and load mitigation. The simulation result shows that the proposed approach is able to control the system lifetime to a predefined value guaranteeing system safety while maximizing power harvested.

5.7 Conclusions

This section proposes a novel adaptive lifetime control strategy for wind turbines. A system health monitoring and prognosis model is integrated into the control loop to provide the information of current system state-of-health and possible future lifetime. The predicted lifetime is used to adapt the parameters and references of the primary load reduction control loop. The trade-off between power production and load mitigation is optimized by regulating the WT lifetime to a predefined design value. The simulation using a high fidelity model shows that the proposed approach is able to control the lifetime of the system, thus avoiding un-scheduled downtime and decrease the operation and maintenance cost of wind turbines.

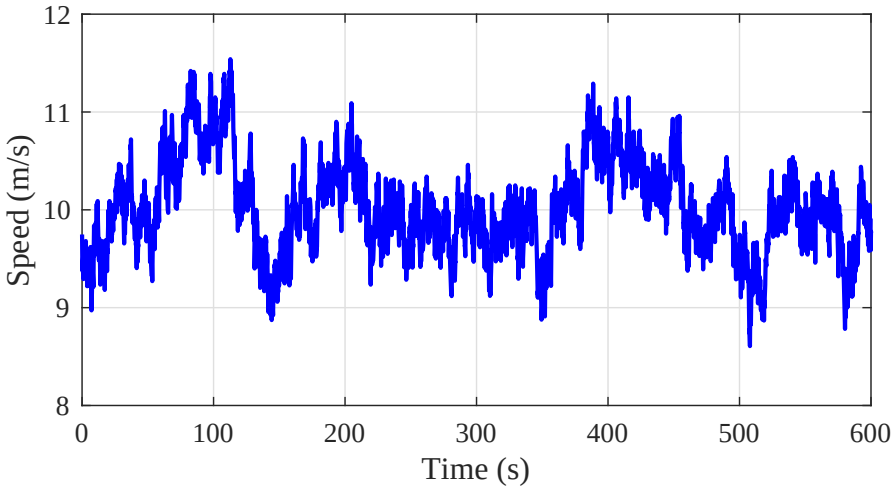

Figure 5.7: Stochastic wind profile [DS20c]

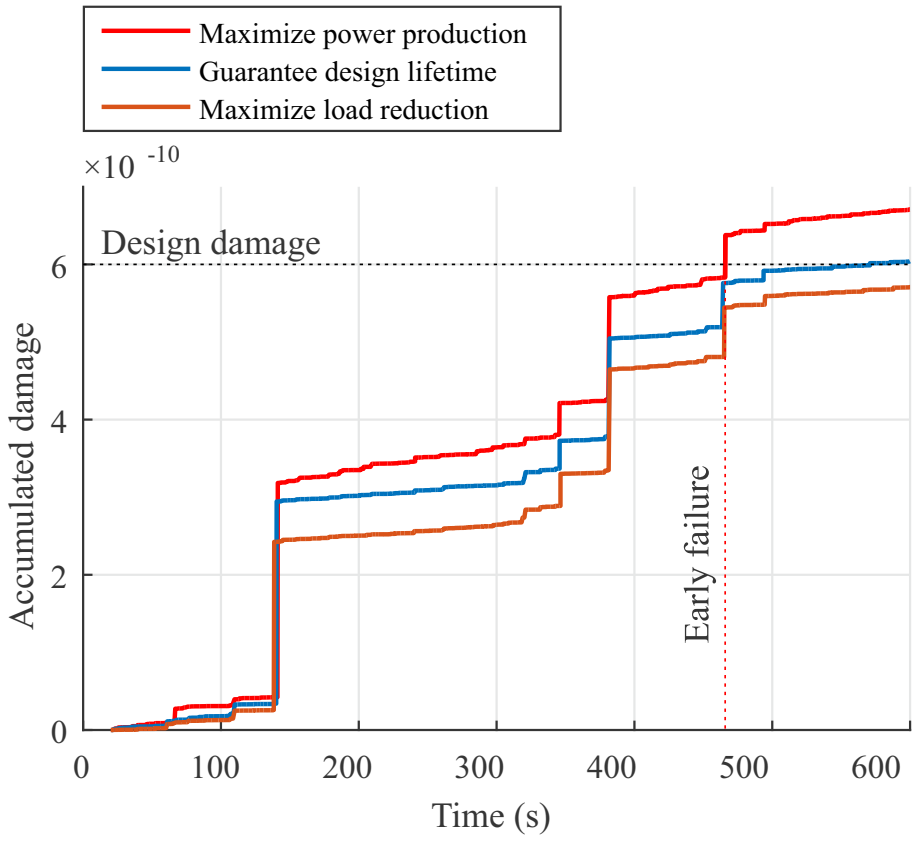

Figure 5.8: Lifetime control results [DS20c]

6 Summary, conclusions, and outlook

6.1 Summary and Conclusions

In the thesis, a new adaptive lifetime control strategy for wind turbines is developed. The approach uses a supervisory control concept to reconfigure the primary load mitigation controller with different load mitigation levels depending on SoH information. By changing the load mitigation levels of the controller, the health degradation behavior can be adjusted, thus the lifetime can be controlled to a predefined value. By guaranteeing the desired lifetime of WT components, unwanted maintenances/repairs can be avoided thus reducing the O&M cost. The proposed control strategy provides an optimal balance between maximize power production and reduce fatigue loading objectives.

The lifetime supervisory control concept requires a primary load mitigation controller, so a robust disturbance accommodating control is developed for both region 2 and region 3 wind turbine control. The robust optimal parameters of a DAC controller are defined by minimizing the H_∞ norm of the generalized system with uncertainties. The proposed method has better performance in both power control and loads mitigation objectives in comparison with that of the baseline controllers. The method also has high robustness against wind speed variation and inaccurate models.

A novel measure based on covariant between power and loads time-series historical data is proposed to compare and evaluate control performance for both power production and load mitigation objectives. The measure considers structural loads, power production and regulation to prove the control performance and to formulate criteria for controller design. The proposed measures allow graphical illustration and numerical criteria describing conflicting control goals and the relationship between goals qualifying control approaches.

6.2 Novel contributions

Within the scope of the thesis and related published papers, the following novel contributions are claimed:

(i) The new method to design DAC controllers based on non-smooth H_∞ synthesis with constrains is developed and evaluated. The proposed approach combines the ability to mitigate disturbance effects of DAC and the robustness of H_∞ synthesis. The parameters of DAC controllers are optimized with respect to both performance and robustness by minimizing the weighted mixed-sensitivity H_∞ norms of the closed-loop system. The method is applied for

both region 2 and region 3 wind turbine control and provide better performances compared with baseline controllers.

(ii) The new covariant diagram measures to compare and evaluate multi-objective control performance for load mitigation and power production of wind turbines is given. The proposed measures are able to describe the different and conflicting control goals of wind turbines thus allow to evaluate different performance dimensions of controllers giving criteria for WT control system designing.

(iii) The generalized and classification of IPHMC concept for wind energy systems are provided for the first time. The concept represents a new research direction for the wind energy field regarding the integration of PHM techniques into WT control systems to improve performances and reliability.

(iv) The new adaptive lifetime control approach for wind turbines is developed based on RUL feedback supervisory control. The controller parameters are adapted to the estimated RUL possible range to control the lifetime of WT components. By regulating the actual lifetime to the desired value, the trade-off between lifetime expansion and power production is optimized thus improve WT performances and reliability.

6.3 Outlook

In the thesis, the collective control approach is used. To further reduce the asymmetrical loads caused by the wind shear, Individual Pitch Control (IPC) approaches can be used in combination with the proposed RDAC approach using Multi-blade Coordinate Transformation (MBC) methods. The pitch angles are controlled individually for each blade to mitigate periodic asymmetrical loads on the blades. However, the pitch activities will increase using IPC thus reduces the actuators' lifetime. To ensure the reliability of the whole system, the lifetime of blade pitch actuators needs to be considered when design control algorithms.

The proposed RDAC approach uses the mix-sensitivity H_∞ norm as a cost function for the optimization problem. The robustness and performance of each output channel can be designed by weight functions for different frequency ranges. In future work, the weight functions can be adapted to the actual wind dynamics with related dominating frequencies for a more effective situation-based balance between robustness and performance. The weights also can be chosen depending on the situation-based demands from grid operators.

The current work focuses only on fatigue damage and uses a linear damage accumulation model based on Miner's rule and rain-flow counting algorithm. In practice, wind turbines contain multiple failure modes caused by different mechanisms. For more precise lifetime control, a better model representing multiple failure modes

need to be developed. In addition, the lifetime degradation rate of WT components varies depending on many factors such as system aging and operation conditions, so a multi-state non-linear degradation model is required to describe correctly the health degradation dynamics for the control purpose. Those developments might contribute to the complexity of the PHM methods thus increase the computational burden. Special attention to the execution time of the PHM methods is required to ensure the practical applicability of the integrated PHM control strategy.

Furthermore, the lifetime expansion of a component might lead to additional loads on others, this trade-off needs to be optimized to ensure the entire turbine reliability and performance. The current work considers a single component case, in future work, the approach can be extended for multiple components. In this case, a MIMO model representing the connection between operation parameters and the health degradation behavior of each component might be required.

Bibliography

[Ago19] Agora Energiewende and Sandbag: *The European Power Sector in 2018. Up-to-date analysis on the electricity transition.* https://www.agora-energiewende.de/fileadmin2/Projekte/2018/EU-Jahresauswertung_2019/Agora-Energiewende_European-Power-Sector-2018_WEB.pdf, 2019. – Accessed: 2019-11-30

[AL14] Ahmadzadeh, F. ; Lundberg, J.: Remaining useful life estimation. In: *International Journal of System Assurance Engineering and Management* 5 (2014), No. 4, pp. 461–474

[AN06] Apkarian, P. ; Noll, D.: Nonsmooth H_∞ Synthesis. In: *IEEE Transactions on Automatic Control* 51 (2006), No. 1, pp. 71–86

[AN17] Apkarian, P. ; Noll, D.: The H_∞ control problem is solved. In: *AerospaceLab Journal* (2017), No. 13, pp. pages–1

[AST17] ASTM: E1049-85. In: *Standard practices for cycle counting in fatigue analysis* (2017)

[AWRF11] Adams, D. ; White, J. ; Rumsey, M. ; Farrar, C.: Structural health monitoring of wind turbines: method and application to a HAWT. In: *Wind Energy* 14 (2011), No. 4, pp. 603–623

[AYTS12] Abdullah, M. A. ; Yatim, A. H. M. ; Tan, C. W. ; Saidur, R.: A review of maximum power point tracking algorithms for wind energy systems. In: *Renewable and sustainable energy reviews* 16 (2012), No. 5, pp. 3220–3227

[BBK89] Boyd, S. ; Balakrishnan, V. ; Kabamba, P.: A bisection method for computing the H_∞ norm of a transfer matrix and related problems. In: *Mathematics of Control, Signals and Systems* 2 (1989), No. 3, pp. 207–219

[BBW16] Barradas-Berglind, J. ; Wisniewski, R.: Representation of fatigue for wind turbine control. In: *Wind Energy* 19 (2016), No. 12, pp. 2189–2203

[BDBM10] Bianchi, F. D. ; De Battista, H. ; Mantz, R. J.: Robust Multivariable Gain-Scheduled Control of Wind Turbines for Variable Power Production. In: *International journal of systems control* 1 (2010), No. 3

[BFW12] Bossanyi, E. ; Fleming, P. ; Wright, A.: Field test results with individual pitch control on the NREL CART3 wind turbine. In: *50th AIAA Aerospace Sciences Meeting Including the New Horizons Forum and Aerospace Exposition, Nashville, TN, January*, 2012, pp. 9–12

[Bir08] Bir, G.: Multi-blade coordinate transformation and its application to wind turbine analysis. In: *46th AIAA aerospace sciences meeting and exhibit*, 2008, pp. 1300

[BLB+16] Buonocore, J. J. ; Lambert, K. F. ; Burtraw, D. ; Sekar, S. ; Driscoll, C. T.: An analysis of costs and health co-benefits for a US power plant carbon standard. In: *PloS one* 11 (2016), No. 6, pp. e0156308

[BLSH07] Boukhezzar, B. ; Lupu, L. ; Siguerdidjane, H. ; Hand, M.: Multivariable control strategy for variable speed, variable pitch wind turbines. In: *Renewable energy* 32 (2007), No. 8, pp. 1273–1287

[BNS18] Beganovic, N. ; Njiri, J. ; Söffker, D.: Reduction of Structural Loads in Wind Turbines Based on an Adapted Control Strategy Concerning Online Fatigue Damage Evaluation Models. In: *Energies* 11 (2018), No. 12, pp. 3429

[Bos03a] Bossanyi, E. A.: Individual blade pitch control for load reduction. In: *Wind Energy: An International Journal for Progress and Applications in Wind Power Conversion Technology* 6 (2003), No. 2, pp. 119–128

[Bos03b] Bossanyi, E. A.: Wind turbine control for load reduction. In: *Wind energy* 6 (2003), No. 3, pp. 229–244

[Bos05] Bossanyi, E. A.: Further load reductions with individual pitch control. In: *Wind Energy: An International Journal for Progress and Applications in Wind Power Conversion Technology* 8 (2005), No. 4, pp. 481–485

[BS90] Bruinsma, N. A. ; Steinbuch, M.: A fast algorithm to compute the H_∞ of a transfer function matrix. In: *Systems & Control Letters* 14 (1990), No. 4, pp. 287–293

[BS16] Beganovic, N. ; Söffker, D.: Structural health management utilization for lifetime prognosis and advanced control strategy deployment of wind turbines: An overview and outlook concerning actual methods, tools, and obtained results. In: *Renewable and Sustainable Energy Reviews* 64 (2016), pp. 68–83

[Cas16] Casini, M.: Small vertical axis wind turbines for energy efficiency of buildings. In: *Journal of Clean Energy Technologies* 4 (2016), No. 1, pp. 56–65

[CCC+12] Ciccarelli, O. ; Corradini, M. L. ; Cucchieri, G. ; Ippoliti, G. ; Orlando, G.: Sliding mode control based robust observer of aerodynamic torque for variable-speed wind turbines. In: *IECon 2012-38th Annual Conference on IEEE Industrial Electronics Society* IEEE, 2012, pp. 4332–4337

[CCC+19] Cetrini, A. ; Cianetti, F. ; Corradini, M. ; Ippoliti, G. ; Orlando, G.: On-line fatigue alleviation for wind turbines by a robust control approach. In: *International Journal of Electrical Power & Energy Systems* 109 (2019), pp. 384–394

[CMM16] Carroll, J. ; McDonald, A. ; McMillan, D.: Failure rate, repair time and unscheduled O&M cost analysis of offshore wind turbines. In: *Wind Energy* 19 (2016), No. 6, pp. 1107–1119

[CQZ+18] Cao, L. ; Qian, Z. ; Zareipour, H. ; Wood, D. ; Mollasalehi, E. ; Tian, S. ; Pei, Y.: Prediction of remaining useful life of wind turbine bearings under non-stationary operating conditions. In: *Energies* 11 (2018), No. 12, pp. 3318

[Dav72] Davison, E.: The output control of linear time-invariant multivariable systems with unmeasurable arbitrary disturbances. In: *IEEE Transactions on Automatic Control* 17 (1972), No. 5, pp. 621–630

[DBS18] Djeziri, M. ; Benmoussa, S. ; Sanchez, R.: Hybrid method for remaining useful life prediction in wind turbine systems. In: *Renewable Energy* 116 (2018), pp. 173–187

[DCPAE+12] De Corcuera, A. D. ; Pujana-Arrese, A. ; Ezquerra, J. M. ; Segurola, E. ; Landaluze, J.: H∞ based control for load mitigation in wind turbines. In: *Energies* 5 (2012), No. 4, pp. 938–967

[DGKF89] Doyle, J. C. ; Glover, K. ; Khargonekar, P. P. ; Francis, B. A.: State-space solutions to standard H_2 and H_∞ control problems. In: *IEEE Transactions on Automatic control* 34 (1989), No. 8, pp. 831–847

[Dhi02] Dhillon, B. S.: *Engineering maintenance: a modern approach*. cRc press, 2002

[DMR+13] Dinwoodie, I. ; McMillan, D. ; Revie, M. ; Lazakis, I. ; Dalgic, Y.: Development of a combined operational and strategic decision

support model for offshore wind. In: *Energy Procedia* 35 (2013), pp. 157–166

[DNS18] Do, M. H. ; Njiri, J. G. ; Söffker, D.: Structural load mitigation control for nonlinear wind turbines with unmodeled dynamics. In: *2018 Annual American Control Conference (ACC)* IEEE, 2018, pp. 3466–3471

[DNS20] Do, M. H. ; Njiri, J. G. ; Söffker, D.: Structural load mitigation control for wind turbines: A new performance measure. In: *Wind Energy* 23 (2020), No. 4, pp. 1085–1098

[DR18] Dykes, K. L. ; Rinker, J.: WindPACT Reference Wind Turbines / National Renewable Energy Laboratory (NREL), Golden, CO (United States). 2018. – Techreport

[DS14] Duckwitz, D. ; Shan, M.: Active tower damping and pitch balancing–design, simulation and field test. In: *Journal of Physics: Conference Series* Vol. 555 IOP Publishing, 2014, pp. 012030

[DS19] Do, M. H. ; Söffker, D.: Robust observer-based load extenuation control for wind turbines. In: *15th International Conference on Multibody Systems, Nonlinear Dynamics, and Control (MSNDC)* ASME, 2019

[DS20a] Do, M. H. ; ; Söffker, D.: State-of-the-Art in Integrated Prognostics and Health Management Control for Utility-Scale Wind Turbines. In: *Renewable and Sustainable Energy Reviews* (2020). – submitted

[DS20b] Do, M. H. ; Söffker, D.: Robust structural load mitigation control for wind turbines in low speed region. In: *European Control Conference (ECC 2020)* IEEE, 2020

[DS20c] Do, M. H. ; Söffker, D.: Wind Turbine Lifetime Control Using Structural Health Monitoring and Prognosis. In: *21st IFAC World Congress* IFAC, 2020

[DS20d] Do, M. H. ; Söffker, D.: Wind Turbine Robust Disturbance Accommodating Control Using Non-smooth H_∞ Optimization. In: *Wind Energy* (2020). – submitted

[DV75] Desoer, C. A. ; Vidyasagar, M.: *Feedback systems: input-output properties*. Vol. 55. Siam, 1975

[ECK14] Evans, M. A. ; Cannon, M. ; Kouvaritakis, B.: Robust MPC tower damping for variable speed wind turbines. In: *IEEE Transactions on Control Systems Technology* 23 (2014), No. 1, pp. 290–296

[EOGA+17] Ekwaro-Osire, S. ; Gonçalves, A. C. ; Alemayehu, F. M. [u. a.]: *Probabilistic prognostics and health management of energy systems*. Springer, 2017

[EPN12] Escobet, T. ; Puig, V. ; Nejjari, F.: Health aware control and model-based prognosis. In: *2012 20th Mediterranean Conference on Control & Automation (MED)* IEEE, 2012, pp. 691–696

[ESLM19] Elasha, F. ; Shanbr, S. ; Li, X. ; Mba, D.: Prognosis of a Wind Turbine Gearbox Bearing Using Supervised Machine Learning. In: *Sensors* 19 (2019), No. 14, pp. 3092

[FC14] Ferguson, D. ; Catterson, V.: Big data techniques for wind turbine condition monitoring. In: *European Wind Energy Association Annual Event (EWEA 2014)* (2014)

[FGO13] Frost, S. A. ; Goebel, K. ; Obrecht, L.: Integrating structural health management with contingency control for wind turbines. In: *International Journal of Prognostics and Health Management* 4 (2013), No. 9, pp. 11–20

[GA94] Gahinet, P. ; Apkarian, P.: A linear matrix inequality approach to H_∞ control. In: *International journal of robust and nonlinear control* 4 (1994), No. 4, pp. 421–448

[GA11] Gahinet, P. ; Apkarian, P.: Structured H_∞ synthesis in MATLAB. In: *IFAC Proceedings Volumes* 44 (2011), No. 1, pp. 1435–1440

[GD12] Girsang, I. P. ; Dhupia, J. S.: Performance of linear control methods for wind turbines dealing with unmodeled structural modes. In: *ASME Dynamic Systems and Control Conference* Vol. 3 Fort Lauderdale Florida, 2012, pp. 645–652

[GD13] Girsang, I. P. ; Dhupia, J. S.: Collective pitch control of wind turbines using stochastic disturbance accommodating control. In: *Wind Engineering* 37 (2013), No. 5, pp. 517–533

[GDC15] Gao, Z. ; Ding, S. X. ; Cecati, C.: Real-time fault diagnosis and fault-tolerant control. In: *IEEE Transactions on industrial Electronics* 62 (2015), No. 6, pp. 3752–3756

[GS01] Grimmett, G. ; Stirzaker, D.: *Probability and random processes*. Oxford university press, 2001

[GS18] Gao, Z. ; Sheng, S.: Real-time monitoring, prognosis, and resilient control for wind turbine systems. In: *Renewable Energy* 116 (2018), pp. 1–4

[GSBDP06] Garcia, M. C. ; Sanz-Bobi, M. A. ; Del Pico, J.: SIMAP: Intelligent System for Predictive Maintenance: Application to the health condition monitoring of a windturbine gearbox. In: *Computers in Industry* 57 (2006), No. 6, pp. 552–568

[Hau13] Hau, E.: *Wind turbines: fundamentals, technologies, application, economics*. Springer Science & Business Media, 2013

[Hay12] Hayman, G.: Mlife theory manual for version 1.00. 2012. – Techreport

[HHS18] Habibi, H. ; Howard, I. ; Simani, S.: Reliability improvement of wind turbine power generation using model-based fault detection and fault tolerant control: A review. In: *Renewable energy* (2018)

[HKE18] Hoek, D. van d. ; Kanev, S. ; Engels, W.: Comparison of Down-Regulation Strategies for Wind Farm Control and their Effects on Fatigue Loads. In: *2018 Annual American Control Conference (ACC)* IEEE, 2018, pp. 3116–3121

[HMN12] Hamdi, H. ; Mrad, C. ; Nasri, R.: Effects of Gyroscopic Coupling on the Dynamics of a Wind Turbine Blade with Horizontal Axis. In: *Condition Monitoring of Machinery in Non-Stationary Operations* (2012), pp. 159–174

[IEC05] IEC: IEC 61400-1: Wind turbines part 1: Design requirements (2005). In: *International Electrotechnical Commission* (2005)

[IHS14] Imran, R. M. ; Hussain, D. A. ; Soltani, M.: DAC with LQR control design for pitch regulated variable speed wind turbine. In: *Telecommunications Energy Conference (INTELEC), 2014 IEEE 36th International* IEEE, 2014, pp. 1–6

[IHS15] Imran, R. M. ; Hussain, D. A. ; Soltani, M.: DAC to mitigate the effect of periodic disturbances on drive train using collective pitch for variable speed wind turbine. In: *Industrial Technology (ICIT), 2015 IEEE International Conference on* IEEE, 2015, pp. 2588–2593

[IRE19] IRENA: Future of wind: Deployment, investment, technology, grid integration and socio-economic aspects (A Global Energy Transformation paper). In: *International Renewable Energy Agency, Abu Dhabi* (2019)

[IRE20] IRENA: Renewable power generation costs in 2019. In: *International Renewable Energy Agency, Abu Dhabi* (2020)

[JBBWS15] Jesus Barradas-Berglind, J. de ; Wisniewski, R. ; Soltani, M.: Fatigue damage estimation and data-based control for wind turbines. In: *IET Control Theory & Applications* 9 (2015), No. 7, pp. 1042–1050

[JBJ05] Jonkman, J. M. ; Buhl Jr, M. L.: FAST User's Guide-Updated August 2005 / National Renewable Energy Laboratory (NREL), Golden, CO. 2005. – Techreport

[JBJ09] Jonkman, B. J. ; Buhl Jr, M. L.: TurbSim user's guide. In: *National Renewable Energy Laboratory* (2009)

[JFBP04] Johnson, K. E. ; Fingersh, L. J. ; Balas, M. J. ; Pao, L. Y.: Methods for increasing region 2 power capture on a variable-speed wind turbine. In: *Journal of solar energy engineering* 126 (2004), No. 4, pp. 1092–1100

[Joh76] Johnson, C. D.: Theory of disturbance-accommodating controllers. In: *Control and Dynamic Systems* 12 (1976), pp. 387–489

[Kad12] Kadry, S.: *Diagnostics and Prognostics of Engineering Systems: Methods and Techniques*. IGI Global, 2012

[KFB19] Komusanac, I. ; Fraile, D. ; Brindley, G.: Wind Energy in Europe in 2018, Trends and statistics. In: *Wind Europe* (2019)

[Koo16] Kooten, G. C.: The economics of wind power. In: *Annual Review of Resource Economics* 8 (2016), pp. 181–205

[KRF18] Kumar, R. ; Raahemifar, K. ; Fung, A. S.: A critical review of vertical axis wind turbines for urban applications. In: *Renewable and Sustainable Energy Reviews* 89 (2018), pp. 281–291

[LFGS20] Luna, J. ; Falkenberg, O. ; Gros, S. ; Schild, A.: Wind turbine fatigue reduction based on economic-tracking NMPC with direct ANN fatigue estimation. In: *Renewable Energy* 147 (2020), pp. 1632–1641

[LS14] Liu, Y. ; Söffker, D.: Robust control approach for input-output linearizable nonlinear systems using high-gain disturbance observer. In: *International Journal of Robust and Nonlinear Control* 24 (2014), pp. 1099–1239

[LSFB+13] Le Son, K. ; Fouladirad, M. ; Barros, A. ; Levrat, E. ; Iung, B.: Remaining useful life estimation based on stochastic deterioration models: A comparative study. In: *Reliability Engineering & System Safety* 112 (2013), pp. 165–175

[ME68] Matsuishi, M. ; Endo, T.: Fatigue of metals subjected to varying stress. In: *Japan Society of Mechanical Engineers, Fukuoka, Japan* 68 (1968), No. 2, pp. 37–40

[MH06] Malcolm, D. ; Hansen, A.: WindPACT Turbine Rotor Design Study: June 2000–June 2002 (Revised) / National Renewable Energy Laboratory (NREL), Golden, CO. (US). 2006. – Techreport

[Min45] Miner, M. A.: Cumulative damage in fatigue. In: *J. Appl. Mech.* 12 (1945), No. 3, pp. A159–A164

[MJ12] Musallam, M. ; Johnson, C. M.: An efficient implementation of the rainflow counting algorithm for life consumption estimation. In: *IEEE Transactions on reliability* 61 (2012), No. 4, pp. 978–986

[MSC15] Ma, Z. ; Shaltout, M. L. ; Chen, D.: An adaptive wind turbine controller considering both the system performance and fatigue loading. In: *Journal of Dynamic Systems, Measurement, and Control* 137 (2015), No. 11, pp. 111007

[MSPN13] Mirzaei, M. ; Soltani, M. ; Poulsen, N. K. ; Niemann, H. H.: An MPC approach to individual pitch control of wind turbines using uncertain LIDAR measurements. In: *2013 European Control Conference (ECC)* IEEE, 2013, pp. 490–495

[NBDS19] Njiri, J. G. ; Beganovic, N. ; Do, M. H. ; Söffker, D.: Consideration of lifetime and fatigue load in wind turbine control. In: *Renewable energy* 131 (2019), pp. 818–828

[NK03] Norton, M. P. ; Karczub, D. G.: *Fundamentals of noise and vibration analysis for engineers*. Cambridge university press, 2003

[NS15] Njiri, J. G. ; Söffker, D.: Multi-Objective Optimal Control of Wind Turbines for Speed Regulation and Load Reduction. In: *ASME 2015 Dynamic Systems and Control Conference* American Society of Mechanical Engineers, 2015, pp. V001T05A002–V001T05A002

[NS16] Njiri, J. G. ; Söffker, D.: State-of-the-art in wind turbine control: Trends and challenges. In: *Renewable and Sustainable Energy Reviews* 60 (2016), pp. 377–393

[OSK13] Odgaard, P. F. ; Stoustrup, J. ; Kinnaert, M.: Fault-tolerant control of wind turbines: A benchmark model. In: *IEEE Transactions on control systems Technology* 21 (2013), No. 4, pp. 1168–1182

[OZZ+13] Ong, J. K. ; Zhang, T. L. ; Zhou, Y. ; Lim, K. P. ; Chen, W. Y. ; Siew, P. Y. ; Nandedkar, K. K. R. ; Ho, J. Y. ; Chin, B. C.: *Method and a system for controlling operation of a wind turbine.* November 5 2013. – US Patent 8,577,509

[PCPB11] Pintea, A. ; Christov, N. ; Popescu, D. ; Borne, P.: LQG control of horizontal wind turbines for blades and tower loads alleviation. In: *IFAC Proceedings Volumes* 44 (2011), No. 1, pp. 1721–1726

[PJ11] Pao, L. Y. ; Johnson, K. E.: Control of wind turbines. In: *IEEE Control systems magazine* 31 (2011), No. 2, pp. 44–62

[RDEH+16] Rogelj, J. ; Den Elzen, M. ; Höhne, N. ; Fransen, T. ; Fekete, H. ; Winkler, H. ; Schaeffer, R. ; Sha, F. ; Riahi, K. ; Meinshausen, M.: Paris Agreement climate proposals need a boost to keep warming well below 2 C. In: *Nature* 534 (2016), No. 7609, pp. 631–639

[SB01] Stol, K. ; Balas, M.: Full-state feedback control of a variable-speed wind turbine: a comparison of periodic and constant gains. In: *Journal of solar energy engineering* 123 (2001), No. 4, pp. 319–326

[SBHS18] Stehly, T. J. ; Beiter, P. C. ; Heimiller, D. M. ; Scott, G. N.: 2017 Cost of Wind Energy Review / National Renewable Energy Laboratory (NREL), Golden, CO. (US). 2018. – Techreport

[Sch96] Schütz, W.: A history of fatigue. In: *Engineering fracture mechanics* 54 (1996), No. 2, pp. 263–300

[SEN+09] Sloth, C. ; Esbensen, T. ; Niss, M. O. ; Stoustrup, J. ; Odgaard, P. F.: Robust LMI-based control of wind turbines with parametric uncertainties. In: *Control Applications,(CCA) & Intelligent Control,(ISIC), 2009 IEEE* IEEE, 2009, pp. 776–781

[SEPO18] Sanchez, H. E. ; Escobet, T. ; Puig, V. ; Odgaard, P. F.: Health-aware model predictive control of wind turbines using fatigue prognosis. In: *International journal of adaptive control and signal processing* 32 (2018), No. 4, pp. 614–627

[SES10] Sloth, C. ; Esbensen, T. ; Stoustrup, J.: Active and passive fault-tolerant LPV control of wind turbines. In: *Proceedings of the 2010 American Control Conference* IEEE, 2010, pp. 4640–4646

[SLQ+07] Söffker, D. ; Liu, Y. ; Qiu, Z. ; Zhang, F. ; Müller, P. C.: Robust Control of Uncertain Systems with Nonlinearities Using Model-Based Online Robustness Measure. In: *ASME 2007 International*

Design Engineering Technical Conferences and Computers and Information in Engineering Conference American Society of Mechanical Engineers, 2007, pp. 33–41

[SP07] Skogestad, S. ; Postlethwaite, I.: *Multivariable feedback control: analysis and design*. Vol. 2. Wiley, 2007

[SPJ11] Sung, H. C. ; Park, J. B. ; Joo, Y. H.: Robust observer-based fuzzy control for variable speed wind power system: LMI approach. In: *International Journal of Control, Automation and Systems* 9 (2011), No. 6, pp. 1103–1110

[SR97] Söffker, D. ; Rakowsky, U.: Perspectives of monitoring and control of vibrating structures by combining new methods of fault detection with new approaches of reliability engineering. In: *A Critical Link: Diagnosis to Prognosis* (1997), pp. 671–682

[SSU+13] Spencer, M. D. ; Stol, K. A. ; Unsworth, C. P. ; Cater, J. E. ; Norris, S. E.: Model predictive control of a wind turbine using short-term wind field predictions. In: *Wind Energy* 16 (2013), No. 3, pp. 417–434

[Sto09] Stol, K. A.: Disturbance tracking and blade load control of wind turbines in variable-speed operation. In: *ASME 2003 Wind Energy Symposium* American Society of Mechanical Engineers Digital Collection, 2009, pp. 317–323

[SYM95a] Söffker, D. ; Yu, T. ; Müller, P. C.: State Estimation of Dynamical Systems with Nonlinearities by using Proportional-Integral Observer. In: *International Journal of Systems Science* 26 (1995), pp. 1571–1582

[SYM95b] Söffker, D. ; Yu, T.-J. ; Müller, P. C.: State estimation of dynamical systems with nonlinearities by using proportional-integral observer. In: *International Journal of Systems Science* 26 (1995), No. 9, pp. 1571–1582

[SZW06] Stol, K. A. ; Zhao, W. ; Wright, A. D.: Individual blade pitch control for the controls advanced research turbine (CART). In: *Journal of solar energy engineering* 128 (2006), No. 4, pp. 498–505

[TB16] Tiwari, R. ; Babu, N. R.: Recent developments of control strategies for wind energy conversion system. In: *Renewable and Sustainable Energy Reviews* 66 (2016), pp. 268–285

[TJWD11] Tian, Z. ; Jin, T. ; Wu, B. ; Ding, F.: Condition based maintenance optimization for wind power generation systems under continuous monitoring. In: *Renewable Energy* 36 (2011), No. 5, pp. 1502–1509

[TKG+08] Tang, L. ; Kacprzynski, G. J. ; Goebel, K. ; Saxena, A. ; Saha, B. ; Vachtsevanos, G.: Prognostics-enhanced automated contingency management for advanced autonomous systems. In: *2008 International Conference on Prognostics and Health Management* IEEE, 2008, pp. 1–9

[TS99] Thomsen, K. ; Sørensen, P.: Fatigue loads for wind turbines operating in wakes. In: *Journal of Wind Engineering and Industrial Aerodynamics* 80 (1999), No. 1-2, pp. 121–136

[WB03] Wright, A. D. ; Balas, M. J.: Design of state-space-based control algorithms for wind turbine speed regulation. In: *Journal of solar energy engineering* 125 (2003), No. 4, pp. 386–395

[WB19] Wiser, R. H. ; Bolinger, M.: 2018 Wind Technologies Market Report / Lawrence Berkeley National Lab. (LBNL), Berkeley, CA (United States). 2019. – Techreport

[WF08] Wright, A. D. ; Fingersh, L.: Advanced control design for wind turbines; Part I: control design, implementation, and initial tests / National Renewable Energy Laboratory (NREL), Golden, CO. (US). 2008. – Techreport

[WFB06] Wright, A. D. ; Fingersh, L. J. ; Balas, M. J.: Testing state-space controls for the controls advanced research turbine. In: *Journal of solar energy engineering* 128 (2006), No. 4, pp. 506–515

[Woo19] Wood Mackenzie: *Unplanned wind turbine repairs to cost industry $ 8 billion+ in 2019.* `https://www.woodmac.com/press-releases/unplanned-wind-turbine-repairs-to-cost-industry-$8-billion-in-2019`, 2019. – Accessed: 2020-07-01

[Wri04] Wright, A. D.: Modern control design for flexible wind turbines / National Renewable Energy Lab., Golden, CO (US). 2004. – Techreport

[WW14] Welte, T. M. ; Wang, K.: Models for lifetime estimation: an overview with focus on applications to wind turbines. In: *Advances in Manufacturing* 2 (2014), No. 1, pp. 79–87

[WWB17] Wang, N. ; Wright, A. D. ; Balas, M. J.: Disturbance accommodating control design for wind turbines using solvability conditions. In:

Journal of Dynamic Systems, Measurement, and Control 139 (2017), No. 4, pp. 041007

[WWJ16] Wang, N. ; Wright, A. D. ; Johnson, K. E.: Independent blade pitch controller design for a three-bladed turbine using disturbance accommodating control. In: *American Control Conference (ACC), 2016* IEEE, 2016, pp. 2301–2306

[XLR16] Xiao, Y. ; Li, Y. ; Rotea, M. A.: Multi-objective Extremum Seeking Control for Enhancement of Wind Turbine Power Capture with Load Reduction. In: *Journal of Physics: Conference Series* Vol. 753 IOP Publishing, 2016, pp. 052025

[YGX+09] Yao, X. ; Guo, C. ; Xing, Z. ; Li, Y. ; Liu, S. ; Wang, X.: Pitch regulated LQG controller design for variable speed wind turbine. In: *Mechatronics and Automation, 2009. ICMA 2009. International Conference on* IEEE, 2009, pp. 845–849

[YL10] Yang, X. ; Liu, X.: Sliding mode control using integral fuzzy method to variable speed wind turbine. In: *Control Conference (CCC), 2010 29th Chinese* IEEE, 2010, pp. 4918–4922

[YS14] Yan, L. ; Söffker, D.: Robust control approach for input–output linearizable nonlinear systems using high-gain disturbance observer. In: *International Journal of Robust and Nonlinear Control* 24 (2014), pp. 1099–1239

[YT17] Yuan, Y. ; Tang, J.: Adaptive pitch control of wind turbine for load mitigation under structural uncertainties. In: *Renewable Energy* 105 (2017), pp. 483–494

[YTC+14] Yang, W. ; Tavner, P. J. ; Crabtree, C. J. ; Feng, Y. ; Qiu, Y.: Wind turbine condition monitoring: technical and commercial challenges. In: *Wind Energy* 17 (2014), No. 5, pp. 673–693

[YWPH18] Yang, W. ; Wei, K. ; Peng, Z. ; Hu, W.: Advanced Health Condition Monitoring of Wind Turbines. (2018), pp. 193–218

The thesis is based on the results and development steps published/submitted in the following journal papers and conference proceedings:

Journal papers

[NBDS19] Njiri, J. G. ; Beganovic, N. ; Do, M. H. ; Söffker, D.: Consideration of lifetime and fatigue load in wind turbine control. In: *Renewable energy* 131 (2019), pp. 818–828

[DNS20] Do, M. H. ; Njiri, J. G. ; Söffker, D.: Structural load mitigation control for wind turbines: A new performance measure. In: *Wind Energy* 23 (2020), No. 4, pp. 1085–1098

[DS20a] Do, M. H. ; ; Söffker, D.: State-of-the-Art in Integrated Prognostics and Health Management Control for Utility-Scale Wind Turbines. In: *Renewable and Sustainable Energy Reviews* (2020). – submitted

[DS20d] Do, M. H. ; Söffker, D.: Wind Turbine Robust Disturbance Accommodating Control Using Non-smooth H_∞ Optimization. In: *Wind Energy* (2020). – submitted

Conference proceedings

[DNS18] Do, M. H. ; Njiri, J. G. ; Söffker, D.: Structural load mitigation control for nonlinear wind turbines with unmodeled dynamics. In: *2018 Annual American Control Conference (ACC)* IEEE, 2018, pp. 3466–3471

[DS19] Do, M. H. ; Söffker, D.: Robust observer-based load extenuation control for wind turbines. In: *15th International Conference on Multibody Systems, Nonlinear Dynamics, and Control (MSNDC)* ASME, 2019

[DS20b] Do, M. H. ; Söffker, D.: Robust structural load mitigation control for wind turbines in low speed region. In: *European Control Conference (ECC 2020)* IEEE, 2020

[DS20c] Do, M. H. ; Söffker, D.: Wind Turbine Lifetime Control Using Structural Health Monitoring and Prognosis. In: *21st IFAC World Congress* IFAC, 2020

In the context of research projects at the Chair of Dynamics and Control, the following student theses have been supervised by Manh Hung Do M.Sc. and Univ.-Prof. Dr.-Ing. Dirk Söffker. Development results of the student theses are not included in this thesis.

[Zha20] Zhang, B.: Development of a variable wind source for VAWT experiments. Bachelor Thesis, 2020.

[Das20] Dash, B.B.: Design and development of a small flywheel energy storage system for wind turbine application using 3D Printing. Master Thesis, 2020.

DOI: 10.17185/duepublico/73535
URN: urn:nbn:de:hbz:464-20201210-083005-1